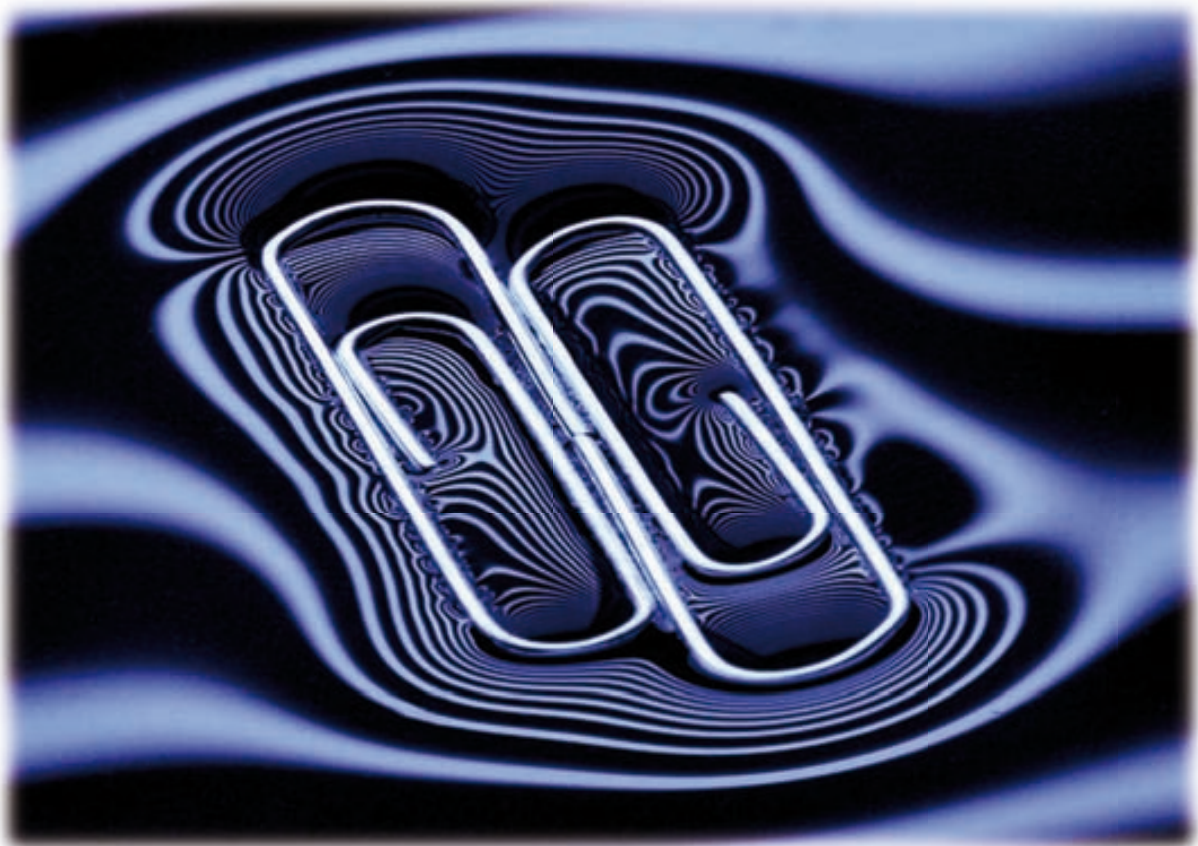


# **MOLECULAR MODELING OF INTERFACIAL PROPERTIES OF INDUSTRIAL RELEVANT FLUIDS**



**BY**

**ORIOI VILASECA I VIDAL**



# **MOLECULAR MODELING OF INTERFACIAL PROPERTIES OF INDUSTRIAL RELEVANT FLUIDS**

A DISSERTATION PRESENTED TO THE DEPARTMENT OF  
PHYSICS AT THE

Universitat Autònoma de Barcelona

in partial fulfillment of the requirements for the degree of

**DOCTOR OF PHILOSOPHY**

Under the supervision Prof. Dr. Lourdes F. Vega

and Dr. Felix Llovell

for the public defense

by

**ORIOL VILASECA I VIDAL**

BELLATERRA, 23<sup>rd</sup> July 2012





# MOLECULAR MODELING OF INTERFACIAL PROPERTIES OF INDUSTRIAL RELEVANT FLUIDS

## **Thesis committee:**

Prof. Dr. Joao A. P. Coutinho  
University of Aveiro, Portugal

Prof. Dr. Rosa Marcos  
Universitat Rovira i Virgili, Spain

Prof. Dr. Carlos Vega  
Universidad Complutense de Madrid, Spain

## **Substitutes:**

Dr. Niall Mac Dowell  
Imperial College, United Kingdom

Dr. Felipe J. Blas  
Universidad de Huelva, Spain



# Declaration

The work reported in this thesis was carried out at the Computational Modeling Group at MATGAS 2000 AIE and at the Molecular Simulation Group of the Institut de Ciència de Materials de Barcelona, Consejo Superior de Investigaciones Científicas (ICMAB-CSIC) (Campus de la Universitat Autònoma de Barcelona, 08193, Bellaterra, Spain). No part of this thesis has been submitted elsewhere for any other degree or qualification and it is all my own work unless referenced to the contrary in the text.

June 2012

---

Oriol Vilaseca i Vidal

PhD Candidate

---

Prof. Dr. Lourdes F. Vega

Supervisor

---

Dr. Felix Llovell

Supervisor





Els sotasignats

FAN CONSTAR

que el present treball, que porta per títol

**MOLECULAR MODELING OF INTERFACIAL  
PROPERTIES OF INDUSTRIAL RELEVANT FLUIDS**

i que presenta n' **Oriol Vilaseca i Vidal** per a optar al grau de doctor en Ciència i Tecnologia dels Materials per la Universitat Autònoma de Barcelona, ha estat realitzat en aquesta universitat sota la seva direcció, i que tots els resultats presentats i l'anàlisi corresponent són fruit de la investigació realitzada per l'esmentat candidat.

I per a que se'n prengui coneixement i als efectes que correspongui, signen aquest certificat.

Lourdes F. Vega

Directora de MATGAS

Investigadora Científica

Felix Llovell i Ferret

MATGAS

Investigador Científic Associat



*To Angels and my kids: Miquel and Aina.*

*“You cannot travel the path until you have become the path itself”*

*Hindu Prince Gautama Siddhartha (563-483 B.C); Buddhism' founder*

# Contents

<b>Acknowledgements</b> .....	<b>xv</b>
<b>Summary</b> .....	<b>xvii</b>
<b>Summary in Catalan</b> .....	<b>xix</b>
<b>Summary in Spanish</b> .....	<b>xxi</b>
<b>Notation</b> .....	<b>xxiii</b>
<b>List of Figures</b> .....	<b>xxvi</b>
<b>List of Tables</b> .....	<b>xxxii</b>

## **1. Introduction..... 1**

1.1. Scope and objectives of this Thesis .....	2
1.2. Organization of this Thesis .....	6
1.3. References.....	7

## **2. Interfacial properties..... 9**

2.1 Introduction.....	10
2.2 Molecular interpretation of interfacial properties .....	13
2.3 Historical Review on Theories for Interfacial Properties .....	15
2.3.1 The interfacial tension concept until Laplace.....	17
2.3.2 From the mechanical to the thermodynamic description .....	19
2.4 Recent approaches to calculate the interfacial properties .....	22
2.4.1 The Parachor .....	22
2.4.2 The corresponding states .....	23
2.4.3 Density Gradient Theory .....	24
2.4.4 Density Functional Approaches .....	26
2.4.5 Molecular simulations .....	27
2.5 References.....	29

<b>3. Methodology .....</b>	<b>33</b>
3.1 Density Gradient Theory.....	34
3.1.1 Density profiles.....	39
3.2 The SAFT Equation of State.....	40
3.2.1 The segment term.....	42
3.2.2 The chain term.....	43
3.2.3 The association term .....	43
3.3 The soft-SAFT equation of state .....	45
3.3.1 The crossover treatment .....	47
3.3.2 The polar term.....	48
3.4 The DGT combined with the soft-SAFT EoS .....	49
3.5 References.....	51
 <b>4. Results and discussion .....</b>	 <b>57</b>
4.1. Assessment of the model: comparison with simulation data.....	59
4.1.1. Lennard-Jones chains .....	60
4.2. Experimental systems: modeling of pure compounds .....	63
4.2.1. Nonassociating compounds .....	67
4.2.1.1. Inorganic compounds .....	68
4.2.1.2. Light n-Alkanes .....	75
4.2.1.3. Heavy n-Alkanes.....	80
4.2.2. Associating compounds .....	83
4.2.2.1. Hydrogen sulfide, ammonia and sulfur dioxide .....	83
4.2.2.2. Water .....	88
4.2.2.3. Light Alkanols .....	91
4.2.2.4. Refrigerants.....	96
4.2.2.5. Nitriles.....	104
4.2.2.6. Ionic liquids.....	107
4.2.3. Comparison between organic families .....	116

4.3. Modeling of binary mixtures .....	118
4.3.1. Nonassociating mixtures .....	118
4.3.1.1. Hydrocarbon mixtures .....	118
4.3.1.2. Carbon dioxide mixtures .....	121
4.3.2. Associating mixtures .....	123
4.3.2.1. n-Alkane + Nitrile mixtures .....	123
4.3.2.2. Refrigerants mixtures .....	124
4.3.2.3. Water + Alkanol mixtures .....	128
4.3.2.4. Ionic liquid + n-Alkane mixtures .....	131
4.4. Surface and critical properties of ionic liquids .....	133
4.4.1. Critical Properties .....	134
4.4.2. Interfacial thermodynamic properties .....	138
4.4.3. Surface thermodynamic properties .....	139
4.5. References .....	143
<b>5. Conclusions and Future Work .....</b>	<b>151</b>
<b>List of publications .....</b>	<b>155</b>
<b>List of conference contributions .....</b>	<b>157</b>
<b>Curriculum Vitæ .....</b>	<b>163</b>
<b>Curriculum Vitæ (Catalan) .....</b>	<b>165</b>

## Acknowledgements

First of all I would like to thank Prof. Lourdes F. Vega for guiding me during all these years. I still remember when I first met her, several years ago, in the thermodynamics course at the University Rovira i Virgili in Tarragona, a nice and a hard subject to deal with. I'm also grateful to her for giving me the opportunity to attain an Erasmus grant to study at the INPT in Toulouse (France) and helping me on obtaining a Seneca grant for my last year at the UAB, when I was first introduced into the research world. Also, my gratitude to her for encouraging me on starting my PhD after some years in the private sector, once I set up my own company in the Contractor & Engineering sector. Prof. Lourdes F. Vega has guided me during all this PhD Thesis project; first teaching me the key facts on interfacial and thermodynamic properties calculations, then after the first steps and establishing the objectives as well as a formal methodology to achieve them, she gave me the right clues and advices for the understanding of molecular models and the physics inside. In conclusion, she has been one the most important persons during my educational live.

I am also thankful to Dr. Felix Llovell, for his help with the code and with some of the last calculations and for his friendship throughout these years. I also want to highlight Prof. João A.P. Coutinho's contributions specially to help me on the understanding of the ionic liquids, and for sharing some of his expertise with me. I also want to thank Prof. Javier Rodriguez Viejo for being the institutional tutor this thesis.

My mum what can I say about her? She has stood my up during all my life, especially concerning my education; even when I was a disobedient boy, she knew that I was clever enough to succeed in life, and she was certainly right. For all the calls she and Charlie made from Spain to France just to say, hello!!

To my travel-mate, Angels for taking care of the kids while I was in my office writing down this PhD thesis, for all the time I have stolen to her, for her comprehension, patience and kindness....for all the dinners she had brought me to the second floor with a kind smile, just saying, how r u....honey? how´s it going? for all the presentations she has listened to at any time. Also I want to mention my kids who have lost some time with his father...but have earned a lot of quality moments...

I also want to thank the ICMA-B-CSIC, where the first part of this PhD thesis has been done, for all the logistic support, and to the MATGAS Research Center for the rest of support during the final part of the thesis.

This research has been possible thanks to the financial support received from the Spanish Government under project CTQ2008-05370/PPQ, as well as CEN2008-01027, a CENIT project belonging to the Programa Ingenio 2010. Additional support from Carbueros Metálicos (Air Products Group), and from the Catalan Government, under projects (SGR2005-00288 and 2009SGR-666), is also acknowledged. The CENIT-SOST-CO2 lead by Carbueros Metálicos and technically coordinated by MATGAS is specially acknowledged, as this work was done in the framework of the project. It is a Spanish Private-Public Project concerning all the carbon dioxide life cycle: from capture, sequestration, transport and to its final applications into the market, in a constant seek for sustainable energy resources under a sustainable point of view.



## Summary

In this PhD thesis, the Density Gradient Theory (DGT) [van der Waals, 1894] combined with a molecular-based Equation of State (EoS); the soft-SAFT [Blas and Vega, 1997], was applied to simultaneously predict the phase behavior and the interfacial properties of industrial relevant fluids. As the equation is based in statistical mechanics, its approximations and assumptions were assessed against simulation data for the same underlying model. Once the model was validated, it was applied to simultaneously calculate the phase equilibria and the interfacial properties of some of the most representative industrial fluids, far from and close to the critical region. In particular, the model has been tested with molecular model fluids as Lennard-Jones chains, giving excellent agreement with simulation data, and then applied to different pure fluids, including: n-alkanes, light alkanols, ionic liquids, refrigerants, nitriles, water, carbon dioxide and ammonia, among others. A step forward has been done by calculating the interfacial properties of the binary mixtures of industrial interest, with associating and nonassociating compounds, in a predictive manner, avoiding the need of additional fitting, and providing information for systems for which there is not experimental data available. In addition, three correlations of the influence parameter as a function of the carbon number have been proposed for the light alkanes, light alkanols and one ionic liquid family, allowing for predictions of properties of compounds not included in the fitting procedure.

A final novel contribution of this Thesis work is the prediction of the critical temperature, density and pressure of the most common used ionic liquids by using soft-SAFT coupled with the DGT. This is to our best knowledge the first time that an EoS is coupled to the DGT to calculate simultaneously the interfacial tension at elevated temperatures, while capturing the asymptotic behavior as the critical region is approached. Moreover, the surface properties, such as surface entropy and surface enthalpy, have been derived from the surface tension dependence on temperature, finding a very good agreement with the <sup>xvii</sup> values reported in the literature from simulation and experimental contributions.

Finally, a throughout study of the different density profiles, including single fluids and different binary mixtures, has been carried out to complete the description of the interfacial phenomena. Absorption and desorption density profiles are also presented given their importance in transport and process control.

The work developed here demonstrates that coupling an accurate molecular-based equation of state for phase properties, the soft-SAFT equation, with a simple and accurate theory for interfacial properties, the Density Gradient Theory, is a reliable tool to simultaneously predict the phase and interfacial properties of nonassociating and associating compounds, as well as their mixtures with a very slight computational effort and great accuracy.

## Summary in Catalan

En aquesta tesi doctoral es presenta la Teoria del Gradient de Densitat (DGT) [van der Waals, 1894] combinada amb una Equació d'Estat (EoS) amb base molecular la soft-SAFT [Blas i Vega, 1997], per predir de forma simultània el comportament de l'equilibri de fases i les propietats interfacials dels fluids industrials més representatius. Atès que l'equació està basada en mètodes estadístics, les aproximacions i condicions de contorn establertes han de ser validades davant les dades de simulació, on s'utilitza mateix model que per a l'equació. Una vegada que el model ha estat validat amb dades de simulació de la literatura, s'ha aplicat per calcular simultàniament els equilibris de fases i les propietats interfacials dels fluids industrials més representatius, tant lluny com a prop de la regió crítica. En particular, el model ha estat provat amb fluids modelats com cadenes de Lennard-Jones i amb fluids purs: n-alcans, alcohols, líquids iònics, refrigerants, nitrils, aigua, diòxid de carboni i altres molècules inorgàniques. Un pas endavant s'ha fet en el càlcul de les propietats interfacials de les mescles binàries d'interès industrial de compostos associants i no associants també d'una manera predictiva, evitant la necessitat d'ajustos addicionals al mateix temps que s'obté informació per als sistemes que no està disponible experimentalment. A més, s'han obtingut tres correlacions per al paràmetre d'influència en funció del nombre de carbonis per: els alcans, els alcohols i una família de líquids iònics per la obtenció predictiva de les propietats dels compostos que no van ser inclosos en el procediment d'ajust.

Una de les contribucions més significatives d'aquesta Tesi és la predicció de les propietats crítiques dels líquids iònics com ara la temperatura, la pressió i la densitat dels líquids iònics més comuns, mitjançant l'acoblament de la soft-SAFT amb la DGT. Aquesta és la primera vegada que una EoS és acoblada a la DGT per calcular simultàniament la tensió interfacial a temperatures elevades, capturant el comportament asimptòtic prop de la regió crítica. A més, les propietats de la superfície, com l'entropia i l'entalpia de superfície, s'han derivat a partir de la dependència de la tensió superficial amb la temperatura, els resultats trobats estan d'acord quantitativament amb els valors reportats a la literatura tant de dades de simulació com de les contribucions experimentals.

Finalment per completar la revisió dels fenòmens interfacials, s'ha dut a terme un estudi dels diferents perfils de densitat, incloent fluids purs i diferents tipus de mescles binàries. Així mateix es presenten alguns perfils de densitat amb fenòmens d'absorció i desorció en la interfase, atès que aquests són de gran rellevància tant per al control de processos com per al transport de gasos i fluids.

En aquesta tesi es demostra que l'acoblament d'una Equació d'Estat amb base molecular per al càlcul de les propietats de les fases, la soft-SAFT, amb una teoria simple i adequada per a les propietats interfacials, la teoria del Gradient de Densitat, es presenta com un mètode elegant per predir les propietats d'equilibri i les propietats interfacials de compostos associants i no associants, així com de les seves mescles, de forma acurada i amb un mínim esforç computacional.

## Summary in Spanish

En esta tesis doctoral se presenta la Teoría del Gradiente de Densidad (DGT) [van der Waals, 1894] combinada con una Ecuación de Estado (EoS) con base molecular, la soft-SAFT [Blas y Vega, 1997], para predecir de forma simultánea el comportamiento del equilibrio de fases y las propiedades interfaciales de los fluidos industriales más representativos. Dado que la ecuación está basada en métodos estadísticos, las aproximaciones y condiciones de contorno establecidas tienen que ser validadas frente a los datos de simulación, donde se utiliza el mismo modelo que para la ecuación, pero sin las aproximaciones que ésta implica. Una vez que el modelo ha sido validado frente a datos de simulación existentes en la literatura, se ha aplicado para calcular simultáneamente los equilibrios de fases y las propiedades interfaciales de los fluidos industriales más representativos, tanto lejos como cerca de la región crítica. En particular, el modelo ha sido probado con fluidos modelados como cadenas de Lennard-Jones y con fluidos puros, incluyendo: n-alcanos, alcoholes, líquidos iónicos, refrigerantes, nitrilos, agua, dióxido de carbono y otras moléculas inorgánicas. Además, se ha llevado a cabo el cálculo de propiedades interfaciales de mezclas binarias de interés industrial de compuestos asociantes y no asociantes de forma predictiva, evitando la necesidad de ajustes adicionales a la vez que se obtiene información para los sistemas que no está disponible experimentalmente. Se han obtenido, asimismo, tres correlaciones para el parámetro de influencia en función del número de carbonos para los alcanos, los alcoholes y una familia de líquidos iónicos, pudiendo así predecir el comportamiento de fases e interfacial de compuestos que no incluidos en el procedimiento de ajuste.

Una de las contribuciones más significativas de esta Tesis es la predicción de las propiedades críticas de los líquidos iónicos tales como la temperatura, la presión y la densidad crítica de los líquidos iónicos más comunes, mediante el acoplamiento de la soft-SAFT con la DGT. Esta es la primera vez que una EoS es acoplada a la DGT para calcular simultáneamente la tensión interfacial a temperaturas elevadas, al mismo tiempo que captura el comportamiento asintótico de estas propiedades en las proximidades de la región crítica. Además, las propiedades de la superficie, como la entropía y la

entalpía de superficie, se han derivado a partir de la dependencia de la tensión superficial con la temperatura, los resultados encontrados están de acuerdo cuantitativamente con los valores reportados en la literatura tanto de datos de simulación como de las contribuciones experimentales.

Finalmente se ha llevado a cabo un estudio de los distintos perfiles de densidad, incluyendo fluidos puros y diferentes tipos de mezclas binarias para completar la revisión de los fenómenos interfaciales. Se presentan algunos perfiles de densidad con fenómenos de absorción y desorción en la interfase, dada su gran relevancia tanto para el control de procesos como para el transporte de gases y fluidos.

En esta tesis se demuestra que el acoplamiento de una Ecuación de Estado con base molecular para el cálculo de las propiedades de las fases, la soft-SAFT, con una teoría simple y precisa para las propiedades interfaciales, la teoría del Gradiente de Densidad, es un método elegante que permite predecir las propiedades de equilibrio y las propiedades interfaciales de compuestos asociantes y no asociantes, así como de sus mezclas, de una manera precisa y con un mínimo esfuerzo computacional.

# Notation

## Abbreviations

CFC	Chlorofluorocarbon
CPA	Cubic Plus Association
DFT	Density Functional Theory
DGT	Density Gradient Theory
EoS(s)	Equation(s) of State
GWP	Global Warming Potential
HCFC	Hydrochlorofluorocarbon
IT	Interfacial tension
LJ	Lennard-Jones
LLE	Liquid-Liquid Equilibria
LLV	Liquid-Liquid-Vapor Equilibria
MD	Molecular Dynamics
ODPs	Ozone Depletion Potentials
PC	Perturbed Chain
PFC	Perfluoroalkanes
PHCT	Perturbed Hard Chain Theory
PSCT	Perturbed Soft Chain Theory
PR	Peng-Robinson
PVT	Pressure-Volume-Temperature
RG	Renormalization Group
RK	Redlich-Kwong
SAFT	Statistical Associating Fluid Theory
SRK	Soave-Redlich-Kwong
TPT1	Thermodynamic Perturbation Theory (First order)
UNIFAC	Universal Functional Activity Coefficient Model
UNIQUAC	Universal Quasi-Chemical Approach
vdW	van der Waals
VLE	Vapor-Liquid Equilibria
VR	Variable range

## Latin symbols

$A$	Helmholtz free energy
$a$	Helmholtz free energy density
$c$	influence parameter
$C_{ij,0}$	direct correlation function of the homogeneous fluid
$CN$	carbon number
$g$	pair correlation function
$k^{HB}$	volume of association
$k_B$	Boltzmann constant
$L$	cutoff length
$M_w$	molecular weight
$m$	number of LJ segments, chain length
$N_A$	Avogadro's number
$P$	pressure
$Q$	quadrupole
$R$	ideal gas constant
$T$	temperature
$T_c$	critical temperature
$Tr$	reduced temperature
$X$	fraction of nonbonded molecules
$x$	mole fraction
$z$	density profile

## Greek symbols

$\square$	adjustable parameter to the interfacial tension measurements
$\sigma$	size parameter of the LJ segments
$\square$	energy well-depth of the LJ intermolecular potential / dispersive energy
$\square_{HB}$	association energy
$\eta$	size parameter of the generalized Lorentz-Berthelot combining rules
$\square$	intermolecular potential
$\phi$	average gradient of the wavelet function (crossover parameter)
$\square$	compressibility
$\square_{HB}$	volume of association
$\square$	chemical potential / Joule-Thomson coefficient



- energy binary parameter of the generalized Lorentz-Berthelot combining rules
- density
- $\gamma$  interfacial tension
- grand thermodynamical potential

### Superscripts

<i>assoc</i>	association term
<i>attr</i>	attraction term
<i>chain</i>	chain term
<i>cross</i>	crossover
<i>disp</i>	dispersion
<i>id</i>	ideal term
<i>LJ</i>	Lennard-Jones
<i>polar</i>	polar term
<i>ref</i>	reference term

### Subscripts

<i>B</i>	Boltzmann constant
<i>HB</i>	parameters of association on soft-SAFT
<i>i,j</i>	the specific compound i or j in a mixture

**Note: the terms interfacial tension and surface tension have been used indistinctly.**

## List of Figures

<b>Figure 2.1:</b> Thermodynamic magnitudes determining the states of carbon dioxide.....	10
<b>Figure 2.2:</b> Interaction forces acting on one molecule on the surface and on the bulk..	11
<b>Figure 2.3:</b> Interfacial tension effects.....	12
<b>Figure 2.4:</b> Thermodynamic factors determining the magnitude of the interfacial tension value. ....	13
<b>Figure 2.5:</b> Sketch of Archimedes's principle.....	15
<b>Figure 2.6:</b> Sketch of capillarity effects.....	16
<b>Figure 2.7:</b> Discontinuous approach for the density variation $\rho(z)$ . ....	18
<b>Figure 2.8:</b> Functional approaches for the density variation $\rho(z)$ .....	20
<b>Figure 3.1:</b> Types of density variation $\rho(z)$ . From: [Rowlinson and Widom, 1998] .....	39
<b>Figure 3.2:</b> Representation of the different interactions included in the SAFT-EoS.....	46
<b>Figure 4.1:</b> Graphical representation of the Lennard-Jones chains in a simulation box. ....	59
<b>Figure 4.2:</b> Phase diagram of LJ chains from $m=1$ to $m=32$ . Symbols are simulation data while lines are the calculations with the soft-SAFT. See text for details. ....	61
<b>Figure 4.3:</b> Vapor-liquid interfacial tension of LJ chains from $m=1$ to $m=32$ . Symbols are simulation data while lines are the calculations with the soft-SAFT combined with the DGT. See text for details.....	62
<b>Figure 4.4:</b> Predicted vapor-liquid equilibrium (left) and interfacial tensions (right) of hydrogen. Symbols represent experimental data from NIST and lines correspond to soft-SAFT+DGT approach.....	70
<b>Figure 4.5:</b> Predicted pressure-temperature diagram of hydrogen. Symbols represent experimental data from NIST and lines correspond to soft-SAFT+DGT approach as obtained in this work.....	70
<b>Figure 4.6:</b> Vapor-liquid equilibria (left) and interfacial tensions (right) of nitrogen, argon and oxygen (from bottom to top). Symbols represent experimental data from NIST and lines correspond to crossover soft-SAFT+DGT approach. See text for details .....	71
<b>Figure 4.7:</b> Vapor-liquid equilibria (left) and interfacial tension as a function of temperature (right) of carbon monoxide. Symbols represent experimental data from NIST and lines correspond to crossover soft-SAFT+DGT approach. ....	72
<b>Figure 4.8:</b> Temperature-density diagram of carbon dioxide. Symbols are experimental data from NIST and the dashed and dotted line is the predictions with the crossover soft-SAFT.....	74

- Figure 4.9:** Vapor-liquid interfacial tension of carbon dioxide as a function of temperature. Circles represent experimental data [NIST] while lines correspond to the crossover soft-SAFT+DGT approach. .... 74
- Figure 4.10:** Example of a Graphical representation of n-pentane. .... 75
- Figure 4.11:** Schema of different hydrocarbons processes. .... 76
- Figure 4.12:** Vapor-liquid equilibria of n-alkanes, from methane to n-octane (from left to right). Symbols are experimental data from references [Landolt-Börnstein; NIST] and the dashed and dotted lines correspond to the crossover soft-SAFT combined with the DGT calculations. .... 78
- Figure 4.13:** Vapor-liquid interfacial tensions of n-alkanes, from methane to n-octane (from left to right). Symbols are experimental data from references [NIST; Landolt-Börnstein] and the full lines correspond to the predictions of the crossover soft-SAFT+DGT approach. .... 79
- Figure 4.14:** Optimized influence parameter for the light members of the n-alkane (circles) series versus the carbon number. Lines correspond to the values obtained from Equation 4.4. .... 79
- Figure 4.15:** Molecular 3D representation of n-eicosane (C=20). .... 80
- Figure 4.16:** Predicted vapor-liquid interfacial tensions of heavy n-alkanes: n-C<sub>10</sub>, n-C<sub>12</sub>, n-C<sub>16</sub>, n-C<sub>20</sub>, n-C<sub>26</sub>, n-C<sub>32</sub> (from bottom to top). Symbols represent experimental data [NIST; Landolt-Börnstein] and lines correspond to the crossover soft-SAFT+DGT approach. See text for details. .... 81
- Figure 4.17:** Vapor-liquid (left) and interfacial tensions (right) of hydrogen sulfide. Symbols represent experimental data [NIST] and solid line corresponds to the soft-SAFT+ DGT approach while the dashed and dotted line corresponds to the crossover soft-SAFT+DGT approach. See text for details .... 86
- Figure 4.18:** Predicted vapor-liquid diagrams (left) and interfacial tensions (right) of ammonia. Symbols represent experimental data [NIST] and solid line corresponds to the soft-SAFT+ DGT approach while the dashed and dotted line corresponds to the crossover soft-SAFT+DGT approach. .... 86
- Figure 4.19:** Phase equilibria of sulfur dioxide. Symbols are experimental data from NIST solid lines are obtained with the soft-SAFT EoS +DGT and the dashed and dotted line are the predictions with the crossover soft-SAFT EoS + DGT. Temperature-density diagram (left) and Interfacial tension-temperature diagram (right). .... 87
- Figure 4.20:** Representation of hydrogen bonding between water molecules and the chosen molecular model. .... 88
- Figure 4.21:** Vapor-liquid interfacial tensions of water: original soft-SAFT + DGT, without the crossover term (solid line) and crossover soft-SAFT + DGT calculations (dotted and dashed line). Crosses represent experimental data from NIST database. .... 89
- Figure 4.22:** Molecular 3D representation of 1-methanol and 1-butanol .... 92

- Figure 4.23:** Vapor-liquid equilibria of light alkanols from ethanol to 1-octanol (from left to right). Symbols represent experimental data [NIST] and dashed and dotted lines correspond to the crossover soft-SAFT+DGT approach. .... 93
- Figure 4.24:** Vapor-liquid interfacial tensions of light alkanols from ethanol to 1-octanol (from left to right). For clarity methanol is shown separately in the inset. Symbols represent experimental data [Jasper, 1972; Landolt-Börnstein; NIST] and dotted lines correspond to the crossover soft-SAFT+DGT approach ..... 94
- Figure 4.25:** Optimized influence parameter for the light members of the light alkanols (squares) series versus the carbon number. Lines correspond to the values obtained from equation 4.5. .... 95
- Figure 4.26:** Schematic representation of a hydrofluorocarbon. .... 99
- Figure 4.27:** Correlations of  $m\sigma^3$  with  $M_w$  for the HFC molecules (equations (4.6a-4.d), continuous lines): fluoromethanes ( $\square$ ), fluoroethanes ( $\square$ ), fluoropropanes ( $\Delta$ ), fluorobutanes ( $\diamond$ ); and other series of molecules (equations (4e-4g), dashed lines): n-alkanes, n-perfluoroalkanes and pentafluoroalkanes..... 101
- Figure 4.28:** Vapor-liquid interfacial tension for (a) R23( $\square$ ), R32( $\Delta$ ) and R41(+); (b) R125( $\Delta$ ), R152a(+), R134a ( $\square$ ); (c) R143a( $\square$ ); (d) R227 ( $\Delta$ ), R236fa (+), R236ea ( $\square$ ), R245fa ( $\square$ ) and R245ca ( $\diamond$ ). Symbols represent the experimental data [NIST] while the lines correspond to the soft-SAFT + DGT modeling. .... 103
- Figure 4.29:** Molecular 3D representation propionitrile..... 104
- Figure 4.30:** Vapor-liquid interfacial tensions of n-nitriles. a) acetonitrile ( $\text{CH}_3\text{CN}$ ), b) from propionitrile ( $\text{C}_2\text{H}_5\text{CN}$ ) to nonanenitrile ( $\text{C}_8\text{H}_{17}\text{CN}$ ), from left to right. Symbols are experimental data from [Landolt-Börnstein] and the full lines correspond to the soft-SAFT+DGT approach..... 105
- Figure 4.31:** (Left) Number of publications about ionic liquids published in journals included in the Web of Science List, year by year in the last decade. (Right) Distribution of topics related to the presentations about ionic liquids at the 17th International Symposium on Thermophysical Properties. See text for details. .... 109
- Figure 4.32:** Representation of ionic liquids molecules [ $\text{C}_n\text{-mim}$ ][ $\text{BF}_4$ ],[ $\text{C}_n\text{-mim}$ ][ $\text{PF}_6$ ] and [ $\text{C}_n\text{-mim}$ ][ $\text{Tf}_2\text{N}$ ]. .... 110
- Figure 4.33:** Interfacial tension as a function of temperature for the ionic liquid family 1,3-methyl-imidazolium tetrafluoroborate [ $\text{C}_n\text{-mim}$ ][ $\text{BF}_4$ ] as a function of temperature. Symbols: [ $\text{C}_2\text{-mim}$ ] (squares), [ $\text{C}_6\text{-mim}$ ] (diamonds) and [ $\text{C}_8\text{-mim}$ ] (triangles) represent experimental data [Freire et al., 2007; Gathee et al., 2008] and lines correspond to the soft-SAFT+DGT approach..... 111
- Figure 4.34:** Interfacial tension as a function of temperature for the ionic liquid family 1,3-methyl-imidazolium hexafluorophosphate [ $\text{C}_n\text{-mim}$ ][ $\text{PF}_6$ ] as a function of temperature. Symbols: [ $\text{C}_2\text{-mim}$ ] (asterisks), [ $\text{C}_6\text{-mim}$ ] (pluses) and [ $\text{C}_8\text{-mim}$ ] (crosses)

- represent experimental data [Freire et al., 2007] and lines correspond to the soft-SAFT+DGT approach..... 112
- Figure 4.35:** a) Vapor-liquid interfacial tensions of the ionic liquid family 1-alkyl-3-methyl-imidazolium bis(trifluoromethylsulfonyl)imide as a function of temperature [C<sub>2</sub>-mim][Tf<sub>2</sub>N], [C<sub>3</sub>-mim][Tf<sub>2</sub>N], [C<sub>4</sub>-mim][Tf<sub>2</sub>N], [C<sub>5</sub>-mim][Tf<sub>2</sub>N], [C<sub>6</sub>-mim][Tf<sub>2</sub>N] and [C<sub>7</sub>-mim][Tf<sub>2</sub>N] (from top to bottom) b) [C<sub>8</sub>-mim][Tf<sub>2</sub>N]. Symbols represent experimental data [Carvalho et al., 2008] and lines correspond to the soft-SAFT+DGT calculations. .... 113
- Figure 4.36:** Optimized influence parameter for the light members of the n-alkyl-3-methyl-imidazolium bis(trifluoromethylsulfonyl)imide: [C<sub>n</sub>-mim][Tf<sub>2</sub>N], versus the carbon number. Solid line corresponds to the values obtained from equation (4.7).. 114
- Figure 4.37:** Predictions for the vapor-liquid interfacial tensions of [C<sub>10</sub>-mim][Tf<sub>2</sub>N]. Symbols represent experimental data [Carvalho et al., 2008] and lines correspond to the soft-SAFT+DGT predictions. .... 115
- Figure 4.38:** Comparison of phase and interfacial properties of a C<sub>4</sub> compound from the three homologous chemical families: butane (squares), perfluorobutane (crosses) and butanol (circles) .a) vapor-liquid equilibria phase diagram, b) interfacial tensions as a function of temperature. Symbols represent the experimental data [[Landolt-Börnstein, NIST] while the lines correspond to the crossover soft-SAFT+DGT approach..... 116
- Figure 4.39:** Comparison of the density profiles of butane (dotted and dashed lines), butanol (dashed lines) and perfluorobutane (solid lines) as predicted from crossover-soft-SAFT + DGT at three reduced temperatures a) T<sub>r</sub>=0.84, b) T<sub>r</sub>=0.91 and c) T<sub>r</sub>= 0.97. .... 117
- Figure 4.40:** Predictions for the vapor-liquid interfacial tensions of the n-hexane + n-decane mixture at: 303.15, 323.15, and 353.15 K (from top to bottom). Crosses represent experimental data [Landolt-Börnstein] and lines correspond to the crossover soft-SAFT+DGT predictions. .... 119
- Figure 4.41:** Predictions for the vapor-liquid interfacial tensions of the n-decane + n-hexadecane mixture at: 293.15, 303.15, 313.15, 323.15 and 333.15 K (from top to bottom). Crosses are experimental [Landolt-Börnstein] and lines correspond to the soft-SAFT+DGT approach..... 119
- Figure 4.42:** Predictions for the vapor-liquid interfacial tensions of the n-hexadecane + n-eicosane mixture at: 313.15, 323.15, 333.15 and 343.15 K (from top to bottom). Crosses are experimental data [Landolt-Börnstein] and lines correspond to the soft-SAFT+DGT approach..... 120
- Figure 4.43:** Vapor-liquid interfacial tensions of the carbon dioxide + n-butane mixture at: 319.3, 344.3 and 377.6 K (from left to right). Symbols represent experimental data [Hsu et al., 1985] and lines are calculations from the crossover soft-SAFT+DGT approach with two binary parameters, close to unity..... 121

- Figure 4.44:** Vapor-liquid interfacial tensions of the carbon dioxide + n-decane mixture at: 319.3, 344.3 and 377.6 K (from left to right). Symbols represent experimental data [Nagarajan et Robinson, 1986] and lines are calculations from the crossover soft-SAFT+DGT approach with two binary parameters, close to unity ..... 122
- Figure 4.45:** Vapor-liquid interfacial tensions of the butanenitrile + pentane mixture at: 293, 303 and 333 K (from top to bottom). Symbols represent experimental data [Landolt-Börnstein] and lines are predictions from the soft-SAFT+DGT approach. ... 123
- Figure 4.46:** Interfacial properties of the systems propane + R152a mixture (a) Interfacial tension for a mass composition fraction  $w_1=0.2008$  ( $\Delta$ ) and  $w_1=0.4922$  ( $\square$ ). Symbols represent the experimental data [NIST] while the lines correspond to the soft-SAFT modeling. .... 125
- Figure 4.47:**  $\square$  1-z and  $\square$  2-z density profiles for the mixture propane + R152a at a fixed mass composition fraction  $w_1=0.2008$  and three temperatures  $T=270K$ , 295K and 315K. The full line represents the propane density profile while the dotted-dash line represents the R152a density profile along the interface..... 126
- Figure 4.48:** Interfacial properties of the systems R32 + R134 mixture (a) Interfacial tension for a mass composition fraction  $w_1=0.2379$  ( $\Delta$ ) and  $w_1=0.4017$  ( $\square$ ). Symbols represent the experimental data [Yuan-Yuan et al., 2003] while the lines correspond to the soft-SAFT modeling. .... 127
- Figure 4.49:** Vapor-liquid interfacial tensions of the water-methanol mixture at: 303, 313 and 323 K (from top to bottom). Symbols represent experimental data [Gonzalo et al., 1995; Landolt-Börnstein] and lines are the soft-SAFT + DGT predictions. .... 129
- Figure 4.50:** Vapor-liquid interfacial tensions of the water-ethanol mixture at: 293, 298, 313 and 323 K (from top to bottom). Symbols represent experimental data [Gonzalo et al., 1995; Landolt-Börnstein] and lines are predictions from the soft-SAFT+DGT approach. See text for details. .... 129
- Figure 4.51:** Liquid-liquid interfacial tensions for the  $[C_4mim][Tf_2N]$  + n-hexane mixture from 293 to 313 K. Symbols represent experimental data [Gardas et al., 2010] and lines are predictions from the soft-SAFT+DGT approach..... 131
- Figure 4.52:** Critical properties for the light members of the  $[C_n-mim][BF_4]$  (circles),  $[C_n-mim][PF_6]$  (diamonds) and  $[C_n-mim][Tf_2N]$  (squares) ionic liquids, versus the carbon number. a) Critical Temperature b) Critical Pressure c) Critical density ..... 135-136
- Figure 4.53:** Corresponding states surface tension  $\gamma_{red}$  as a function of the reduced temperature  $T_{red}$ . Experimental data [Landolt-Börnstein] for argon (dashed line) and for R32 (solid line) and ethanol (dotted line). Results from soft-SAFT + DGT calculations for two ionic liquids  $[C_4-mim][PF_6]$  (circles) and  $[C_4-mim][Tf_2N]$ (stars) are represented. .... 137
- .....xxx.....
- Figure 4.54:** Interfacial tension as a function of temperature for  $[C_4-mim][PF_6]$ . Symbols represent simulation data YASP (stars) and GROMACS (triangles up) [Weiss et al,

2010a,b], and experimental data from Freire et al., [2007] (circles) and Gathee et al., [2008] (squares) while the solid line represents the soft-SAFT+DGT calculations..... 138

**Figure 4.55:** Representation of a ionic liquid in a planar interface. See text for details.  
..... 140

## List of Tables

<b>Table 4.1.</b> Crossover optimized parameters for flexible LJ chains studied in this work. Simulation data from different references. See text for details.....	60
<b>Table 4.2.</b> Molecular models used in this thesis .....	66
<b>Table 4.3.</b> Molecular sketch for the compounds studied in this section .....	68
<b>Table 4.4.</b> Molecular parameters for the inorganic compounds, together with the references were the parameters were originally obtained.....	69
<b>Table 4.5.</b> Molecular parameters for the light alkanes studied in this work. [Llovell et al. 2004] .....	77
<b>Table 4.6.</b> Optimized influence parameters for the light alkanes studied in this work.....	77
<b>Table 4.7.</b> Molecular sketch for the compounds studied in this section .....	84
<b>Table 4.8.</b> Optimized parameters for the inorganic associating compounds .....	85
<b>Table 4.9.</b> Molecular parameters for water (with and without crossover, together with the references were the parameters were originally obtained).....	90
<b>Table 4.10.</b> Optimized influence parameters for water .....	90
<b>Table 4.11.</b> Molecular parameters for the light alkanols studied in this work [Llovell et al. 2006] See text for details.....	92
<b>Table 4.12.</b> Optimized influence parameters for the light alkanols studied in this work.....	93
<b>Table 4.13.</b> Name, code and structure of the refrigerants studied in this section.....	98
<b>Table 4.14.</b> Optimized influence parameters for the refrigerants studied in this work .....	102
<b>Table 4.15.</b> Molecular parameters for the nitriles studied in this work, together with the references were the parameters were originally obtained.....	104-105
<b>Table 4.16.</b> Optimized influence parameters for the nitriles studied in this work.....	106
<b>Table 4.17.</b> Optimized influence parameters for the ionic liquids studied in this work. See text for details.....	113
<b>Table 4.18.</b> Critical properties for the compounds studied in this work. See text for details. ....	141
<b>Table 4.19.</b> Surface properties for the compounds studied in this work. See text for details .....	142



# 1. Introduction

*“Originality consists of returning to the origin. Thus, originality means returning, through one’s resources, to the simplicity of the early solutions”*

*Antoni Gaudí i Cornet (1852-1926); Catalan Architect*

## 1.1. Scope and objectives of this Thesis

Interfacial tension, interfacial thickness or relative Gibbs adsorption of one component are ubiquitous in industrial practice. Examples include design, scale up and optimization of industrial processes, such as the mass transfer operations or distillation, extraction, absorption and adsorption or CO<sub>2</sub> technologies; they all need the knowledge of the interfacial properties. However, experimental interfacial tension data is not always available, especially near the critical region or when dealing with mixtures [Rolo *et al.*, 2002]. Consequently, there is a clear need for the development of reliable predictive tools [Chapman, 1998]. A prediction of interfacial tension can be achieved by different modeling approaches, from classical to molecular [Carey *et al.*, 1978a;1978b;1980; Chapman, 1988; Queimada *et al.*, 2001; 2003; 2005; 2006]. It has been demonstrated that the choice of a suitable molecular model [Davis and Scriven, 1982] and the use of molecular modeling tools, can accurately represent real systems taking into account inter and intra-molecular forces, providing microscopic insights into the macroscopic phenomena. In addition, an advantage of using a molecular-based approach versus macroscopic approaches is that the model and parameters can be used to extend calculations for the same compounds at different thermodynamic conditions, and for other similar compounds, making these methods transferable and predictive [Cornelisse *et al.*, 1993; 1996; Miqueu, 2001; Vilaseca *et al.*, 2010; Vilaseca and Vega, 2011; 2012] compared to more traditional methods. Hence, given their importance, reliable predictive methods are needed.

A very successful molecular approach to calculate thermodynamic properties is the Statistical Associating Fluid Theory (SAFT) [Chapman *et al.*, 1988], which is a modeling approach rather than an equation. SAFT describes the free energy of the system as the summation of different microscopic contributions, including a reference term (usually considering the segments forming a chain), a chain term (which takes into account the molecular shape)

and an association term (which takes into account the hydrogen bonding formation and other specific interactions) [Blas and Vega, 1997; 1998]. In the original equation, the reference fluid was a hard-sphere system and a mean-field perturbation term was added to take into account the effect of weaker attractive intermolecular forces, like dispersion and induction; in contrast, when a Lennard-Jones term or a square-well term are considered as the reference fluid, such as in the soft-SAFT and SAFT-VR versions, respectively, the same reference term takes into account the attractive and repulsive interactions.

This PhD Thesis is devoted to the modeling of relevant fluids using the Density Gradient Theory (DGT) proposed by Johannes Diderik van der Waals [1894], and modified by several authors [Cahn and Hilliard, 1958; Bongiorno and Davis, 1975; Carey *et al.*, 1978a;1978b;1980; Cornelisse *et al.*, 1993] combined with a molecular-based equation of state (soft-SAFT), developed by Vega and co-workers [Blas and Vega, 1997;1998; Pàmies and Vega, 2001; Llovel *et al.*, 2004] in order to simultaneously predict the phase equilibria and the interfacial behavior of industrial relevant fluids and their mixtures. The main objective of the present PhD thesis is to perform a systematic application of the crossover soft-SAFT equation [Blas and Vega, 1997; Llovel *et al.*, 2004] coupled with DGT [van der Waals, 1894] for the quantitative prediction of several industrial systems, advancing a step forward into applying modeling tools with physical insight for engineering purposes. Soft-SAFT is implemented through a computer code developed in the research group in which this thesis work has been developed, and conveniently modified, to take into account new properties and systems.

The use of soft-SAFT requires the adoption of a model for each system for which molecular parameters are obtained by fitting to vapor-liquid equilibria data, when available. In order to obtain a reliable molecular model, parameters should have values with physical meaning, i.e.  $\nu$  is related to the volume occupied by the groups making-up the molecules,  $\epsilon$  is related to their energy of interaction and  $m$  to the chain length, etc.; hence, their values should be of the order of what is known by experimental or simulation techniques [Pàmies and Vega, 2001; Duque and Vega, 2004; Duque *et al.*, 2004; Mejía *et al.*, 2005; Mejía and Vega, 2006]. For instance, in previous

works it has been observed that for regular chemical families, such as n-alkanes, light alkanols or ionic liquids the molecular parameters of soft-SAFT correlate with the molecular weight of the compounds [Pàmies and Vega, 2001]. These correlations allow us to obtain the behavior of heavier compounds of the series [Pàmies, 2003] not included in the fitting procedure, as well as the behavior of mixtures formed by these compounds. In this work the same tendency is searched for the influence parameter in the case of interfacial properties [Pàmies, 2003, Vilaseca *et al.*, 2010; Vilaseca and Vega, 2011; 2012].

Specific objectives of this work include:

- Validation of the theory and its approximations with molecular simulations.
- Proposal of molecular models for the different inorganic compounds as well as organic, to follow with the optimization of their molecular parameters.
- Calculation of the phase equilibrium properties with the optimized molecular parameters of the soft-SAFT equation.
- Optimization of the influence parameter with the soft-SAFT equation in combination with DGT by fitting the model to the available interfacial properties data.
- Calculation of the interfacial tension with the obtained influence parameter and validation of the model by comparing the results obtained with the experimental or simulation interfacial tension data.
- Search for trends in the values of the influence parameter for different families, in order to make the model more predictive.
- Prediction of the phase and interfacial properties for associating and nonassociating mixtures of industrial interest.
- Application of the tools to the description of the critical and surface properties of ionic liquids.

Using soft-SAFT combined with DGT, selected associating and nonassociating fluids and mixtures of industrial interest were modeled. A throughout study of properties of ionic liquids at the interface and their mixtures is presented in detail here. We provide accurate predictions of interfacial properties far from and close to the critical region, advancing a step forward the existing works in

## *Introduction*

the literature [Cornelisse *et al.*, 1993;1996; Coutinho and collaborators, 2008; Enders and collaborators, 2000; 2002; 2005; 2008; 2010; Miqueu *et al.*, 2000; 2003; Pàmies, 2003] that employed a DGT approach with classical equations, in which the description of interfacial tensions near the critical point is rather poor as a consequence of the classical formulation of the chosen EoS. In addition, we search for trends to make the model as robust and predictive as possible.

## 1.2. Organization of this Thesis

A description of the content of each chapter is presented next, guiding the reader through the whole document.

In chapter 2, a brief historical review of interfacial properties is presented, starting from the first approaches concerning capillarity phenomena, to theories proposed by van der Waals at the end of the 19<sup>th</sup> century, rediscovered and improved by Cahn and Hilliard in the 20<sup>th</sup> century. The classical and the molecular theories are presented to walk through the main contributions to the field of thermophysical properties with particular emphasis on interfacial properties.

In chapter 3, a general description of the theories and the tools used in this work are given. The soft-SAFT EoS and the DGT are presented in detail, as they are chosen in this PhD Thesis as the main tools to develop a predictive model for the description of interfacial properties of some relevant fluids. Details on the implementation of these methods to the systems of interest are also given in this chapter.

Chapter 4 provides the results obtained through the implementation of the methodology explained in the previous chapter. It presents modeling results concerning the phase equilibria and interfacial behavior of the selected compounds and their mixtures as compared to simulation and experimental data. In particular, the systems that have been studied in this thesis are: Lennard-Jones chain-like fluids, n-alkanes, 1-alkanols, nitriles, refrigerants and inorganic molecules -including water, ionic liquids, carbon dioxide and ammonia-, among others. The last section of the chapter is devoted to the study in detail of the surface and critical properties of selected ionic liquids by a combination of soft-SAFT and DFT.

In chapter 5, a summary of the work is given with main conclusions; the future work is also outlined here.

## 1.3. References

- Blas, F.J.; Vega, L.F. *Mol. Phys.* **92**, 135 (1997).
- Blas, F.J.; Vega, L.F. *Ind. Eng. Chem. Res.* **37**, 660 (1998).
- Bongiorno, V.; Davis, H.T. *Phys.Rev. A* **12**, 2213 (1975).
- Cahn, J.W.; Hilliard, J.E. *J. Chem. Phys.* **28**, 258 (1958).
- Carey, B.S.; Scriven, L.E.; Davis, H.T. *AIChE J.* **24**, 1076 (1978)a.
- Carey, B.S.; Scriven, L.E.; Davis, H.T. *J. Chem. Phys.* **69**, 5040 (1978)b.
- Carey, B.S.; Scriven, L. E.; Davis, H.T. *AIChE J.* **26**, 705 (1980).
- Chapman, W.G. *PhD Thesis*, Cornell University, Ithaca, NY, USA, 1988.
- Cornelisse, P.M.W.; Peters, C.J.; de Swaan Arons, J. *Fluid Phase Equilib.* **82**,109 (1993).
- Cornelisse, P.M.W.; Peters, C.J.; de Swaan Arons, J. *Fluid Phase Equilib.* **117**, 312 (1996).
- Cornelisse, P.M.W. *Ph.D. Thesis*, Delft University of Technology, Netherlands,1997.
- Davis, H.; Scriven, L.E. *T. Adv. Chem. Phys.* **49** , 357 (1982).
- Duque, D.; Vega, L.F. *J. Chem. Phys.* **121**, 17 (2004).
- Duque, D.; Pàmies, J.C.; Vega, L.F. *J. Chem. Phys.* **121**, 11395 (2004).
- Enders S; Kahl, H.; Winkelmann, J. *Fluid Phase Equilib.* **228-229**, 511(2005).
- Kahl, H.; Enders, S. *Fluid Phase Equilib.* **172**, 27 (2000).
- Kahl, H.; Enders, S. *Phys. Chem.Phys.* **4**, 931 (2002).
- Kahl, H.; Enders S. *Fluid Phase Equilib.* **263**, 160 (2008).
- Llovell,F.; Pàmies, J.C.; Vega, L.F. *J. Chem. Phys.* **121**, 21 (2004).
- Mejía, A.; Pàmies, J.C.; Duque, D.; Segura, H.; Vega, L.F. *J. Chem. Phys.* **123**, 034505.1 (2005).
- Mejía, A.; Vega, L.F. *J. Chem. Phys.* **124**, 244505 (2006).

- Miqueu, C. *PhD Thesis*, Université de Pau et des Pays de l'Adour, France. 2001.
- Miqueu, C.; Broseta, D.; Satherley, J.; Mendiboure, B.; Lachaise, J.; Graciaa, A. *Fluid Phase Equilib.* **172**, 169 (2000).
- Miqueu, C.; Mendiboure, B.; Graciaa, A.; Lachaise, J. *Fluid Phase Equilib.* **207**, 225 (2003).
- Niño Amezquita, O.G.; Enders, S.; Jaeger, P.T.; Eggers R. *Ind. Eng. Chem.Res.* **49**, 592 (2010).
- Niño Amezquita, O.G.; Enders, S.; Jaeger, P.T.; Eggers R. *J. Supercrit. Fluids* **55**, 724 (2010).
- Oliveira, M.B.; Marrucho, I. M.; Coutinho, J.A.P.; Queimada, A.J. *Fluid Phase Equilib.* **267**, 93 (2008).
- Pàmies, J.C.; Vega, L. F. *Ind. Eng. Chem. Res.* **40**, 2532 (2001).
- Pàmies, J.C. *Ph.D. Thesis*, Universitat Rovira i Virgili, Tarragona, 2003.
- Queimada, A. J.; Marrucho, I. M.; Coutinho, J. A. P. *Fluid Phase Equilib.*, **183-184**, 229 (2001).
- Queimada, A. J.; Stenby, E.H.; Marrucho, I. M.; Coutinho, J.A.P. *Fluid Phase Equilib.*, **212**, 303 (2003).
- Queimada, A. J.; Marrucho, I. M.; Coutinho, J.A.P.; Stenby, E.H. *Int. J. of Thermophys.* **26**, 47 (2005)
- Queimada, A.J.; Rolo, L.I.; Caço, A.I.; Marrucho, I.M.; Stenby, E.H. Coutinho, J.A.P. *Fuel* **85**, 874 (2006).
- Rolo, L.I.; Caço, A.I.; Queimada, A.J.;Marrucho, I.M.; Coutinho, J.A.P. *J. Chem. Eng. Data.* **47**, 1442 (2002).
- van der Waals, J. D. *Z. Phys. Chem.* **13**, 657 (1894).
- Vilaseca, O.; Llovell, F.; Yustos, J.; Marcos, R.M.; Vega, L.F. *J. Supercrit. Fluids* **55**, 755 (2010).
- Vilaseca, O.; Vega, L.F. *Fluid Phase Equilib.* **306**, 4 (2011).
- Vilaseca, O.; Vega, L.F. *submitted* [2012].



# 2. Interfacial properties

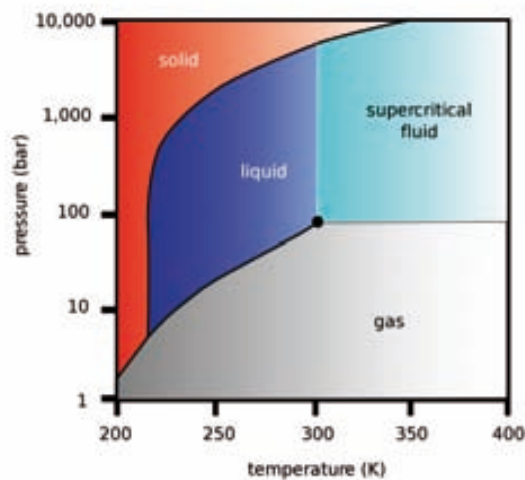
*“The nature is really comfortable and consistent with itself”*

*Sir Isaac Newton (1642-1727); English Scientist*

## 2.1 Introduction

Immense efforts have been made over history to discern the conduct of matter under different conditions of pressure, temperature, size and shape. The three states of matter, solid, liquid and vapor, have led to different theories about the matter's behavior and its interaction with the universe from both, macroscopic and microscopic points of view.

Physics provides different approaches and tools to comprehend the key properties that govern the nature of matter, especially in the field of thermodynamics, when a breakthrough happened introducing the concept of the energy instead of the mechanical arguments, to figure out some of the key aspects of soft-matter. One of them is the *interfacial tension*, which was not completely understood by mechanical arguments until a thermodynamic interpretation was given at the end of the 19<sup>th</sup> century [van der Waals, 1873; 1894].



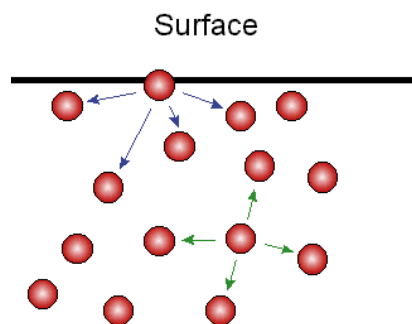
**Figure 2.1:** Thermodynamic magnitudes determining the states of carbon dioxide.

<http://www.nextbigfuture.com>

The interfacial tension can be defined, in general, as the force required bringing one molecule from the bulk liquid to the surface of a liquid; conversely, it can also be defined as the reversible stored energy resulting from an increase of one unit in the surface area, expressed by force per unit

length [N/m] or by work per area [J/m<sup>2</sup>]. From a thermodynamic point of view, the interfacial tension can be considered as the property that makes liquids condensed materials, and also, as the origin of the vapor-liquid surface separation, the *interface*, where differential characteristics between liquid and gases appear.

The molecular origin of this property is sketched in Figure 2.2., in which molecules at the surface experience a net attraction to the rest of the fluid because of the lower density of the molecules on the air side of the interface, while molecules in the bulk are subjected to uniform cohesive forces in all directions, and experience no net attraction; consequently, the surface of a liquid tends to contract while in the bulk the intermolecular attractions are responsible of the spherical shape of drops. In fact, it is the interplay between bulk and interface contributions to the *free energy* of a system which leads to the broad variety of what it is known as interfacial phenomena [Pàmies, 2003].



**Figure 2.2:** Interaction forces acting on one molecule on the surface and on the bulk.

<http://www.mikeblaber.org/oldwine/chm1045/notes/Forces/Liquids/tension.gif>

In our day to day life there are present plenty of phenomena in which the interfacial tension plays an important role. The movement of the blood on our tiny vessels (*capillaries*), the water transported by plants from roots to leaves, the air-liquid interface in our lungs, the formation of bubbles, the stability of colloids in emulsions (ink, mayonnaise, milk, creams, oils or paintings), the molecular mechanism of lipid bilayers membranes, the oil spilt out on the seas, the formation of tears of wine, surfactants (which are molecules which high affinity for the interfaces) such as soap or oil, the water rising or the

mercury falling in a capillary tube, to mention a few examples, all depend on the type and magnitude of the relevant *molecular interactions* that occur at the interfaces in these inhomogeneous systems.



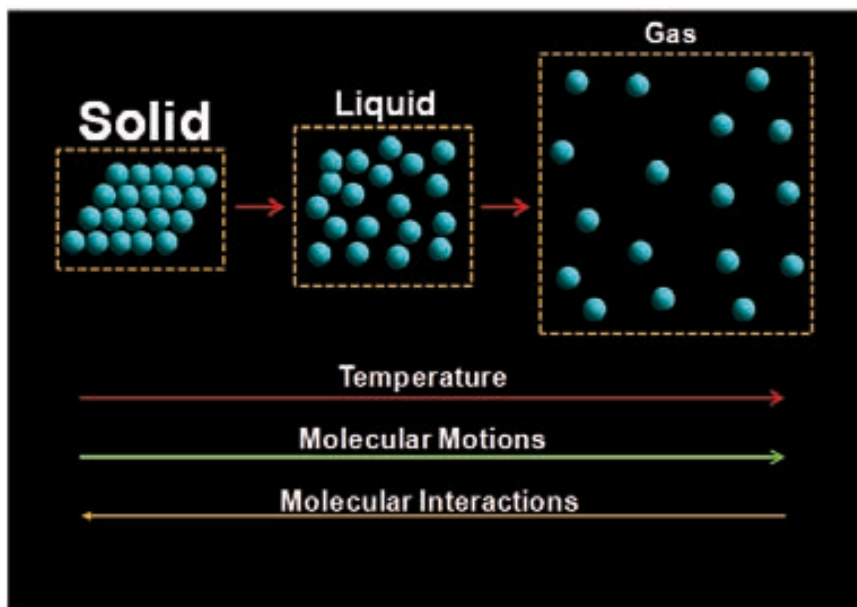
**Figure 2.3:** Interfacial tension effects.

[wwwswt.informatik.uni-rostock.de](http://wwwswt.informatik.uni-rostock.de); [www.darkroastedblend.com/](http://www.darkroastedblend.com/); [th03.deviantart.net/](http://th03.deviantart.net/)

Also, the interfacial phenomena is crucial in many industrial and environmental processes, for example, in surfactants production, in food industry, pharmaceutical or chemical products involving emulsion or suspension processes, polymerization processes, heterogeneous catalysis, the development of detergents, liquid/liquid extraction, soil vapor extraction, soil remediation, enhanced oil recovery or even refrigerated nuclear reactors. All require a good knowledge of the liquid-vapor coexistence behavior for the understanding and control of all these processes. As a particular example, in fluids for petroleum industry, the optimization of the nonthermal secondary and tertiary oil extraction from depleted reservoirs by miscible displacement needs reliable interfacial tension predictions for n-alkanes mixtures pressurized by a soluble gas (methane, nitrogen or, most commonly, carbon dioxide) [Islam, 1999].

## 2.2 Molecular interpretation of interfacial properties

As observed in Figure 2.4, there is an intimate relation between the temperature, the volume and the pressure with the *molecular state* of a given material. If we heat up a bulk material in its solid state at a constant pressure, the molecular motions will raise up the system until reaching the liquid state, so the molecular interactions due to the increased intermolecular distance between molecules will decrease, as the molecules are far apart. If we continue heating up, the gas state will be reached and, consequently, the molecular motion will boost considerably compared to those in the liquid. This thermal expansion increases the volume occupied by the molecules, hence reducing the density of the system, so the molecules in the gas state are more dispersed into the space; it is obvious that the molecules will have a lower cohesion in the gas state than in the liquid or in the solid state. In the same way, if the molecules are more dispersed in the space, the molecular interactions will considerably diminish so the value of the interfacial tension will do so.



**Figure 2.4:** Thermodynamic factors determining the magnitude of the interfacial tension value.

Another factor that determines the magnitude of the interfacial tension value is the type of molecular interactions within the fluid, i.e. van der Waals interactions, hydrogen bonds, ionic interactions, etc. For example, for the same chain length, an alcohol (able to form hydrogen bonds) will have a higher surface tension than the corresponding n-alkane (unable to form hydrogen bonds). The type of atomic bonds also play an important role in the value of the interfacial tension, the metallic compounds have a higher interfacial tension at a given temperature than that of an inorganic compound or an organic compound, respectively. Therefore, at the same thermodynamic conditions, mercury will have a higher interfacial tension than sodium chloride or n-pentane.

As stated, in this PhD thesis we have decided to account on all these molecular contributions for the prediction of phase and interface properties by coupling the soft-SAFT Eos [Blas and Vega, 1997] with the DGT [van der Waals, 1894], as both of them are molecular in nature. Within the soft-SAFT approach almost all the inter- and intra- molecular interactions can be described by different molecular contributions to the Helmholtz energy, providing accurate descriptions of bulk phase equilibria, as explained in the next chapter, while with the DGT the gradient of the density at the interface between the two phases is explicitly considered. Hence, the value of the interfacial tension can be calculated taking into account all the thermodynamic changes and interactions between molecules.

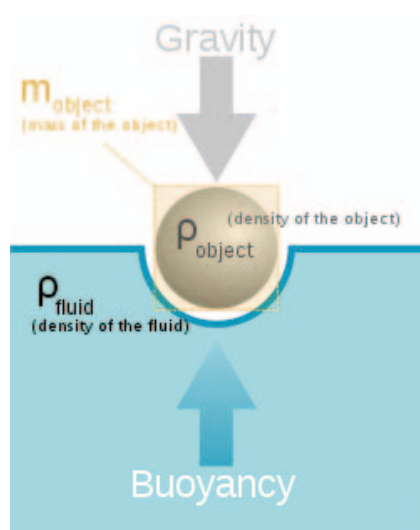
In the following section a historical review of the most known approaches and theories related to the interfacial phenomena are presented, while a summary of the SAFT and the DGT approaches is given in more detail in Chapter 3 of this Dissertation.

## 2.3 Historical Review on Theories for Interfacial Properties

In this section, a brief summary on the development of the capillarity phenomena and the interfacial tension is provided. As most of the ancient scientific discoveries, it started by the simple observation of the nature. The first author reporting information of various organic molecules affecting the surface tension of water was Pliny the Elder (23-79 AD) [Bush, 2004] who wrote about spear-fishermen pouring oil on water to increase their ability to see the bottom. This is the first *natural phenomena* related to interfacial tension described in literature. He also noted that the absence of capillary waves in the wake of ships was due to the ships stirring up the biomaterial present into the sea, which acts as a surfactant.

Archimedes (287-212 BC) was the first who seriously studied the behavior of fluids with his well known principle of flotation:

*“An object, when deposited into a bath of liquid, displaces a volume of liquid having mass equal to the effective mass of the object.”*

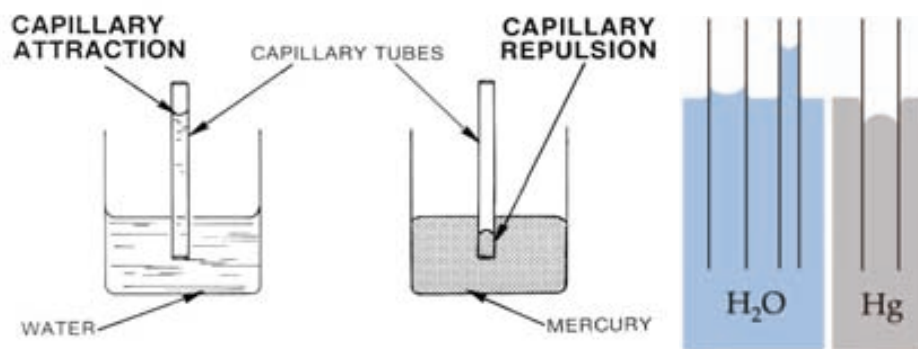


**Figure 2.5:** Sketch of Archimedes's principle.

[www.wikipedia.org](http://www.wikipedia.org)

The principle, unfortunately, does not take into account the effect of the surface tension associated with wetting; however, it establishes the principles of *hydrostatics* besides describing how the solids act on the surface of a fluid.

The definition given by Encyclopaedia Britannica refers to the concept of capillarity as: “the result of surface, or interfacial, forces”. The rise of water in a thin tube inserted in water is caused by forces of attraction between the molecules of water and the glass walls and among the molecules of water themselves. These attractive forces just balance the force of gravity of the column of water that has risen to a characteristic height. The narrower the bore of the capillary tube, the higher the water rises. Mercury, conversely, is depressed to a greater degree, the narrower the bore. The liquid climbs until the adhesive and cohesive forces are balanced by the force of gravity. This fact can be stated by submerging some capillary glasses into water and mercury as in Figure 2.6. The rise of a liquid in capillarity tube is a macroscopical evidence of the existence of attractive forces between the ultimate particles of matter.



**Figure 2.6:** Sketch of capillarity effects. [www.wikipedia.org](http://www.wikipedia.org)

As already mentioned, the first steps towards understanding the interfacial phenomena were done by observing the natural facts that occur into our day to day life. Leonardo da Vinci (1452-1519) was the first scientist to apply the Latin word *capillaris* to the tiny blood vessels, and there were the physicists as Jurin, Segner or Young who first studied the capillarity effects from a scientific point of view.

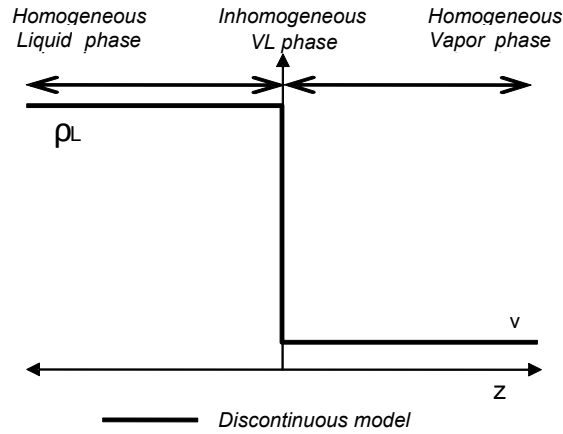


### **2.3.1 The interfacial tension concept until Laplace**

Over the last centuries several attempts have been made to describe the behavior of the optical and capillarity effects from direct observation of nature. The main interest on interfacial properties at that time came because of the apparent contradiction of the capillarity phenomena with the gravitational laws proposed by Newton. This contradiction was clarified by Francis Hauksbee [1706; 1709], (Newton's assistant in The Royal Society), who postulated the existence of short range attractive forces between the liquid layers in contact with a solid. Afterwards, James Jurin [1718; 1719] tested this theory by way of experiments with water and mercury, where the liquid-liquid and solid-liquid attractions were described. The next step on the understanding of interfacial phenomena was made by Clariout [1743], through the observation of tiny water drops. He realized that the dimension of the drops was small enough not to be affected by the gravitational forces; nevertheless, his contribution to the science of capillarity cannot be considered important [Bikerman, 1978].

In the middle of the 18<sup>th</sup> century, J. A. Segner synthesized all these phenomena under the work *Interfacial Tension Phenomena* [1752], providing a comprehensive review on the topic. He stated that in the absence of gravitation every drop would be a sphere. Nevertheless, it was not until the beginning of the 19<sup>th</sup> century when the cohesive forces theories appeared, giving a new focus to the problem. The first approximations about the density variation  $\rho(z)$  were made separately by Young [1805] in London, and Pierre Simon Laplace [1805] in Paris; giving a mechanical explanation to the capillarity phenomena by proposing a discontinuous model. Although during the first half of the century, the problems involving cohesive forces were worked out, some other questions remained unsolved, like the static treatment given to the fluids, which are not static at all.

They proposed a step shift between the liquid and the gas state, as shown in Figure 2.7; obviously, as pointed out years later this oversimplified theory did not describe the correct phase transition of the fluids.



**Figure 2.7:** Discontinuous approach for the density variation  $\rho(z)$ .

However, an important principle was determined by Laplace and Young using a discontinuous model that states that the required work per unit area ( $H$ ) to separate two liquids at a distance equal or larger than  $d$  can be defined as:

$$H = \int_0^d K(r) dr = -\pi N_{av}^2 \rho^2 \int_0^d \varphi_{at}(r) r^3 dr \quad (2.1)$$

From this equation Laplace established the connection between attractive forces and the interfacial tension  $H=2\gamma$ , and also deduced the relation between the internal and the external pressure ( $P_{int}$  and  $P_{ext}$ ) of a drop of radius  $R$ , by the following relation:

$$P_{int} - P_{ext} = \frac{H}{R} = \frac{2\gamma}{R} \quad (2.2)$$

## 2.3.2 From the mechanical to the thermodynamic description

It was in 1869, when Athanase Dupré (Paris) recalculated the attractive forces postulated by Laplace. He reformulated the forces balance quantifying the energy necessary to remove one by one each particle existing in the surface of a liquid. This counter example was useful to reveal that Laplace's discontinuous model was incorrect. Later on, James C. Maxwell [1876] revisited the Dupré's work to solve the unbalanced forces difficulty, but he was unsuccessful. After all, Josiah Willard Gibbs in New Haven [1875-1878] gave a thermodynamic interpretation based on the first and the second thermodynamics law, but still using a discontinuous treatment model for  $\rho(z)$ . If we have a surface which hypothetically divides the two homogeneous phases ( $\alpha$  and  $\beta$ ) of density  $\rho$  and the arbitrary chosen position is  $(z_0)$ , we can define the interfacial behavior as:

$$\int_{-\infty}^{z_0} [\rho(z) - \rho^\alpha] dz + \int_{z_0}^{\infty} [\rho(z) - \rho^\beta] dz = 0 \quad (2.3)$$

These ideas were followed in the academic community until 1888, when Karl Fuchs in Bratislava [1888], Lord Rayleigh in Terling [1892] and Johannes Diderik van der Waals in Amsterdam [1894], independently proposed the description of the concentration variation within the interfacial region, suggesting a continuous model for  $\rho(z)$ . It was van der Waals the only one who obtained this model without mechanical arguments, relating the interfacial tension to the Helmholtz free energy density and not to the internal energy as Fuchs and Rayleigh postulated. In 1894, van der Waals proposed what it is known as the Density Gradient Theory (DGT), which leads to a general expression for the Helmholtz energy of an inhomogeneous system in an elegant and simple way. The theory remained forgotten during more than half a century until it was re-discovered by Cahn and Hilliard [1958] and Carey *et al.*, [1978a; 1978b; 1980], who made it friendly for implementations with other models, so as to predict the interfacial tensions of pure fluids and mixtures for practical applications.

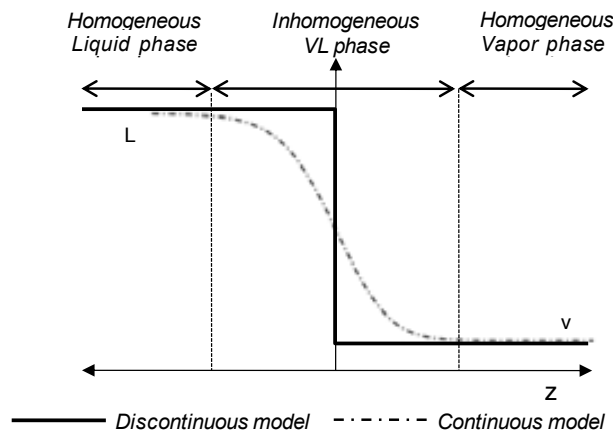
In its original form, the van der Waals's development could be expressed as:

$$\frac{A}{V}(z) = a(z) = a_0 [\rho(z)] + \frac{1}{2}c \left[ \frac{d\rho(z)}{dz} \right]^2 \quad (2.4)$$

where  $a_0$  is the Helmholtz's energy density of a homogenous fluid with a constant concentration and  $c$  is a positive constant, known as the influence parameter, corresponding to the 4<sup>th</sup> moment of the intermolecular potential  $\varphi_{at}$ :

$$c = \frac{2\pi}{3} \int r^4 \varphi_{at}(r) dr \quad (2.5)$$

Due to its formulation and the shape of equation (2.4), the theory is known as the Density Gradient Theory (DGT). DGT was not appreciated in the scientific community until ten years later when Kamerlingh Onnes presented the experimental results obtained by E.C.Vries (Onnes's assistant), about the determination of the interfacial tension of ether. He experimentally confirmed that near the critical point, the interfacial tension tends tangentially to zero, according to the continuous model proposed by van der Waals (vdW). The great advantage of this model (which caused controversy in the scientific community for years) is the ability to describe the inhomogeneous behavior of the fluids by means of a model hypothetically continuous.



**Figure 2.8:** Functional approaches for the density variation  $\rho(z)$ .

As can be observed in Figure 2.8 the two treatments lead to very different phase transition profiles: while the discontinuous model provides a step change between liquid and gas phases, the continuous model results in a smooth profile to describe (under a realistic approach) the continuity of the gas and liquid states.

As a curiosity, other attempts of Fowler [1937], Yvon [1948]<sup>1</sup> or some considerations about the capillarity phenomena interpretation coming from great known scientists as Einstein [1901], Schrödinger or Bohr, were given without specifying any contribution to the model.

<sup>1</sup> Yvon proposed a model evaluating the density gradients at different heights of the interface, which was never finished.

## 2.4 Recent approaches to calculate the interfacial properties<sup>1</sup>

Several attempts have been made in the last century to relate the interfacial tension of pure fluids to other physical properties such as density, refractive index, critical constants, compressibility and speed of sound, from both, theoretical-based or empirical approaches. However, most of these theories have parameters with little physical meaning, and, hence, their predictive capability and applicability to mixtures is very limited.

### 2.4.1 The Parachor

In the petrochemical industry, the most common method used to determine the interfacial tension of pure fluids and mixtures is the Parachor [Macleod, 1923; Sugden, 1924; Quayle, 1953]. It consists on empirically relating the interfacial tension to the difference between phase densities by means of a temperature-independent parameter, as it can be observed in equation 2.6.

The first relation proposed by Macleod [1923] was:

$$\gamma = C (\rho_L - \rho_V)^4 \quad (2.6)$$

where  $\gamma$  is the interfacial tension,  $\rho_L$  et  $\rho_V$  are the liquid and the vapor densities, respectively, and C is a constant.

Sugden proposed in 1923 an analogous relation introducing the chemical composition to the equation:

$$P_a = \frac{MW}{\rho_L - \rho_V} \gamma^{\frac{1}{4}} \quad (2.7)$$

---

<sup>1</sup> Part of this section has been published in Vilaseca, O. and Vega, L.F. Direct calculation of interfacial properties of fluids close to the critical region by a molecular-based equation of state. *Fluid Phase Equilib.* **2011**, 306, 4-14.

where MW is the molar weight and  $P_a$  is the Parachor. The word “Parachor” comes from the Greek “para” means *aside* and “chor” means *space*, which in thermodynamics, is normally related to the volume. As deduced from equation (2.7) each compound has a characteristic parachor value.

A step forward was made in the 40's by Weinaug and Katz [1943], when they proposed a linear combination of the pure compounds equations, weighted with the molar fractions, to calculate mixtures of constituents, especially applicable in the petrochemical industry.

$$\gamma^{\frac{1}{n}} = \sum_{i=1}^N P_{ai} \left( x_i \frac{\rho_L}{MW_L} - y_i \frac{\rho_V}{MW_V} \right) \quad (2.8)$$

As described, the Parachor method is quite simple but it strongly depends on the chosen scaling exponent [Miqueu, 2001; Galliero, 2010]. Very recently, this simple principle has been used to the study of simple molecules [Galliero, 2010].

## 2.4.2 The corresponding states

Another frequently used method for the estimation of interfacial tensions is the corresponding states principle [Guggenheim, 1945; Zuo, 1997]. This is one the greatest advances that the van der Waals' equation of state indirectly introduced in the physics of the liquid and vapor states.

Pitzer was the first in stating that this principle was able to accurately describe the properties of some noble gases such as argon, krypton and xenon [Pitzer, 1938]. Guggenheim used it to calculate the thermodynamic properties of methane, nitrogen, oxygen and carbon monoxide [Guggenheim, 1945].

The temperature dependence of the surface tension can be described by means of this theory following the expression:

$$\gamma = \gamma_0 \left( 1 - \frac{T}{T_c} \right)^{1+r} \quad (2.9)$$

where  $\gamma$  is the surface tension and  $T$  represents the temperature,  $r$  is a constant; van der Waals suggested a value of  $r=0.234$  and Guggenheim

proposed a value of  $r = 2/9$ , which adequately represents the value of some simple compounds. We can read that the surface of a liquid decreases with temperature and is equal to zero at the critical point.

An approach based on the corresponding states principle may provide very accurate predictions, but its predictive power strongly depends on the reference fluid chosen and the empirical equations used to describe its thermodynamic properties.

A step forward in the method was provided by Queimada *et al.* [2001; 2003; 2005; 2006] as they presented two predictive corresponding states approaches for the surface tension of the n-alkanes, which afforded very accurate results. Very recently, the standard approach has proved to be useful to identify universal behavior of simple fluids and also can be employed as a simple test for surface tension theories based on SAFT-like EoS combined with the DGT [Galliero, 2010].

### 2.4.3 Density Gradient Theory

The Density Gradient Theory (DGT) [van der Waals, 1894; Cahn and Hilliard, 1958] allows relating an equation of state to interfacial properties of a classical fluid system, leading to a general expression for the Helmholtz energy of the total system. In essence, DGT provides a density functional for the local Helmholtz energy density of a fluid system, which consists of a 'homogeneous' term and a 'nonhomogeneous' term. The former is represented by the Helmholtz energy density of a homogeneous fluid, evaluated at a local density in between the bulk densities, while the latter is proportional to the square of the molar density gradient. In their derivation Cahn and Hilliard [1958] assumed that the Helmholtz energy density  $a$  of the inhomogeneous fluid is a function of the mole density and its derivatives with respect to the space coordinates. It was also assumed that the density gradient is small compared to the reciprocal value of the intermolecular distance, thus allowing treating the density and its derivatives as independent variables. They expanded the function  $a$  in a Taylor series about  $a_0(\rho)$ , the Helmholtz energy density of the homogeneous fluid at the local density  $\rho$ , and truncated it after the second order term.



In the absence of an external potential, the expression for the Helmholtz energy of the system  $A$  reads:

$$A = \equiv a_0(\rho, T) + \frac{1}{2} \sum_{i,j} c_{ij} \int d^3r \quad (2.10)$$

where the integration is performed in the entire system volume,  $\rho_n$  is the molar density of component  $i$  and  $j$ . The only quantity required then, is an expression for the coefficient of proportionality that goes prior the square gradient, the influence parameter  $c_{ij}$ , in terms of density and/or temperature. The influence parameter was originally related to the mean square range of the direct correlation function  $C_{ij,0}$  of a homogeneous fluid:

$$c_{ij}(\rho, T) = \frac{T}{6} \int r^2 C_{ij,0}(r, \rho) d^3r \quad (2.11)$$

Details on the derivation of this expression are given elsewhere [Bongiorno and Davis, 1975; Bongiorno *et al.*, 1976; Cornelisse *et al.*, 1993;1996; Cornelisse, 1997; Yang, 1975; Yang *et al.*, 1976].

Because no direct correlation functions are available for most systems of practical interest, several estimation methods have been used [Cornelisse *et al.*, 1997]. For instance, Carey *et al.*, 1978a;1978b;1980] connected this parameter to those from the Peng-Robinson EoS, arguing that the ratio  $c/ab^{(2/3)}$  for real nonpolar fluids might be a slowly varying function of temperature and density, while other authors neglected the dependence on thermodynamic properties and treated  $c_{ij}$  as a constant parameter to be fitted to experimental data [Pàmies, 2003; Vilaseca and Vega, 2011].

An attractive feature of DGT is that it does not prescribe the particular theory from which to obtain an expression to define the 'homogeneous' term in the free energy density. The definition of this 'homogeneous' free energy density leads to a unique definition of the Helmholtz energy of the inhomogeneous system. Consequently this might be obtained from an expression based on statistical mechanics, but also from semi-empirical equations of state or from equations without molecular basis. The accuracy of the approach will then rely on the accuracy of the chosen equation.

## 2.4.4 Density Functional Approaches

An alternative approach for the theoretical study of inhomogeneous fluid systems is the Density Functional Theory (DFT) [Chapman, 1988; Evans, 1992]. The DFT formalism offers, in principle, an entirely predictive approach with no adjustable parameters. DFT methods are based on the construction of a free-energy functional from which the thermodynamic properties of the inhomogeneous system can be calculated. DFT methodologies express the thermodynamic properties of the system as a functional of the single particle density, and the interfacial density profile is obtained by numerically solving the condition that the functional is a minimum at equilibria.

$$\frac{\partial \Omega [\{\rho_m(r)\}]}{\partial \rho_i(r)} = \frac{\delta A [\{\rho_m(r)\}]}{\delta \rho_i(r)} - \mu_i = 0 \quad \forall i \quad (2.12)$$

These  $n$  Euler-Lagrange equations are equivalent to requiring that the Helmholtz free-energy functional be a minimum subject to a constraint of constant number of particles; the undetermined multipliers correspond to the chemical potentials of each component  $\mu_i$  in the bulk coexisting phases.

In fact, DFT is a particular case of the DFT approach. In the case of DFT, the free-energy functional  $A [\{\rho_m(r)\}] = A [\rho_1(r); \rho_2(r) \dots \rho_n(r)]$  (to denote the functional dependency of  $A$  on all the densities  $\rho_m(r)$  at each point  $r$ ) is always of the square-gradient form and a unique description is obtained for a given equation of state and values of the influence parameters. With a DFT treatment the choice of functional affects the representation of the interfacial properties depending on the approximations that are employed. Usually, the functional is constructed by partitioning the free energy density into a reference term (which incorporates all of the short-range interactions and is treated locally) and an attractive perturbation (which incorporates the long-range dispersion interactions).

Chapman and co-workers first suggested the use of Wertheim's thermodynamic perturbation theory (TPT) within a DFT approach [Chapman, 1988; Segura *et al.*, 1990]. They proposed a perturbation DFT for inhomogeneous associating fluids. In the same way, the SAFT-VR and PC-

SAFT equations have also been coupled with a DFT approach [Jackson and collaborators 2001; 2002; 2010, Gross 2009].

As mentioned, the main advantage of using a SAFT-DFT method versus the other methods is that it does not use any empirical parameter for the prediction of interfacial properties, hence being truly molecular and predictive. However, this may turn out to be a difficulty when predicting interfacial properties of systems for which the free energy functional is not accurately known, losing accuracy versus experimental data. In addition, DFT requires more computational effort than the simple DGT approach.

## **2.4.5 Molecular simulations**

The use of computers for statistical mechanics calculations started and was considerably extended during the Second World War as part of the Manhattan Project, with the development of what Metropolis called the Monte Carlo method. Molecular Dynamics emerged in the 50s and the 60s, and it was the other way to develop computer assisted simulations for the prediction of thermodynamic properties, using the concepts of statistical mechanics. After this, several authors has developed different techniques to study by computer simulation phase and interfacial properties being the first one the group led by Sir Rowlinson [Chapela *et al.*,1975,1977].

Molecular Simulations provide an additional and complementary tool for the calculation of interfacial properties, but the added complications due to the appropriate treatment of long-range contributions [Duque and Vega, 2004; Blas *et al.*, 2008] and the intensive use of computer time make nowadays difficult the use of molecular simulations for the extensive computation of interfacial properties of real complex fluids, as those needed for engineering calculations. However, they can be used as an excellent tool to check the accuracy of the approximations made in the theory before applying the model to experimental systems. In this sense, Vega and co-workers [2004a; 2004b; 2005; 2006] have performed molecular dynamic simulations of Lennard-Jones (LJ) chains and mixtures to test the accuracy of the soft-SAFT equation coupled with DGT for these systems. Their work shows that the theory is very

accurate for both, phase equilibria and interfacial properties, including interfacial tensions and density profiles, to model pure fluids and binary mixtures and, hence, it can be applied to experimental systems with confidence. In a recent work, Müller and Mejía [2009] have presented MD simulations of asymmetric mixtures of alkanes and have compared these results with predictions obtained with the DGT coupled with the SAFT version of Huang and Radosz [1990a,b], as well as with available experimental results. They concluded that both, the theoretical approach and MD simulations, are able to describe the bulk phase equilibria and its interfacial tension with a relatively low absolute average deviation values with respect to the experimental data. The approach allows to describing other interfacial properties such as concentration profiles along the interfacial region, surface activity (or absolute adsorption), relative Gibbs adsorption isotherms for mixtures or density profiles.

## 2.5 References

- Bikerman, J.J. *Arch. Hist. Exact. Sci.* **18**, 103 (1978).
- Blas, F.J.; Martín del Río, E.; de Miguel, E.; Jackson, G. *Molec. Phys.* **99**, 1581 (2001).
- Blas, F.J.; MacDowell, L.G.; de Miguel, E.; Jackson, G. *J.Chem.Phys*, **129**, 144073 (2008).
- Blas, F.J.; Vega, L.F. *Mol. Phys.* **92**, 135 (1997).
- Bongiorno, V.; Davis, H.T. *Phys.Rev. A* **12**, 2213 (1975).
- Bongiorno, V. ; Scriven, L.E.; Davis, H.T. *J. Colloid Interface Sci.* **57** ,462 (1976).
- Bush, J.W.M., *Surface tension lectures*. MIT (2004).
- Cahn, J.W.; Hilliard, J.E. *J. Chem. Phys.* **28**, 258 (1958).
- Carey, B.S.; Striven, L.E.; Davis, H. T. *AIChE J.* **24**, 1076 (1978).
- Carey, B.S.; Striven, L.E.; Davis, H. T. *J. Chem. Phys.* **69**, 5040 (1978).
- Carey, B.S.; Striven, L.E.; Davis, H. T. *AIChE J.* **26**, 705 (1980).
- Chapman, W. G. *PhD Thesis*, Cornell University, Ithaca, NY, USA, 1988.
- Chapela, G.A.; Saville, G.; Rowlinson, J.S. *Faraday Disc. Chem. Soc.*, , **59**, 22 (1975).
- Chapela, G.A.; Saville, G.; Thompson, S.M.; Rowlinson, J.S *J. Chem. Soc., Faraday Trans. 2*, **73**, 1133 (1977).
- Clairaut, A.C. "*Theorie de la Figure de la terre, tirée des principes de l'hydrostatique*" (1743).
- Cornelisse, P.M.W.; Peters, C.J.; de Swaan Arons, J. *Fluid Phase Equilib.* **82**,109 (1993).
- Cornelisse, P.M.W.; Peters, C.J.; de Swaan Arons, J. *Fluid Phase Equilib.* **117**, 312 (1996).
- Cornelisse, P.M.W. *PhD Thesis*, Delft University of Technology, The Netherlands,1997.
- Dupré, A. Gauthier-Villars, Paris, (1869).

- Duque, D.; Vega, L.F. *J. Chem. Phys.* **121**, 17 (2004)a.
- Duque, D.; Pàmies, J.C.; Vega, L.F. *J. Chem. Phys.* **121**, 11395 (2004)b.
- Einstein, A. *Ann. Phys.* **309**, 513(1901).
- Evans, R. *Density Functionals in the Theory of Nonuniform Fluids in Fundamentals of Inhomogeneous* (Dekker, New York, 1992).
- Fowler, R.H. *Proc. Roy. Soc. A.* **159**, 229 (1937).
- Fuchs, K. *Rep. Phys.* **24**, 141(1888).
- Gibbs, J.W. *On the equilibrium of heterogeneous substances.* Trans. Connecticut, Acad. 3, 108, 343 (1875 - 1878). [Reprint of The scientific papers of J. Willard. Gibbs, 1:55 (Dover, New York, 1961)]
- Gloor, G.J.; Blas, F.J; Martín del Río, E.; de Miguel, E.; Jackson, G *Fluid Phase Equilib.* **521**, 194 (2002).
- Gross, J.; *J. Chem. Phys.* **131**, 204705 (2009).
- Guggenheim, E.A. *J. Chem. Phys.* **13**, 253 (1945).
- Hauksbee, F. *Phil. Trans. Roy. Soc.* **25**, 2223 (1706).
- Hauksbee, F. *Phil. Trans. Roy. Soc.* **26**, 258 (1709).
- Huang, S.H. ; Radosz, M. *Ind. Eng. Chem. Res.* **29**, 2284 (1990a).
- Huang, S.H. ; Radosz, M. *Ind. Eng. Chem. Res.* **30**, 1994 (1990)b.
- Islam, M.R. *Energy Sources* **21**, 97 (1999).
- Jurin, J. *Phil. Trans. Roy. Soc.* **355**, 739 (1718).
- Jurin, J. *Phil. Trans. Roy. Soc.* **363**, 1083 (1719).
- Laplace, P.S. *Mécanique céleste.* Supplement to the tenth book in vol.IV. Imprim. Imperiale, Paris (1805).
- Mac Dowell, N.; Llovel, F.; Adjiman, C.S.; Jackson, G.; Galindo, A. *Ind. Eng. Chem. Res.* **49**, 1883 (2010).
- Macleod, D.B. *Trans. Faraday Soc.* **19**, 38 (1923).
- Maxwell, J.C. *Capillary Action.* Encyclopaedia Britannica.(1876).
- Mejía, A.; Pàmies, J.C.; Duque, D.; Segura, H.; Vega, L.F. *J. Chem. Phys.* **123**, 034505.1 (2005).
- Mejía, A.; Vega, L.F. *J. Chem. Phys.* **124**, 244505 (2006).

- Miqueu, C. *PhD Thesis*, Université de Pau et des Pays de l'Adour, France. 2001.
- Müller, E.; Mejía, A. *Fluid Phase Equilibria* **282**, 68 (2009).
- Pàmies, J.C. *Ph. D. Thesis*, Universitat Rovira i Virgili, Tarragona, 2003.
- Pitzer, K. *J. Chem. Phys.* **7**, 583 (1939).
- Quayle, O.R. *Chem. Rev.* **53**, 439 (1953).
- Queimada, A. J.; Marrucho, I.M.; Coutinho, J.A.P. *Fluid Phase Equilib.* **183-184**, 229 (2001).
- Queimada, A.J.; Stenby, E.H.; Marrucho, I.M.; Coutinho, J.A.P. *Fluid Phase Equilib.*, **212**, 303 (2003).
- Queimada, A.J.; Marrucho, I.M.; Coutinho, J.A.P.; Stenby, E.H. *Int. J. of Thermophys.* **26**, 47 (2005)
- Queimada, A.J.; Rolo, L.I.; Caço, A.I.; Marrucho, I.M.; Stenby, E.H. Coutinho, J.A.P. *Fuel* **85**, 874 (2006).
- Rayleigh, Lord *Philos. Mag.* **33**, 209 (1892).
- Segner, J.A. *Commentarii Societ. Regiae Scientiarum Gottingensis* **1**, 301 (1752).
- Segura, C.J.; Chapman, W.G.; Shukla, K.P. *Molec. Phys.* **90**, 759 (1990).
- Sugden, S. *J. Chem. Soc.* **125**, 32 (1924).
- van der Waals, J.D. *Over de Continuïet Van Den Gas- En Vloeïstof-Toestrand (On the Continuity of the Gaseous and Liquid States); Translation by J.S. Rowlinson. PhD thesis, University of Leiden, Netherlands, 1873.*
- van der Waals, J.D. *Z. Phys. Chem.* **13**, 657 (1894).
- Weinaug, C.F.; Katz, D.L. *Ind.Eng.Chem.* **35(2)**, 239 (1943).
- Yang, A. *PhD. Thesis*, Molecular theory of surface tension, Brown University, 1975.
- Yang, A.J.M.; Fleming, P.D.; Gibbs, J.H. *J. Chem. Phys.* **64**, 3732 (1976).
- Young, T. *Philos. Trans. R. Soc.*, **95**, 65 (1805).

## Chapter 2

Yvon, J. *Le problème de la condensation de la tension et du point critique.*  
Colloque de thermodynamique. Int. Union Pure and Applied  
Physics, Brussels, 9 - 15, (1948).

Zuo, Y.-X; Stenby, E.H. *Can. J. Chem. Eng.* **75**, 1130 (1997).

<http://www.nextbigfuture.com>

<http://www.mikeblaber.org/oldwine/chm1045/notes/Forces/Liquids/>

<wwwswt.informatik.uni-rostock.de>

[www.darkroastedblend.com/](http://www.darkroastedblend.com/)

[th03.deviantart.net/](http://th03.deviantart.net/)

[www.wikipedia.org](http://www.wikipedia.org)



# 3. Methodology

*“There are two objectionable types of believers: those who believe the incredible and those who believe that 'belief' must be discarded and replaced by 'the scientific method”*

*Max Born (1882-1970); German Physicist*

## 3.1 Density Gradient Theory<sup>2</sup>

As stated already, van der Waals [van der Waals, 1873] was the first to propose a continuous model for the transition between the liquid and vapor states. He established that there was a continuous function of the pressure and the density, introducing the modern concept of the equation of state (EoS). Van der Waals's EoS included a repulsive contribution to the free energy as a function of the molecular size, and an attractive contribution related to the average of molecular attractions also known as the mean field approximation. This equation was the first cubic equation of state in history; at a temperature and pressure where there are three real density roots, a coexisting vapor-liquid phase must exist, the equilibrium constraint being an equality of the chemical potential in both phases, a concept introduced by Gibbs some years earlier [Gibbs, 1875]. This explained the principle that a liquid in coexistence with its vapor can have one stable liquid and one stable vapor density, and presented a graphic explanation of why, at constant pressure, the addition of energy to a coexisting vapor-liquid system did not result in a temperature rise, but in a phase change.

Later on, in his famous contribution [van der Waals, 1894] provided an approach for relating an equation of state to interfacial properties of a classical fluid system through DGT. His theory leads to a general expression for the Helmholtz energy of an inhomogeneous system. Cahn and Hilliard in 1958, and Carey *et al.* [1978a;1978b;1980] made this theory friendly to be used for predictions of interfacial tensions of pure fluids and mixtures. DGT provides a density functional for the local Helmholtz energy density of a fluid system, which consists of a 'homogeneous' term and a 'non-homogeneous' term. The previous is represented by the Helmholtz energy density of a homogeneous fluid, evaluated at a local density in between the bulk densities, while the second is proportional to the square of the molar density gradient. In their derivation Cahn and Hilliard assumed that the Helmholtz energy density  $a$  of the inhomogeneous fluid is a function of the mole density and its

---

<sup>2</sup> Part of this section has been published in Vilaseca, O. and Vega, L.F. Direct calculation of interfacial properties of fluids close to the critical region by a molecular-based equation of state. *Fluid Phase Equilib.* **2011**, 306, 4-14.

derivatives with respect to the space coordinates. It was also assumed that the density gradient is small compared to the reciprocal value of the intermolecular distance, thus allowing treating the density and its derivatives as independent variables. They expanded the  $a$  function in a Taylor series about  $a_0(\rho)$ , the Helmholtz energy density of the homogeneous fluid at the local density  $\rho$ , and truncated it after the second order term [Pàmies, 2003].

The theory explicitly considers the local free energy density within the interface, hence providing a route to obtain density profiles across the interface and the interfacial thickness, which cannot be calculated by empirical methods. Van der Waals originally developed a theory for a diffuse interface in which there was a smooth gradient density [van der Waals, 1894; Cahn and Hilliard, 1958]. Nevertheless, the theory also gives good results close to the triple point [Davis and Scriven, 1982]. Several publications explaining the theory in different manners are available in the literature (see, for instance, Rowlinson and Widom [1982]), therefore, instead of rewriting it; we have decided to keep here the main basic equations of the theory and its implementation as done in our simulation code.

Density profiles can be obtained by DGT by the minimization of the total free energy of the system. Davis and Scriven [1982] proved that the chemical potential of a species remains constant across the interface. From the application of these statements to equation 3.0:

$$A = \int_V a_0(\rho) + \frac{1}{2} \sum_{i,j} c_{ij} \rho_i \rho_j d^3r \quad (3.0)$$

Equation (3.0) expressed as an Euler-Lagrange equation results:

$$\sum_j \left( c_{ij} \rho_j \right) \frac{1}{2} \sum_k \frac{\partial c_{kj}}{\partial \rho_i} \rho_k = \frac{\partial \left( a_0(\rho) \right)}{\partial \rho_i} \quad (3.1)$$

$i, j, k = 1, \dots, N$

Equation (3.1) is mathematically a nonlinear boundary value problem. For details of the various numerical approaches to solve this equation, the reader

is referred to the existing literature and references therein [Bongiorno *et al.*, 1976; Carey *et al.*, 1978a; 1978b; 1980; Davis and Scriven, 1982; Cornelisse, 1997; Yang *et al.*, 1976]. The existence of a fluid microstructure (e.g., planar interface, spherical drop, thin film, periodic structure) is governed by the right hand side of equation (3.1) and  $c_{ij}$ , which was named influence parameter because it affects the stability and characteristic length scales of these microstructures.

The interfacial tension is a macroscopically consequence of the density profile. Considering a planar interface and assuming that the density dependence of the influence parameter can be neglected, an expression that relates the interfacial tension to the square of the density gradients can be derived from equation (3.1) [Carey *et al.*, 1978a; 1978b; 1980; Davis and Scriven, 1982; Chapman, 1988; Segura *et al.*, 1990; Queimada *et al.*, 2001]:

$$\sigma = \int_{-\infty}^{\infty} \sum_{i,j} c_{ij} \frac{d\rho_i}{dz} \frac{d\rho_j}{dz} dz = 2 \int_{-\infty}^{\infty} a_0(\rho) \sum_i \rho_i \rho_{0i} p_0 dz \quad (3.2)$$

where  $a_0$  is the free Helmholtz's energy density of a homogenous fluid with a constant concentration,  $\rho_{0i}$  and  $p_0$  are the equilibrium chemical potential and pressure, respectively, and  $z$  is the direction perpendicular to the interface.  $c_{ij}$ , previously defined, is a positive constant, the influence parameter, whose value is proportional to the inhomogeneity of the system.

The approximation  $\partial c_{ij} / \partial \rho = 0$  is supported by the works of McCoy and Davis [1979] and those of Carey *et al.* [1978a; 1978b; 1980].

Equation (3.2) would be of more practical use if it were expressed in terms of density space. Poser and Sanchez [1981] employed a transformation from location space to density space, the integration of which provides a way to calculate density profiles:

$$z = z_0 + \int_{\rho_2(z_0)}^{\rho_2(z)} \sqrt{\frac{c}{|\rho_1, \rho_2|}} d\rho_2 \quad (3.3)$$

The following equations are reduced to the particular case of binary mixtures, for simplicity. The expressions for pure fluids can be straightforwardly derived. In equation (3.3),  $z_0$  denotes an arbitrarily chosen origin,  $\omega(\rho_1, \rho_2) = a_0(\rho_1, \rho_2) \cdot \rho_1 \rho_2$  is the reduced grand thermodynamic potential,  $\omega(\rho_1, \rho_2) = a_0(\rho_1, \rho_2) \cdot \rho_1 \rho_2 + p_0$  and  $c$  results from the influence parameters of the pure components and the density profiles across the interface:

$$c = c_2 + 2c_{12} \frac{d\rho_1}{d\rho_2} + c_1 \left( \frac{d\rho_1}{d\rho_2} \right)^2 \quad (3.4)$$

For simplicity the crossed influence parameter  $c_{12}$  is assumed to be given by the geometric mean combination rule  $c_{12} = \sqrt{c_1 c_2}$ , which leads to a useful simplification of equation (3.4).  $\alpha$  is an adjustable parameter, which can be fitted to interfacial tension measurements of the mixture or kept equal to one for predictive purposes.

Using the above mentioned transformation, Poser and Sanchez [1981] also derived an equation for the interfacial tension in binary mixtures that considers the change in the partial densities  $\rho_1$  and  $\rho_2$  within the interface:

$$\sigma = \sqrt{2} \int_{\rho_2^I}^{\rho_2^{II}} \sqrt{c(\rho_1, \rho_2)} d\rho_2 \quad (3.5)$$

The limits of integration are the bulk densities of component 2 in the coexisting phases, indistinctly labeled by I and II.

The computation of the grand thermodynamic potential for binary mixtures can be performed, with the following expression:

$$\begin{aligned} \omega(\rho_1, \rho_2) &= (\rho_1 + \rho_2) A(\rho_1, \rho_2) - \rho_1 \int_{\rho_1^I}^{\rho_1} \omega(\rho_1, \rho_2^I) d\rho_1 - \rho_2 \int_{\rho_2^I}^{\rho_2} \omega(\rho_1^I, \rho_2) d\rho_2 + p_0 \\ &= \rho_1 \int_{\rho_1^I}^{\rho_1} \omega(\rho_1, \rho_2^I) d\rho_1 + \rho_2 \int_{\rho_2^I}^{\rho_2} \omega(\rho_1^I, \rho_2) d\rho_2 \end{aligned} \quad (3.6)$$

For binary mixtures, it is clear from equations (3.7)-(3.9) that the determination of  $\gamma \left( \rho_1, \rho_2 \right)$  and  $c_{12}$  requires the knowledge of  $\rho_1$  for each value of  $\rho_2$  within the interface. This dependence conforms to the density profiles across the interface. Minimization of the interfacial tension leads to a system of equations [Poser and Sanchez, 1981] by which the partial density profiles can be obtained:

$$\frac{\partial \gamma \left( \rho_1, \rho_2 \right)}{\partial \rho_1} = c_1 \frac{\partial^2 \rho_1}{\partial z^2} + c_{12} \frac{\partial^2 \rho_2}{\partial z^2} \quad (3.7)$$

$$\frac{\partial \gamma \left( \rho_1, \rho_2 \right)}{\partial \rho_2} = c_{12} \frac{\partial^2 \rho_1}{\partial z^2} + c_2 \frac{\partial^2 \rho_2}{\partial z^2} \quad (3.8)$$

This second-order system of partial differential equations can be numerically solved by finite-difference or finite-element methods. For a detailed discussion about the numerical solution of these coupled equations, the reader is referred to the PhD thesis of Cornelisse [1997].

The above system of equations can be reduced to a single algebraic equation if the simple geometric mixing rule for  $c_{12}$  (with  $\rho = 1$ ) is used:

$$\sqrt{c_2} \frac{\partial \gamma \left( \rho_1, \rho_2 \right)}{\partial \rho_1} = \sqrt{c_1} \frac{\partial \gamma \left( \rho_1, \rho_2 \right)}{\partial \rho_2} \quad (3.9)$$

Combining equations (3.6) and (3.9), the simple relation:

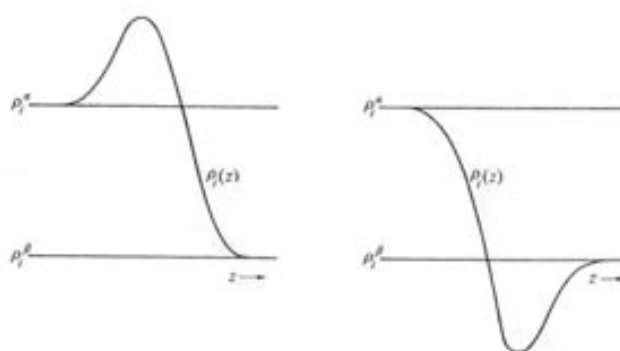
$$\sqrt{c_2} \gamma \left( \rho_1, \rho_2 \right) - \rho_1 \left( \frac{\partial \gamma}{\partial \rho_1} \right) = \sqrt{c_1} \gamma \left( \rho_1, \rho_2 \right) - \rho_2 \left( \frac{\partial \gamma}{\partial \rho_2} \right) \quad (3.10)$$

can be used to compute  $\rho_1$  at every sampling point value of  $\rho_2$  within the interface.

### 3.1.1 Density profiles

DGT does not only allow calculating the interfacial tension of fluids or mixtures, but also offers the possibility of getting insides into the mixture behavior at molecular level by allowing the calculation of the density profiles. The theory explicitly considers the local free energy density within the interface, hence providing a route to obtain density profiles, adsorption and desorption profiles, or the interfacial thickness which cannot be measured experimentally. The strength of this approach is that simple analytical expressions can be used to obtain the density profiles and for surface tension calculations, as explained in the last section. The interfacial thickness can also be obtained directly from the density profiles equations.

As sketch in the following Figure, absorption (left) and desorption (right) phenomena have a direct impact on the density profile shape.



**Figure 3.1:** Types of density variation  $\rho(z)$ . From: [Rowlinson and Widom, 1998]

The absorption phenomena at the interface leads to a minimized interfacial tension of the mixture, compared to the pure compounds forming the same, because of the minimized free energy at the interface. When dealing with mixtures, the compound has its own free energy and, hence, an associated value of interfacial tension; therefore, the compound having the highest interfacial tension (so the highest free energy) will never be absorbed on the vapor-liquid interface of the mixture. This compound must be chosen as the reference fluid as it will never reach a maximum and will change monotonically from vapor to liquid phase. This section will be completed in chapter 4 with examples of some types of density profiles for pure fluids and mixtures.

## 3.2 The SAFT Equation of State<sup>3</sup>

As stated, the calculation of interfacial properties by DGT requires the evaluation of the bulk the properties with a complementary approach. For this purpose it is necessary to choose an accurate equation of state. One EoS that has been proven to be very accurate is the *Statistical Associating Fluid Theory* (SAFT) which is an equation based on statistical mechanics.

The origin of the SAFT equation of state has its roots in Wertheim's work [1984a; 1984b; 1986a; 1986b], who developed a Thermodynamic Perturbation Theory of first and second order (TPT1 and TPT2) for describing the properties of associating fluids. Later on, Chapman *et al.* used Wertheim's theory to construct an equation of state for associating fluids known as the *Statistical Associating Fluid Theory* (SAFT). SAFT, which is a modeling approach rather than an equation, describes the free energy of the system as the summation of different microscopic contributions, including a reference term (hard spheres in the original formulation plus a perturbation term to take into account the dispersive forces), a chain term (which takes into account the molecular shape) and an association term (which takes into account the hydrogen bonding formation and some other specific interactions). Different versions of SAFT have been proposed over the years, most of them different only in the reference term, while Wertheim's approach is kept for the chain and association term.

As stated, SAFT, more than an equation, is a modeling approach that provides a framework in which structural and thermophysical properties of a given fluid can be calculated at the molecular level with some specific methods (theories or simulations). A good description of the SAFT approach can be found in the original papers [Chapman *et al.*, 1989; 1990] and further reviews [Müller and Gubbins, 2001; Economou *et al.*, 2002; Pàmies, 2003; Tan *et al.*, 2008]. In the following lines a brief review of the SAFT equations is enunciated in order to show the different terms that conform the mathematical development of the theory.

---

<sup>3</sup> Part of this section has been published in Vilaseca, O. and Vega, L.F. Direct calculation of interfacial properties of fluids close to the critical region by a molecular-based equation of state. *Fluid Phase Equilib.* **2011**, 306, 4-14.



The SAFT equation is expressed in terms of the residual Helmholtz energy, defined as the difference between the total Helmholtz energy and that of an ideal gas at the same temperature and density. The residual Helmholtz energy of a system of associating chains can be expressed as the sum of contributions due to different intermolecular effects:

$$\begin{aligned}
 A^{res} &= A^{total} - A^{ideal} = \\
 &= A^{seg}(\rho, T; \sigma, \epsilon) + A^{chain}(\rho, T, x_i; \sigma, \epsilon, m_i) + A^{assoc}(\rho, T, x_i; \sigma, \epsilon, m_i, \epsilon_{HB}^{i,j}, k_{HB}^{i,j}) + \dots
 \end{aligned}
 \tag{3.11}$$

where  $\rho$  is the (chain) molecular density;  $T$  is the absolute temperature;  $x_i$  is the composition of species  $i$  in the mixture, and the molecular parameters are:

- $m$ , the number of spherical segments forming a chain molecule,
- $\sigma$ , the diameter of the segments,
- $\epsilon$ , the dispersive energy of the segments,
- $\epsilon_{HB}^{i,j}$ , the energy of association between site  $\alpha$  on specie  $i$  and site  $\beta$  on specie  $j$ ,
- $k_{HB}^{i,j}$ , the volume of association between site  $\alpha$  on specie  $i$  and site  $\beta$  on specie  $j$ .

With the obtained value of the Helmholtz energy, all other thermodynamic properties, such as temperature, pressure or composition can be calculated by classical thermodynamics relations.

In equation (3.11) SAFT considers three major microscopic contributions to the total intermolecular potential of a given associating molecule:

- $A^{seg}$ , the repulsion-dispersion contribution due to the presence of the individual segments,
- $A^{chain}$ , the contribution due to the fact that these segments can form a chain,
- $A^{assoc}$ , the contribution due to the possibility that some segment(s) form association complexes with other molecules.

Additional perturbation molecular terms have been added as extensions of the SAFT versions, all based on the molecular structure of the chosen systems. These terms deal with additional features of the molecules, such as quadrupolar terms, dipolar terms, electrolyte terms, etc. Other extensions of the equation allow the calculation of other properties or other regions of the phase diagram; this is the case of adding a crossover treatment to take into account the density fluctuations in the near critical region [Llovell *et al.*, 2006], the calculation of second order thermodynamic derivative properties [Llovell *et al.*, 2006] and the combination with DGT to study interfacial properties [Pàmies 2003, Vega and coworkers, 2004; 2005; 2006; 2010; 2012].

### 3.2.1 The segment term

Molecular chains can be approximated as spherical segments (atoms, functional groups, monomers, etc.) that interact with isotropic repulsion and dispersion (attraction) forces. The segment term,  $A^{seg}$ , in SAFT describes the properties of the individual units that compose the chain, and corresponds to the sum of all monomers (being  $A^{monomer}$  the molar Helmholtz energy of the fluid if no chain connectivity occurred, evaluated at the monomer molar density):

$$A^{seg} = RT \sum_i x_i m_i \frac{A^{monomer}}{RT} \quad (3.12)$$

where  $R = k_B N_A$  is the ideal gas constant,  $k_B$  the Boltzmann constant and  $N_A$  the Avogadro's number,  $x_i$  the molar fraction of component  $i$  and  $m_i$  its chain length.

SAFT does not specify the description of  $A^{monomer}$ , as Wertheim's theory does not specify it. Although, originally, a perturbation expansion with a hard-sphere fluid as a reference and a dispersion term as a perturbation was used [Chapman *et al.*, 1989; 1990], other more refined intermolecular potentials have been applied, leading to more accurate versions of the SAFT equation. Among them I want to highlight the soft-SAFT equation, using a Lennard-Jones potential [Blas and Vega, 1997;1998; Johnson *et al.*,1994], the SAFT-VR EoS, using square-well potential of variable range [Gil-Villegas *et al.*, 1997] and the SAFT-VR-Mie which uses a generalized Lennard-Jones potential with

variable exponents [Lafitte *et al.*, 2006]; they all use the same formal term for chain and association and different versions of the segment term. Conversely, there are also other approaches, such as PC-SAFT, based on perturbed hard chains [Gross and Sadowski, 2001], that applies the TPT1 on the chain term interactions, (see section 3.4.2.) and the GC-SAFT [Tamouza *et al.*, 2004] or the SAFT- $\square$  [Lymperiadis *et al.*, 2007], based on Group Contribution methods.

### 3.2.2 The chain term

The SAFT model accounts for the nonspherical shape of molecules allowing for the connectivity of segments to form long chainlike molecules. This is accomplished by taking the limit of complete bonding in Wertheim's theory [Wertheim, 1984a;1984b;1986a;1986b] in which infinitely strong bonding on an infinitely small association site placed at the edge of a given segment leads to the formation of chains.

The chain term  $A^{chain}$  takes into account the contribution to the Helmholtz energy due to the formation of chains from  $m_i$  spherical monomers:

$$A^{chain} = RT \sum_i x_i (1 - m_i) \ln g_r(\sigma) \quad (3.13)$$

where  $g_r(\sigma)$  is the radial distribution function of the reference fluid for the interaction of two segments in a mixture of segments, evaluated at the contact length  $\sigma$ . This term is formally identical in all versions of SAFT, and it comes directly from Wertheim's theory [Wertheim, 1984a; 1984b; 1986a; 1986b].

### 3.2.3 The association term

The presence of noncentral directional and strong attractions is taken into account in SAFT by including an additional perturbation term describing intermolecular association. The association term  $A^{assoc}$  is added when the fluid under study has an associating behavior (e.g. possible formation of hydrogen bonds):

$$A^{assoc} = RT \sum_i x_i \left[ \sum_{\alpha} \left( \ln X_i^{\alpha} - \frac{X_i^{\alpha}}{2} \right) + \frac{M_i}{2} \right] \quad \alpha = A, B, C, \dots \quad (3.14)$$

where  $X_i$  is the fraction of molecules of specie  $i$  that are not bonded at site  $\alpha$ ,  $M_i$  is the number of association sites per molecule (which have to be

included in the model) and  $\alpha$  is the running label for the associating sites. The calculation is performed over all association sites (A,B,C,...) on the molecule and for all the associating species present in the mixture.

The values of the X's are obtained from the solution of the mass balances with a statistical approach. The value of  $A^{assoc}$  ultimately depends on the association strength between sites and this is related to the radial distribution function and the reference intermolecular potential.

The association term introduces two additional molecular parameters  $\varepsilon_{HB} = \varepsilon_{HB}^{i,j}$  (energy of the association site) and  $K_{HB} = k_{HB}^{i,j}$  (volume of association). The selected reference fluid also influences the chain formation (as it depends on the  $g(r)$  of the reference fluid) and the geometry of the association sites. In the case of a LJ reference fluid, the association sites are allowed to be fully embedded inside the reference core, which can describe a realistic situation of overlapping between the segments that contain the two association sites involved in a bond in experimental situations.

The number of molecular parameters to be used within a SAFT approach depends on the molecular structure of the system under study. SAFT requires a minimum of two molecular parameters,  $\sigma$  and  $\varepsilon$ , to describe simple conformal fluids. A third parameter,  $m$ , is required to describe the nonsphericity for nonassociating fluids. For quadrupolar fluids, such as CO<sub>2</sub>, the quadrupolar moment Q appears as an additional parameter if the quadrupolar term is explicitly considered. For associating fluids, one must also assign two more parameters,  $\varepsilon_{HB}$  and  $\kappa_{HB}$ . For each species, the associating sites and their bonding correspondence, which site bonds to which, must be defined. These molecular parameters are independent on the thermodynamic conditions. Hence, once the molecular model is tested against available experimental data, the same model can be used to confidently predict the thermodynamic properties of the same system at other conditions. Usually, these parameters are regressed from experimental vapor-liquid phase equilibria properties. Nevertheless, because of the well-defined physical meaning of each parameter, in principle they could be estimated from *ab initio* calculations or from direct measurements, such as FT-IR.

In summary, SAFT-type equations are based on statistical mechanics, which lets a physical interpretation of the system. Consequently, the effects of molecular shape and interactions on the thermodynamic properties can be separated and quantified. In addition, the small number of parameters, with physical meaning and transferable, makes SAFT a powerful tool for engineering predictions.

### 3.3 The soft-SAFT equation of state<sup>4</sup>

Several modifications of the original SAFT equation have been presented during these years. Most of them differ on the reference term used, being soft-SAFT one of the most successful in the description of physicochemical properties of a wide of complex systems. As mentioned, the success of the description of the interfacial properties with DGT depends on the underlying theory for the bulk. For instance, if the coexistence phase region is not accurately predicted, then the density profiles will not have the proper asymptotic behavior, and they will not be trustworthy, neither the surface tension.

Soft-SAFT [Blas and Vega, 1997] is a modified version of the original SAFT equation, the main difference being the fact that the reference term is a Lennard-Jones term (soft), instead of a hard-sphere and a perturbation attractive term. Soft-SAFT has been developed and extended over the last fifteen years by our group in a systematic manner [Vega and collaborators, 1997; 1998; 2001; 2002; 2005; 2006; 2009], expanding its capability to other regions of the phase space [Duque *et al.*, 2004; Llovel *et al.*, 2004] and for the calculation of additional properties [Llovel and Vega, 2006]. One of the objectives of the present PhD thesis is to use the crossover approach, proved to accurately represent the vapor-liquid critical region, for the prediction of the interfacial tension in this region. This is the first time that DGT has been used coupled with a non-classical method to correctly describe the interfacial properties in the near critical region of experimental systems.

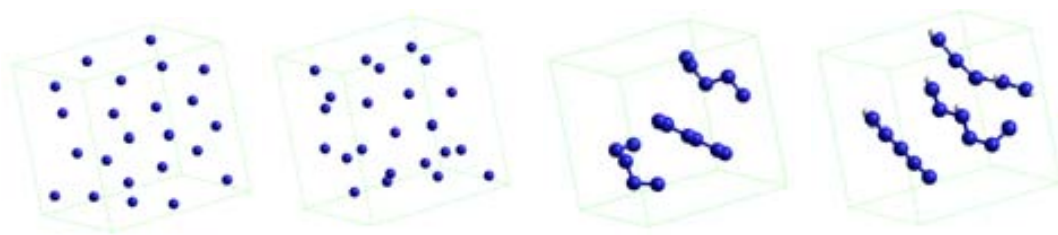
---

<sup>4</sup> Part of this section has been published in Vilaseca, O. and Vega, L.F. Direct calculation of interfacial properties of fluids close to the critical region by a molecular-based equation of state. *Fluid Phase Equilib.* **2011**, 306, 4-14.

As soft-SAFT and its crossover version have been extensively presented in the literature, only the main equations are kept here for completeness. Further details regarding the theory and its implementation have been widely discussed and can be found in the literature and references therein [Llovel et al, 2004; Llovel and Vega, 2006; Vega and collaborators, 1997; 1998; 2001; 2002; 2006; 2009]. All SAFT-type equations are written as a sum of contributions to the total free energy of the system, in which the molecular effects are separated and quantified. Soft-SAFT [Blas and Vega, 1997] mainly differs from the original SAFT in the reference term, which is a LJ fluid, instead of a hard sphere plus a perturbative attractive term. As stated, the LJ term accounts for both, the repulsive and attractive interactions of the monomers forming the chain in a single term, which turns out to be very important in some systems in which the fluid structure greatly affects the thermodynamic behavior. The Helmholtz energy density of these systems is given as:

$$\frac{A}{V} = a_0 = a^{id} + a^{ref} + a^{chain} + a^{assoc} \quad (3.15)$$

where  $a^{id}$  states for the ideal term,  $a^{ref}$  refers to the Helmholtz energy density of the reference LJ fluid and  $a^{chain}$  and  $a^{assoc}$  are the chain and association term, both coming from TPT1 of Wertheim.



**Figure 3.2:** Representation of the different interactions included in the SAFT-EoS.

In addition to the mathematical model, a molecular model for each of the systems of interest is needed in order to apply the SAFT approach to experimental systems. Typically, the molecular parameters of the model are obtained by fitting to vapor-liquid equilibrium data and used in a transferable manner for other properties' calculations. During the last years the MOLSIM group in which it was conceived (Vega and collaborators), has developed a

multioptional code which allows the calculation of different properties in an optimized manner. These properties are, among others, thermodynamic properties of one, two and three phases in equilibria, solubilities, heat capacities, speed of sound, compressibilities, critical properties of pure, binary and ternary mixtures, interfacial properties of pure and binary mixtures, free energies, entropies and enthalpies of mixing, excess properties, etc. For this thesis the computational code has been conveniently modified in order to extend the calculations to different families and mixtures.

### 3.3.1 The crossover treatment

The classical formulation of SAFT makes the theory unable to correctly describe the scaling of thermodynamic properties as the critical point is approached. This can be overcome by splicing together an equation which incorporates the fluctuation-induced scaled thermodynamic behavior of fluids asymptotically close to the critical point, but that also accounts for a crossover to classical behavior of the thermodynamic properties far away from the critical point, where the effect of fluctuations becomes negligible. This contribution is obtained when the renormalization group (RG) theory [Wilson, 1971, Wilson *et al.*, 1972] is applied. The treatment followed in the crossover soft-SAFT EoS, based on White's work [White, 1992;1999;2000; Salvino and White, 1992; White and Zhang, 1993;1995], is done by incorporating the scaling laws governing the asymptotic behavior close to the critical point, while reducing to the original EoS far from the critical point. This approach is mathematically expressed as a set of recursive equations that incorporate the fluctuations in a progressive way:

$$a = k_B T \bullet \left( a_{n-1} + a_n^{cross} \right) \quad (3.16)$$

The value of  $a_{n-1}$  for the first iteration corresponds to the original soft-SAFT value. The inclusion of the crossover treatment leads to two additional parameters, the cutoff length,  $L$ , related to the maximum wavelength fluctuations that are accounted for in the uncorrected free energy, and  $\phi$  which is the average gradient of the wavelet function. Details on the implementation of the crossover term can be found in the original references [Llovell *et al.*, 2004; 2005 ; Llovell and Vega, 2006].

### 3.3.2 The polar term

The multipolar term for fluids of linear symmetrical molecules, such as CO<sub>2</sub> or SO<sub>2</sub>, which are of interest for this work, is the quadrupole-quadrupole potential. This term can be incorporated into soft-SAFT by using an extension of the theory of Gubbins and Twu [1978] (originally developed for spherical molecules) to chain fluids. Following the ideas of Jog *et al.*, [2001], the methodology is based in a perturbative approach of the Helmholtz free energy density due to the polarity effects. The free energy is expanded in a series of terms, written with the Padé approximation Stell *et al.* [1974]:

$$a^{qq} = a_2^{qq} \left( 1 - \frac{a_3^{qq}}{a_2^{qq}} \right)^{-1} \quad (3.17)$$

$a_2^{qq}$  is the second-order term in the perturbation expansion and  $a_3^{qq}$  is the third-order term. Expressions for  $a_2^{qq}$  and  $a_3^{qq}$  were obtained for an arbitrary intermolecular reference potential and involve state variables, molecular parameters and the integral  $J$  for the reference fluid [Jog *et al.*, 2001]. The previous expressions include the quadrupole moment,  $Q_i$ , of the molecule. Moreover, the extension to chain fluids assumes that the polar moments are well-localized on certain segments of the chain [Jog *et al.*, 2001]. As a consequence; a fraction  $x_{pi}$  has to be defined as the fraction of the molecule affected by the quadrupole.

Some of the chosen molecules studied in this work present polar interactions that are taken into account through the quadrupolar term, for example, the carbon dioxide molecule is modeled [Belkadi *et al.*, 2008; Dias *et al.*, 2006] as a LJ chain in which explicit quadrupolar interactions are taken into account. This model has already been used with success to describe the behavior of CO<sub>2</sub> on different systems [Dias *et al.*, 2006; Belkadi *et al.*, 2008; 2010; Andreu and Vega, 2007;2008; Vilaseca and Vega, 2011], it has also been applied in this thesis also with great success, accounting on association effects and polar interactions for the dipole-dipole, quadrupole-quadrupole and cross dipole-quadrupole interactions.



### 3.4 The DGT combined with the soft-SAFT EoS<sup>5</sup>

In last decades several authors have combined DGT to different EoS models, mostly the Peng-Robinson, although some other equations have also been used. In their pioneering work Cornelisse *et al.* [1993] computed interfacial tensions for carbon dioxide, n-butane, n-decane, and their binary and ternary mixtures with the modified Peng Robinson EoS of Chou and Prausnitz. They obtained good agreement in general, but the scaling behavior did not agree with experiments, due to the classical formulation of the chosen EoS. In a later work [Cornelisse *et al.*, 1996] they provided a temperature-dependent model for the influence parameter that provided critical exponents closer to experimental values, thus improving the description of equilibria densities and interfacial tensions near the critical point. Miqueu *et al.* [2003] employed the DGT and the Peng Robinson EoS with volume corrections for the calculation of interfacial tensions of hydrocarbons, gases and refrigerants. From their results, they stated that the temperature dependence of the influence parameter needs to be conserved. They provided a simple correlation to account for this temperature dependence. Contrarily, Enders and co-workers [Enders and co-workers, 2000; 2002; 2005; 2008; 2010] neglected the temperature dependence of the influence parameter and used the Peng Robinson EoS, the Sanchez-Lacombe and the original SAFT EoS models to compute interfacial tensions for hexane, benzene, methanol and water. They showed that predictions strongly depend on the choice of the model. Although SAFT has a significant advantage for associating substances, Kahl and Enders obtained that the Peng-Robinson EoS seems to perform better than the original SAFT for the description of interfacial properties of non-polar fluids, probably due to the fact that the Peng Robinson EoS provided more accurate bulk properties than the original SAFT equation. Oliveira et al [2008] have coupled DGT with the Cubic Plus Association (CPA) EoS to describe the surface tensions of a broad range of homologue families of nonassociating (n-alkanes and n-fluoroalkanes) and associating components (1-alkanols). The authors used a quadratic correlation of the influence

---

<sup>5</sup> Part of this section has been published in Vilaseca, O. and Vega, L.F. Direct calculation of interfacial properties of fluids close to the critical region by a molecular-based equation of state. *Fluid Phase Equilib.* **2011**, 306, 4-14.

parameter in Tr obtaining accurate estimations of surface tensions in the  $0.45 < Tr < 0.85$  range. In a very recent work [Dias *et al.*, 2009] have modeled the interfacial tensions of highly fluorinated compounds combining DGT with crossover soft-SAFT [Llovell, Pàmies and Vega, 2004] as part of a throughout characterization of this family of compounds by a molecular-based equation of state, obtaining excellent results.

During the last years several authors have been interested on DGT for calculating interfacial properties [Yang, 1975; Yang *et al.*, 1976; Vargas *et al.*, 1976; Bongiorno and Davis, 1975; Bongiorno *et al.*, 1976; Carey *et al.*, 1978a; 1978b; 1980; Cornelisse *et al.*, 1993; 1996; Davis *et al.*, 1978; 1980; Davis and Scriven, 1982; Duque *et al.*, 2004; Enders and coworkers, 2000; 2002; 2005; 2008; 2010; Mejía *et al.*, 2005; Mejía and Vega, 2006; Miqueu, 2000; 2003; Pàmies, 2003; Oliveira *et al.*, 2008; Rowlinson, 1979; Vilaseca *et al.*, 2010; Galliero, 2010; Vilaseca and Vega, 2011]. All of them have concluded that good predictions for the interfacial properties of simple molecules can be achieved by means of this theory.

## 3.5 References

- Andreu, J.S.; Vega, L.F. *J. Phys. Chem. C* **111**, 16028 (2007).
- Andreu, J.S.; Vega, L.F. *J. Phys. Chem. B* **112**, 15398 (2008).
- Belkadi, A.; Llovell, F. ; Gerbaud, V.; Vega, L.F. *Fluid Phase Equilib.* **266**, 154 (2008).
- Belkadi, A.; Llovell, F.; Gerbaud, V.; Vega, L.F. *Fluid Phase Equilib.* **289**,191 (2010).
- Blas, F.J.; Vega, L.F. *Mol. Phys.* **92**, 135 (1997).
- Blas, F.J.; Vega, L.F.; *Ind. Eng. Chem. Res.* **37**, 660 (1998).
- Bongiorno, V.; Davis, H.T. *Phys.Rev. A* **12**, 2213 (1975).
- Bongiorno, V. ; Scriven, L.E.; Davis, H.T. *J. Colloid Interface Sci.* **57** ,462 (1976).
- Cahn, J.W.; Hilliard, J.E. *J. Chem. Phys.* **28**, 258 (1958).
- Carey, B.S.; Striven, L.E.; Davis, H.T. *AIChE J.* **24**, 1076 (1978).
- Carey, B.S.; Striven, L.E.; Davis, H.T. *J. Chem. Phys.* **69**, 5040 (1978).
- Carey, B.S.; Striven, L.E.; Davis, H.T. *AIChE J.* **26**, 705 (1980).
- Chapman, W. G. *PhD Thesis*, Cornell University, Ithaca, NY, USA, 1988.
- Chapman, W.G.; Gubbins, K.E.; Jackson, G.; Radosz, M. *Fluid Phase Equilib.* , **52**, 3 (1989).
- Chapman, W.G.; Gubbins, K.E.; Jackson, G.; Radosz, M. *Ind. Eng. Chem. Res.*, **29 (8)**, 1709 (1990).
- Cornelisse, P.M.W.; Peters, C.J.; de Swaan Arons, J. *Fluid Phase Equilib.* **82**,109 (1993).
- Cornelisse, P.M.W.; Peters, C.J.; de Swaan Arons, J. *Fluid Phase Equilib.* **117**, 312 (1996).
- Cornelisse, P.M.W. *PhD Thesis*, Delft University of Technology, Netherlands, 1997.
- Davis, H. T.; Scriven, L.E. *Adv. Chem. Phys.* **49** , 357 (1982).

- Dias, A.M.A; Pàmies, J.C.; Coutinho, J.A.P; Marrucho, I.M., Vega, L.F. *J. Phys. Chem. B* **108**, 1450 (2004).
- Dias, A.M.A.; Carrier, H.; Daridon, J.L.;Pàmies, J.C.; Vega, L.F.; Coutinho, J.A.P.; Marrucho, I.M. *Ind. Eng. Chem. Res.* **45**, 2341 (2006).
- Dias, A.M.A; Llovell, F.; Coutinho, J.A.P; Marrucho, I.M., Vega, L.F. *Fluid Phase Equilib.* **286**, 134 (2009).
- Duque, D.; Pàmies, J.C.; Vega, L.F. *J. Chem. Phys.* **121**, 11395 (2004).
- Duque, D.; Vega, L.F. *J. Chem. Phys.* **121**, 17 (2004).
- Economou, I.G. *Ind. Eng. Chem. Res.* **41**, 953 (2002).
- Enders S; Kahl, H.; Winkelmann, J. *Fluid Phase Equilib.* **228-229**, 511(2005).
- Jog, P.K.; Sauer, S. G.; Blaesing, J.; Chapman, W.G. *Ind. Eng. Chem. Res.* **4641-4648**, 40 (2001).
- Evans, W.V. *J. Chem. Educ.* **19** ,539 (1942).
- Galliero,G. *J. Chem. Phys.* **133**, 074705(2010).
- Gil-Villegas, A.; Galindo, A.; Whitehand, P.J.; Mills, S.J.; Jackson, G. *J. Chem. Phys.* **106**, 4168. (1997)
- Gross, J.; Sadowski, G. *Ind. Eng. Chem. Res.* **40**, 1244 (2001).
- Gubbins, K. E.; Twu, C. H. *Chem. Eng. Sci.* **863-878**, 33 (1978).
- Johnson, J.K.;Müller, E.A.; Gubbins, K.E. *J. Phys. Chem.* **98**, 6413 (1994).
- Kahl, H.; Enders, S. *Fluid Phase Equilib.* **172**, 27 (2000).
- Kahl, H.; Enders, S. *Phys. Chem.Phys.* **4**, 931 (2002).
- Kahl, H.; Enders S. *Fluid Phase Equilib.* **263**, 160 (2008).
- Lafitte, T.; Bessieres, D.; Piñeiro, M.M.; Daridon, J.L. *J. Phys. Chem.* **124**, 024509 (2006).
- Levine, R.D., *Quantum mechanics of molecular rate processes*. (Dover, New York, 1999)

- Lymperiadis, A.A.; Adjiman, C.S.; Galindo, A.; Jackson, G. *J. Chem Phys* **127**, 23 (2007)
- Llovell, F.; Pàmies, J.C.; Vega, L.F. *J. Chem. Phys.* **121**, 21 (2004).
- Llovell, F.; Vega, L.F. *J. Phys. Chem.* **110**, 1350 (2005).
- Llovell, F.; Vega, L.F. *J. Phys. Chem.* **110**, 1350 (2006).
- Llovell, F.; Vega, L.F. *J. Phys. Chem. B* **110**, 11427 (2006).
- McCoy, B.F.; Davis, H.T. *Phys. Rev. A* **20**, 1201 (1979).
- Mejía, A.; Pàmies, J.C.; Duque, D.; Segura, H.; Vega, L.F. *J. Chem. Phys.* **123**, 034505.1 (2005).
- Mejía, A.; Vega, L.F. *J. Chem. Phys.* **124**, 244505 (2006).
- Miqueu, C.; Broseta, D.; Satherley, J.; Mendiboure, B.; Lachaise, J.; Graciaa, A. *Fluid Phase Equilib.* **172**, 169 (2000).
- Miqueu, C. *PhD Thesis*, Université de Pau et des Pays de l'Adour, France. 2001.
- Miqueu, C.; Mendiboure, B.; Graciaa, A.; Lachaise, J. *Fluid Phase Equilib.* **207**, 225 (2003).
- Muller, E.; Gubbins, K.E. *Ind. Eng. Chem. Res.* **40**, 2193 (2001).
- Müller, E.; Mejía, A. *Fluid Phase Equilibria* **282**, 68 (2009).
- Niño Amezquita, O.G.; Enders, S.; Jaeger, P.T.; Eggers R. *Ind. Eng. Chem. Res.* **49**, 592 (2010).
- Niño Amezquita, O.G.; Enders, S.; Jaeger, P.T.; Eggers R. *J. Supercrit. Fluids* **55**, 724 (2010).
- Oliveira, M.B.; Marrucho, I. M.; Coutinho, J.A.P.; Queimada, A.J. *Fluid Phase Equilib.* **267**, 93 (2008).
- Pàmies, J.C.; Vega, L. F., *Ind. Eng. Chem. Res.* **40**, 2532 (2001).
- Pàmies, J.C.; Vega, L. F., *Mol. Phys.* **100**, 2519 (2002).
- Pàmies, J.C. *Ph. D. Thesis*, Universitat Rovira i Virgili, Tarragona, 2003.
- Poser, C.I.; Sanchez, I.C. *Macromol.* **14**, 361 (1981).

- Queimada, A. J.; Marrucho, I. M.; Coutinho, J. A. P. *Fluid Phase Equilib.* **183-184**, 229 (2001).
- Rowlinson, J.S. *J. Stat. Phys.* **20**, 197 (1979).
- Rowlinson, J.S. and Widom, B., *Molecular Theory of Capillarity*. Oxford University Press, Oxford, UK, 1982.
- Salvino, L.W.; White, J.A. *J. Chem. Phys.* **96**, 4559 (1992).
- Segura, C.J.; Chapman, W.G.; Shukla, K.P. *Molec. Phys.* **90**, 759 (1990).
- Stell, G.; Rasaiah, J.C.; Narang, H. *Mol. Phys.* **27**, 1393 (1974).
- Tamouza, S.; Passarello, J.P; Tobaly, P.; de Hemptinne, J.C. *Fluid Phase Equilib.* **222-223**, 67 (2004).
- Tan, S.; Adidharma, H.; Radosz, M. *Ind. Eng. Chem. Res.* **47 (21)**, 8063 (2008).
- van der Waals, J.D. *Over de Continuïet Van Den Gas- En Vloeistof-Toestand (On the Continuity of the Gaseous and Liquid States); Translation by J. S. Rowlinson. PhD thesis, University of Leiden, Netherlands, 1873.*
- van der Waals, J.D. *Z. Phys. Chem.* **13**, 657 (1894).
- Vargas, A. S. *PhD Thesis, University of Minnesota, USA, 1976.*
- Vega, L.F.; Llovel, F.; Blas, F.J. *J. Phys. Chem. B* **113**, 7621 (2009).
- Vilaseca, O.; Llovel, F.; Yustos, J.; Marcos, R.M.; Vega, L.F. *J. Supercrit. Fluids* **55**, 755 (2010).
- Vilaseca, O.; Vega, L.F. *Fluid Phase Equilib.* **306**, 4 (2011).
- Wertheim, M.S. *J. Stat. Phys.* **35**, 19 (1984) a.
- Wertheim, M.S. *J. Stat. Phys.* **35**, 35 (1984)b.
- Wertheim, M.S. *J. Stat. Phys.* **42**, 459 (1986)a.
- Wertheim, M.S. *J. Stat. Phys.* **42**, 477 (1986)b.
- White, J.A. *Fluid Phase Equilib.* **75**, 53 (1992).
- White, J.A.; Zhang, S.J. *J. Chem. Phys.* **99**, 2012 (1993).
- White, J.A.; Zhang, S.J. *J. Chem. Phys.* **103**, 1922 (1995).

*Methodology*

White, J.A. *J. Chem. Phys.* **111** ,9352 (1999).

White, J.A. *J. Chem. Phys.* **112** ,3236 (2000).

Wilson, K.G. *Phy. Rev. B* **4** ,3174(1971).

Wilson, K.G.; Fisher, M.E. *Phys. Rev. Lett.* **28** ,240 (1972).

Yang, A. *Ph.D. Thesis* Molecular theory of surface tension, Brown University, 1975.

Yang, A.J.M.; Fleming, P.D.; Gibbs, J.H. *J. Chem. Phys.* **64**, 3732 (1976).





# 4. Results and discussion

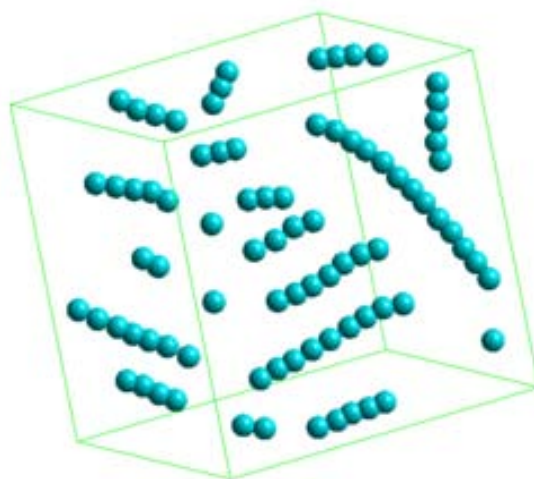
*“Wisdom is the daughter of the experience”*

*Leonardo da Vinci (1452-1519); Italian Polymath*

In this chapter results concerning the application of the crossover soft-SAFT equation coupled with DGT for the prediction of interfacial tensions of pure fluids and mixtures, including non-polar and polar compounds, far from and near to the critical region, are presented. The section has been divided in three main blocks: phase and interfacial properties of pure fluids (associating and non-associating), interfacial properties of selected industrial relevant mixtures and interfacial, surface and critical properties of ionic liquids. A comparison with available simulation and experimental data is performed in all cases.

## 4.1. Assessment of the model: comparison with simulation data

A fundamental test for any equation of state based in Statistical Mechanics is its validation against molecular simulation data for the same underlying model. Molecular simulations provide the exact numerical solution of a model, allowing corroborating and validating the approximations made in the theory. Keeping this principle in mind, we have compared the soft-SAFT equation of state proposed by Blas and Vega [1997] in combination with the DGT [van der Waals, 1894], against the molecular simulation data for the same model reported by several authors [Lofti *et al.*, 1992; Escobedo and de Pablo, 1996; Vega *et al.*, 2003; Duque *et al.*, 2004; McDowell and Blas, 2009; Galliero, 2010]. The comparison was already carried out for some specific Lennard-Jones chains but, here the range of compounds is extended as new simulation data has also appeared [Duque and Vega, 2004; Mejía *et al.*, 2005; Mejía and Vega, 2006]. We have compared the Lennard-Jones simulation data with soft-SAFT + DGT for both equilibria and interfacial calculations. Excellent agreement is obtained in all cases, corroborating the strength of the theoretical approach and enabling the equation to be used with confidence for experimental systems.



**Figure 4.1:** Graphical representation of the Lennard-Jones chains in a simulation box.

### 4.1.1. Lennard-Jones chains

In order to assess the validity of combining soft-SAFT with DFT for simultaneous predictions of phase and interfacial properties nonassociating Lennard-Jones chains have been considered first.

The same Lennard-Jones chain model (with the same parameters value,  $m$ ,  $\sigma$  and  $\epsilon$ ) has been used for both, soft-SAFT and molecular simulations. For the crossover version of soft-SAFT the value of the cutoff length,  $L$ , related to the maximum wavelength fluctuations that are accounted for in the uncorrected free energy, and  $\phi$  which is the average gradient of the wavelet function [Llovel et al, 2004] are obtained by fitting to phase equilibria simulation data up to  $m=16$ . The influence parameter  $c$  is obtained as a temperature independent parameter fitted to interfacial tension data for the same simulation model. The values of the crossover parameters are listed, together with the chain length of the system under consideration and the influence parameter  $c$  in Table 4.1.

**Table 4.1** Crossover optimized parameters from simulation data for flexible LJ chains studied in this work.

$m$	$\phi$	$L/\sigma$	Reference	$10^{19} c$
1	10	1.26	Lofti <i>et al.</i> , 1992; Duque <i>et al.</i> ,2004	4.5
2	10.5	1.35	Vega <i>et al.</i> , 2003;Galliero, 2010	20
3	10.75	1.42	Galliero, 2010	42
4	10.9	1.48	Galliero, 2010; McDowell and Blas, 2009	80
5	11.5	1.59	Galliero, 2010	115
8	13	1.83	McDowell and Blas, 2009	360
12	15.3	2.05	McDowell and Blas, 2009	880
16	17	2.25	Escobedo and de Pablo, 1996	1580

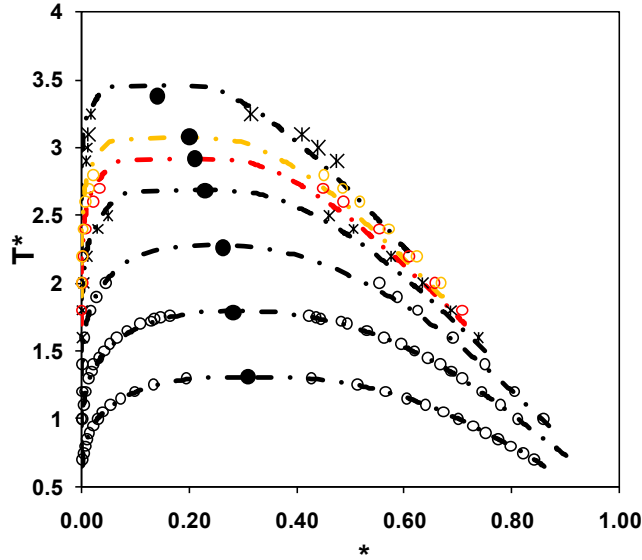
We have observed that the values obtained for crossover and influence parameters can be correlated as a function of the chain length  $m$ :

$$= 0.0051 m^2 + 0.3947 m + 9.521 \quad (4.1)$$

$$\frac{L}{\rho} = 0.0016 m^2 + 0.9392 m + 1.1591 \quad (4.2)$$

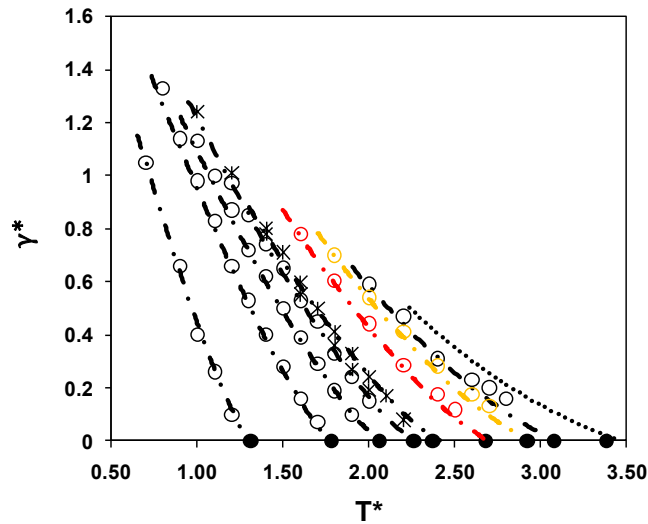
$$10^{19} c_{LJ} = 6.7608 m^2 - 9.5306 m + 7.3377 \quad (4.3)$$

These correlations can be used to predict the behavior of other LJ chains for which simulation data are not available. As a test of their validity, the predicted parameters for  $m=32$  have been obtained using the correlations Eq (4.1)-(4.3) reaching good agreement when compared with simulation data. In all the rest of cases ( $m=1$  to  $m=16$ ) the calculations are in very good agreement, within the associated error of the simulation points, with the data reported in the literature [Lofti *et al.*, 1992; Escobedo and de Pablo, 1996; Duque *et al.*, 2004; McDowell and Blas, 2009; Vega *et al.*, 2003; Galliero, 2010].



**Figure 4.2:** Phase equilibria diagram of LJ chains from  $m=1$  to  $m=32$  (from bottom to top). Symbols are simulation data while lines are the calculations with the crossover soft-SAFT. See text for details.

The calculation of the interfacial tension with soft-SAFT + DGT is shown in Figure 4.3. For the all studied fluids, an excellent agreement between simulation data [Lofti *et al.*, 1992; Escobedo and de Pablo, 1996; Duque *et al.*, 2004; McDowell and Blas, 2009; Vega *et al.*, 2003; Galliero, 2010] and the calculations with the crossover soft-SAFT + DGT approach has been obtained, far from and near to the critical point, due to the inclusion of the crossover term. The combination of the renormalization-group technique with the DGT allows the right description of the critical region up to the critical point, where the interfacial tension vanishes.



**Figure 4.3.:** Vapor-liquid interfacial tension of LJ chains from  $m=1$  to  $m=32$  (from left to right). Symbols are simulation data while lines are the calculations with the crossover soft-SAFT combined with the DGT. The dotted line is a prediction using Eqs. (4.1)-(4.3). See text for details.

## 4.2. Experimental systems: modeling of pure compounds

As explained already, it is necessary to build a physically meaningful molecular model for each compound before proceeding to the optimization of the molecular parameters with soft-SAFT. The main advantage of using a statistical-mechanics based equation of state versus to other classical approaches lays on the physical description of the molecule built into the equation by a coarse-grained model. Here, I have kept a relatively simple model while retaining the main physical features of the different systems investigated. Particular care needs to be taken in the choice of the model and the optimization of the molecular parameters. A short explanation for the different type of molecular models used for this thesis follows.

**Hydrocarbon, perfluorocarbon and inorganic molecules** are represented as united atoms or sites with non polar and non-associating interactions. Each site is assigned parameter values to represent a group of atoms in the molecule of interest, such as O-O, N-O, CH<sub>3</sub>, CH<sub>2</sub> or CH groups. In the soft-SAFT approach, these molecules are modeled as  $m$  LJ segments of equal diameter,  $\sigma$ , and the same dispersive energy,  $\epsilon$ , bonded to form the chain.

**Nitriles** and **sulfur dioxide** are polar molecules and different models can take into account this polar nature. Following other authors [Belkadi *et al.*, 2010] I have modeled **nitriles** as chains with a single association site,  $A$ , located on the CN group, representing the dipolar moment. Hence, although the dipolar moment is not explicitly taken into account its effect is implicitly considered in the association parameters.

**Sulphur dioxide** (SO<sub>2</sub>) is a bent molecule surrounded by 4 electron pairs and can be described as a hypervalent molecule. Its structure has some similarities with the NO<sub>2</sub> molecule, although in this case, no dimerization has been observed. There are three regions of electron density around the central sulphur atom. The SO<sub>2</sub> molecule is characterized by a relatively small polar moment, including dipolar and quadrupolar interactions. I have decided to

account for the polar interactions in the soft-SAFT model, mimicking the dipole moment in an effective manner with two associating sites of different nature (1 positive and 1 negative). This approach has been followed for other polar molecules, such as HCl [Llovel *et al.*, 2007], obtaining a good representation of the phase diagram of the fluid. Hence, SO<sub>2</sub> is modeled as an associating molecule with two specific association sites, *A* and *B*, and only *AB* association interactions are allowed [Llovel *et al.*, 2012].

**1-Alkanols** are similar to n-alkanes molecules but with a hydroxyl group in the end of the chain. This OH group in alkanols is mimicked by two square-well sites embedded off-center in one of the LJ segments, with volume and energy of association  $k_{HB}$  and  $\epsilon_{HB}$ , respectively. These two associating sites are represented by *A* and *B* in the model and only *AB* association is allowed. Different approximations with three and four association sites have been used to describe other molecules such as **hydrogen sulfide** (2*A*,1*B*), **ammonia** (3*A*,1*B*) or **water**, modeled with 2*A* sites and two *B* sites.

Two of the families of ionic liquids considered, **alkyl-imidazolium-[BF<sub>4</sub>]** and **alkyl-imidazolium-[PF<sub>6</sub>]** ionic liquids are modeled as homonuclear LJ chainlike molecules with one associating site, *A*, in each molecule, mimicking the anisotropic interaction felt when one cation-anion pair approaches another. This model mimics the neutral pairs (anion plus cation) as a single chain molecule with this association site describing the specific interactions because of the charges and the asymmetry.

The model used for the third family of ionic liquids, the **[Tf<sub>2</sub>N]<sup>-</sup>imidazolium** family is slightly different, taking into account the delocalization of the anion electric charge due to the oxygen groups, which enhance the possibility of interaction with the surrounding cations through them. Hence, [C<sub>n</sub>-mim][Tf<sub>2</sub>N] ILs are modeled as homonuclear chainlike molecules with three associating sites: one associating *A* type site represents the nitrogen atom interactions with the cation, while two *B* sites represent the delocalized charge due the oxygen molecules on the anion, allowing only *AB* interactions between different IL molecules [Andreu and Vega, 2008].






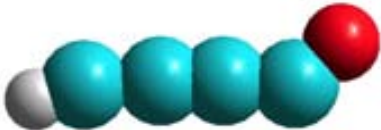

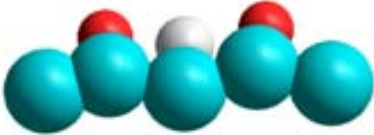




The **carbon dioxide** molecule is modeled as a LJ chain in which explicit quadrupolar interactions are taken into account. In this case, the molecule is represented by five molecular parameters:  $m$ , the chain length,  $\sigma$ , the segment size,  $\epsilon$ , the energy parameter of the segments making the chain and those related to the quadrupolar interactions: the quadrupolar moment  $Q$  and  $x_p$ , defined as the fraction of segments in the chain that contains the quadrupole. This model has already been used with success to describe the behavior of CO<sub>2</sub> on different systems [Andreu and Vega, 2007;2008; Belkadi *et al.*, 2008; 2010; Dias *et al.*, 2006; Vega *et al.*, 2010; Vilaseca and Vega, 2011].

For consistency, I have used here the n-alkanes, 1-alkanols, nitriles and ionic liquids models and parameters from previous published work from the research group, in a transferable manner [Pàmies and Vega, 2001; Dias *et al.*, 2004; Llovel *et al.*, 2004; Llovel and Vega, 2006 a,b; Andreu and Vega, 2007; Belkadi *et al.*, 2010; Llovel *et al.*, 2011].

In all cases, as stated, two additional parameters,  $L$  and  $\phi$ , previously defined, are needed when the crossover term is added.

After this introductory part, a more detailed explanation of the model used for each compound or family of compounds is given in each section, when needed. In Table 4.2 the molecular model used for each molecule or family studied in this thesis have been compiled and presented:

**Table 4.2** Molecular models used in this thesis.

MOLECULAR MODEL	# of association SITES	COMPOUNDS
	0	n-Alkanes, Ar, H <sub>2</sub> , O <sub>2</sub> , N <sub>2</sub> , CO, PFC
	1	[C-mim][BF <sub>4</sub> ] [C-mim][PF <sub>6</sub> ]
	1A 1B	Light Alkanols
	1A 1B	Nitriles, HFC
	1A 1B	SO <sub>2</sub>
	1A 2B	[C-mim][Tf <sub>2</sub> N]
	2A 1B	H <sub>2</sub> S
	3A 1B	NH <sub>3</sub>
	2A 2B	H <sub>2</sub> O
	*	CO <sub>2</sub> *Quadrupole

### 4.2.1. Nonassociating compounds<sup>6</sup>

In the context of the soft-SAFT equation, the simplest molecular fluids that can be modeled are the nonassociating compounds. As stated, they are modeled as  $m$  LJ segments of equal diameter,  $\sigma$ , and the same dispersive energy,  $\epsilon$ , bonded to form the chain. The first modeled compounds are monatomic and diatomic gases as is the case of argon, oxygen, hydrogen or nitrogen. After dealing with these inorganic compounds other industrially relevant gases, such as carbon monoxide or carbon dioxide are also modeled, followed by the most common industrial common nonassociating compounds like n-alkanes, including heavy alkanes. All of them are presented in this section.



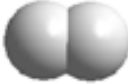



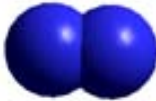
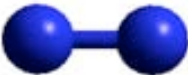

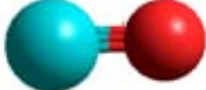

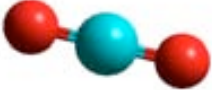
---

<sup>6</sup> Part of this section has been published in Vilaseca, O. and Vega, L.F. Direct calculation of interfacial properties of fluids close to the critical region by a molecular-based equation of state. *Fluid Phase Equilib.* **2011**, 306, 4-14.

### 4.2.1.1. Inorganic compounds

Nonassociating inorganic molecules are generally the effortless molecules to model, as most classical approaches accurately describe their behavior. Regarding their molecular structure some of them are formed by two equal atoms with simple, double or triple bonding or as in the case of noble gases with only one atom forming each molecule. This section starts from one of the simplest molecules, argon and oxygen, to finish with carbon dioxide. In Table 4.3., the model used for each inorganic compound presented within this section, in their atomistic and coarsed grain model, is shown.

**Table 4.3** Molecular sketch for the compounds studied in this section.

<b>COMPOUND</b>	<b>COARSED GRAIN MODEL</b>	<b>ATOMISTIC MODEL</b>
<b>Ar</b>		
<b>H<sub>2</sub></b>		
<b>O<sub>2</sub></b>		
<b>N<sub>2</sub></b>		
<b>CO</b>		
<b>CO<sub>2</sub></b>		

The simplest real gases that can be found in nature (most of them present in the atmosphere that surrounds the earth) like argon, hydrogen, oxygen and

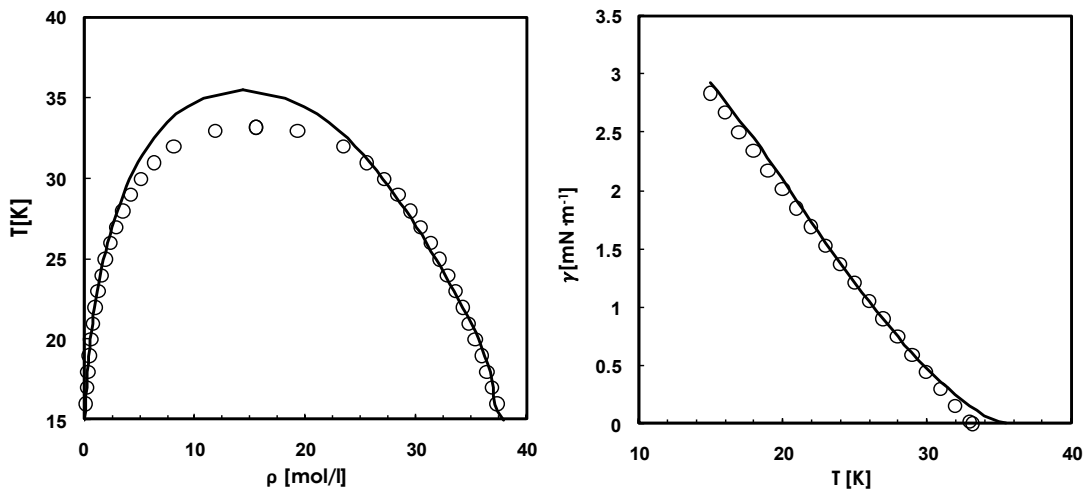
nitrogen are firstly presented. They also have great importance for industrial purposes; hydrogen is expected to be one of the “future fuels”, oxygen is a raw material for a wide variety of industrial processes, also to environmentally improve some of them, as well as key for human life. Nitrogen is also used in several applications, for instance, as a surface cleaning agent in pipes or reactors [United States Patent 5294261], for cryogenic applications, for inertitation, etc. Carbon monoxide is used in the modified packaging industry or in the Monsanto process as a raw material for the production of acetic acid [Sunley and Watson, 2000]. Nevertheless, the Fischer-Tropsch is the most important industrial process in which carbon monoxide is employed [Iglesia, 1997]. It consists on the hydrogenation of carbon monoxide for the production of liquid hydrocarbon fuels or methanol. Also, this technology is employed to convert coal or biomass into biodiesel. As explained before, when the soft-SAFT approach is used to model these compounds, the molecular parameters are obtained by fitting with vapor pressure and liquid density correlated experimental data. In this work we have used, when possible, the NIST database. The calculation of the interfacial tension requires an additional parameter, the influence parameter  $c$ , optimized with the surface tension data. The molecular parameters used with soft-SAFT + DGT for these compounds are compiled in Table 4.4

**Table 4.4** Molecular parameters for the inorganic compounds, together with the references from where the parameters were originally obtained.

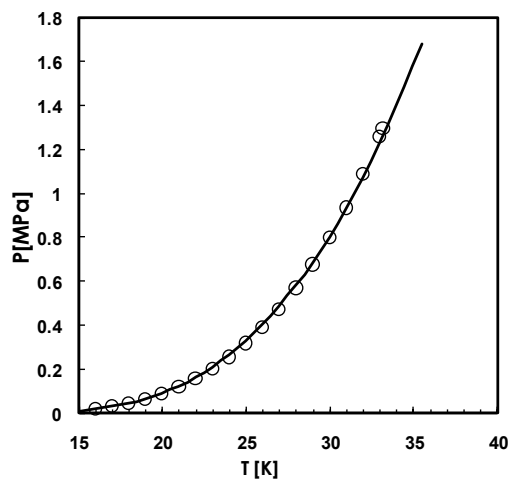
COMPOUND	$m$	$\sigma(\text{\AA})$	$\epsilon/k_B(K)$	$\phi$	$L/\sigma$	$Q(C\cdot m^2)$	Reference	$10^{19} c$ ( $J m^5 mol^{-2}$ )
H <sub>2</sub>	0.487	4.244	33.85				Pàmies, 2003	0.0135
Ar	1.106	3.280	110.90				Pàmies, 2003	0.1050
O <sub>2</sub>	1.168	3.198	111.50				Pàmies, 2003	0.0114
N <sub>2</sub>	1.427	3.181	82.90				Pàmies, 2003	0.0114
CO	1.466	3.170	85.63				Pàmies, 2003	0.1350
CO <sub>2</sub>	1.610	3.172	160.00	5.70	1.13	$4.4010^{-40}$	Belkadi <i>et al.</i> , 2008	0.2625

## Hydrogen

In Figure 4.4 the vapor liquid equilibria and the interfacial tension of hydrogen obtained with the soft-SAFT coupled with the DGT approach as compared to available experimental data are presented. As hydrogen will be always used far away from the critical point no crossover corrections have been applied. This is the reason why the critical properties are overestimated. Nevertheless a good agreement in the phase envelope and interfacial tension is achieved. As an example, in Figure 4.5 a  $P$ - $T$  diagram is presented in order to show the capability of the approach for the calculation of thermal and mechanical properties.



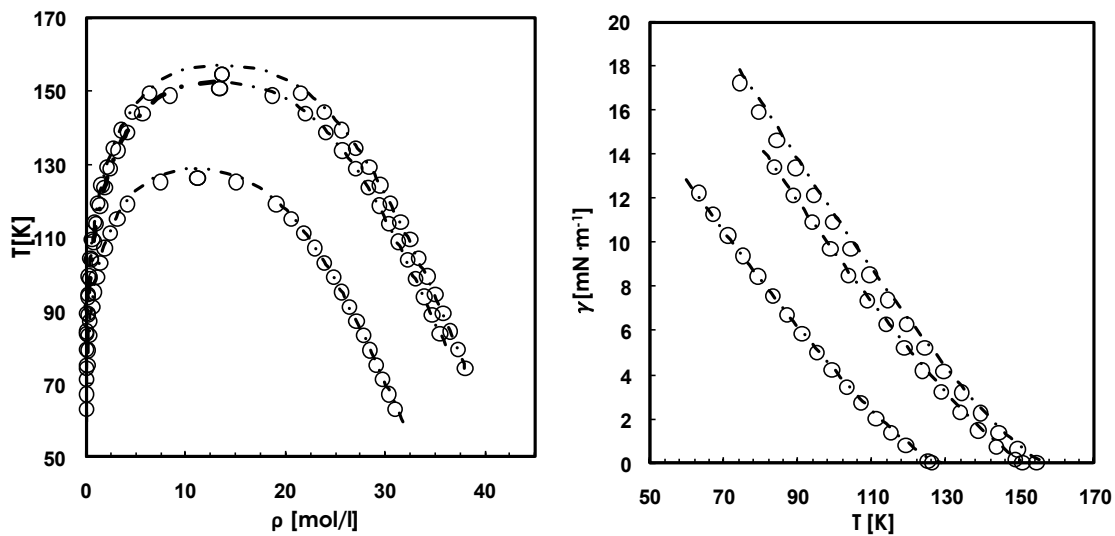
**Figure 4.4:** Vapor-liquid equilibrium (left) and interfacial tensions (right) of hydrogen. Symbols represent experimental data from NIST and lines correspond to soft-SAFT+DGT approach.



**Figure 4.5:** Predicted pressure-temperature diagram of hydrogen. Symbols represent experimental data from NIST and lines correspond to soft-SAFT+DGT approach as obtained in this work.

## Nitrogen, Argon and Oxygen

These three compounds are presented together as they represent compounds that mainly conform the air that we breathe away and they can also appear in an industrial flow. The vapor-liquid equilibria and the interfacial tension of argon, oxygen and nitrogen are obtained by crossover soft-SAFT combined with DGT as compared to available experimental data is depicted in Figure 4.6. As can be observed, soft-SAFT provides an excellent description of the phase envelope, with the application of the crossover [Llovel *et al.*, 2004] term capturing the critical region. The combination of crossover soft-SAFT with DGT provides equally accurate results for the interfacial tensions of these compounds.



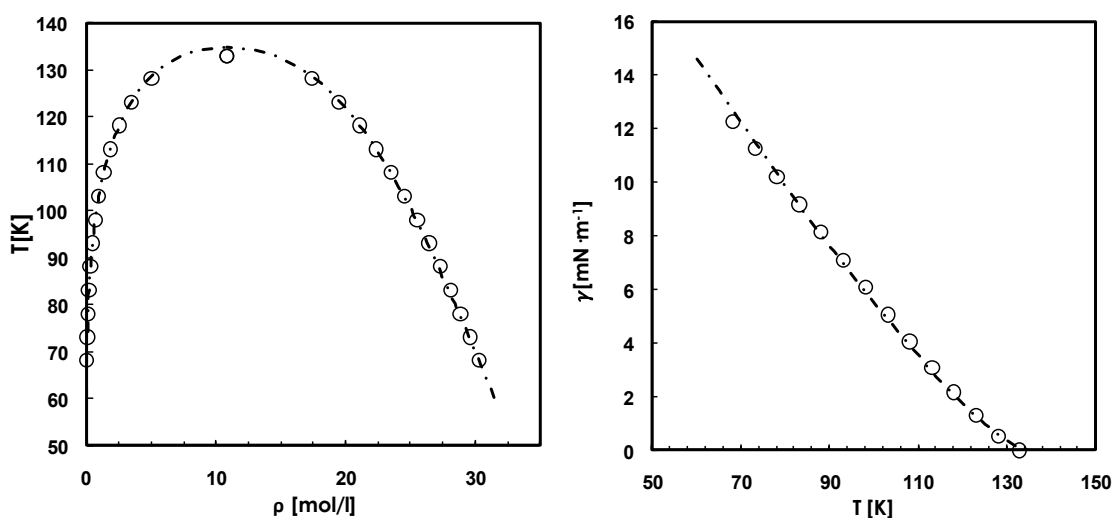
**Figure 4.6:** Vapor-liquid equilibria (left) and interfacial tensions (right) of nitrogen, argon and oxygen (from bottom to top). Symbols represent experimental data from NIST and lines correspond to crossover soft-SAFT+DGT approach. See text for details.

Note that for all the fluids, and the whole range of conditions good agreement between the soft-SAFT calculations and the experimental data is obtained. The interfacial tension is also in very good agreement with experimental data, even capturing the different shapes of the interfacial tension as a function of temperature.

## Carbon monoxide

As stated, carbon monoxide has multiple applications from food industry to petrochemical industry but it also represents a problem for the urban pollution. The main sources of this compound are the internal combustion engines and the incomplete combustion of several fuels including wood, natural gas, coal or trash. It also plays an important role in the ozone cycle at tropospheric level and it is responsible of some of the series of chemical reactions that produces photochemical smog. [Westberg *et al.*, 1971]

The interfacial tension of carbon monoxide obtained by crossover soft-SAFT combined with DGT as compared to available experimental data is depicted in Figure 4.7. As shown in the Figure, the equation is able to provide an excellent agreement in the whole temperature range, far from and close to the critical point.



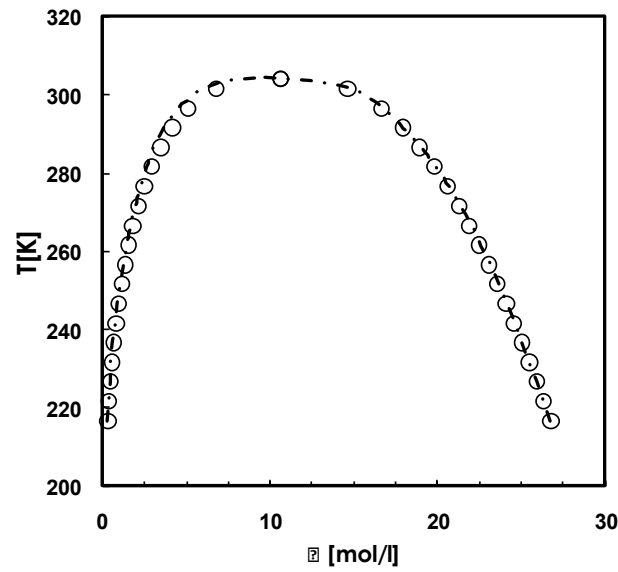
**Figure 4.7:** Vapor-liquid equilibria (left) and interfacial tension as a function of temperature (right) of carbon monoxide. Symbols represent experimental data from NIST and lines correspond to crossover soft-SAFT+DGT approach.



## **Carbon dioxide**

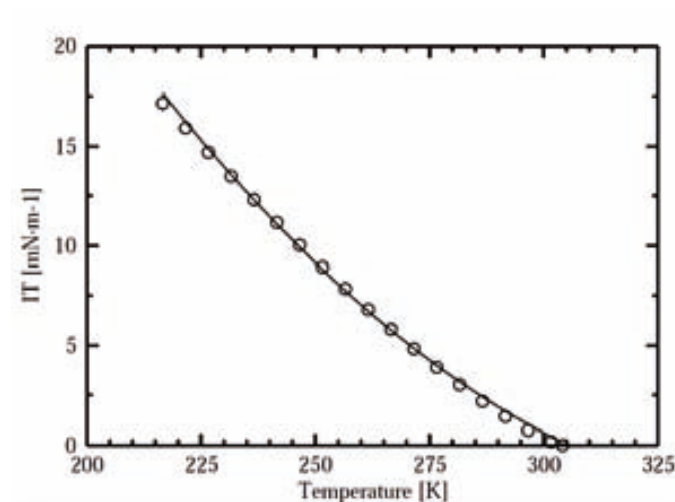
CO<sub>2</sub> is composed of two oxygen atoms covalently bonded to a single carbon atom. At standard conditions, it is a gas and it is present in the Earth's atmosphere. At low temperatures, below 195 K, it is in the solid state and it is known as dry ice, which has some industrial applications. The current average concentration of CO<sub>2</sub> in the atmosphere is approximately of 397 ppm by volume [co2now.org]. The human being is increasing its global concentration by the combustion of fossil fuels, but natural processes are also producing huge quantities of carbon dioxide, including volcanoes or during the breathing of vivacious beings. Carbon dioxide is one of the most studied molecules at the moment due to its contribution to the climate change and also because of its many possible industrial applications. In fact the Global Warming Potential is referenced to the amount of energy trapped by a certain mass of a compound compared with carbon dioxide [GWP (CO<sub>2</sub>=1)]. New projects on capture and utilization of the CO<sub>2</sub> are being carried on all over the world, the storage of the captured CO<sub>2</sub> are being planned under high pressure and temperature conditions, so that means that a robust modeling for the understanding of the physical and chemical properties of carbon dioxide and its mixtures is needed in order to optimize the conditions for separation, storage and utilization of carbon dioxide.

I present next the vapor liquid equilibria and interfacial tensions of carbon dioxide as compared with available the experimental data from literature. As can be observed in Figure 4.8., an excellent description of both the liquid and the vapor phases are given by the soft-SAFT equation with the crossover treatment near and far from the critical point.



**Figure 4.8:** Temperature-density diagram of carbon dioxide. Symbols are experimental data from NIST and the dashed and dotted line is the prediction with the crossover soft-SAFT.

The interfacial tension of carbon dioxide obtained by crossover soft-SAFT combined with DGT as compared to available experimental data is depicted in Figure 4.9. As shown in the Figure, the equation is able to provide an excellent agreement in the whole temperature range with the same accuracy.



**Figure 4.9:** Vapor-liquid interfacial tension of carbon dioxide as a function of temperature. Circles represent experimental data [NIST] while lines correspond to the crossover soft-SAFT+DGT approach.

#### 4.2.1.2. Light n-Alkanes

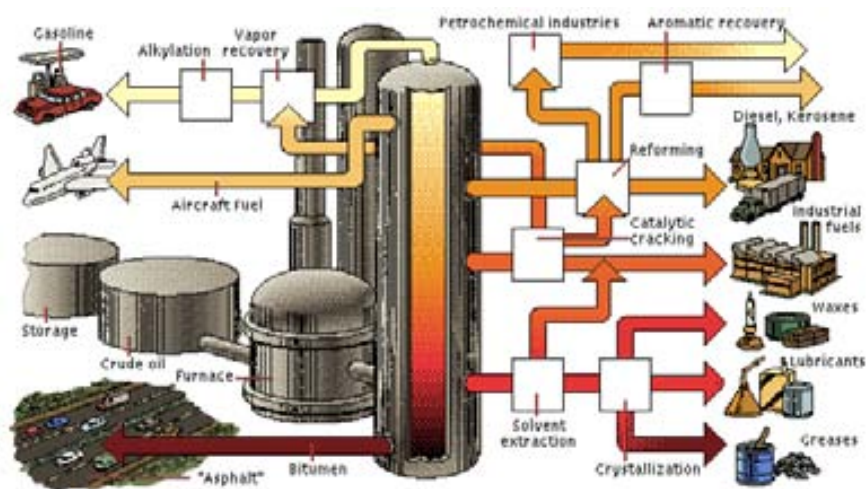
n-Alkanes are organic compounds formed by carbon and hydrogen atoms that have simple bonding C-C or C-H, which are known as saturated hydrocarbons. They are formed by the union of carbon molecules and a determined number of hydrogen atoms, making a neutral compound with no associating sites. Their simple lineal chain structure, their regularity as a chemical family and their importance for industrial purposes, make them almost the most studied compounds in the chemical engineering field [Heintz *et al.*, 2001]; also they are perfect candidate to test any new model developed, given their regularity. Other scientific related areas like physics or chemists are involved in the research of new models for the prediction of thermophysical properties especially in the critical region, without carrying on costly experiments under high pressure and temperature conditions, saving time and money so making the optimization of industrial processes faster and cheaper.



**Figure 4.10:** Example of a Graphical representation of n-pentane.

In the 20<sup>th</sup> century, possibly the most important molecules in the petrochemical industry have been the n-alkanes and derivatives. The petrochemical is based in this family of organic compounds, so the distillation of the petrol gives different cuts from methane to asphaltenes. They are then processed to obtain fuels, solvents, plastics, lubricants, candles or pharmaceutical products to enumerate some of them. Hydrocarbons play an important role in the chemical but also in the energetic field, where crude oil or the natural gas are blends of these molecules.

These examples give us an order of magnitude of the huge importance of hydrocarbons and its derivatives in our day to day life, see the schema below:



**Figure 4.11:** Schema of different hydrocarbons processes  
<http://www.emt-india.net/process/petrochemical/Petroleum.htm>

The chosen molecular model for the n-alkanes family used in this work is the same than the one adopted by Vega and collaborators [Blas and Vega, 1998; Pàmies and Vega, 2001; Llovel and Vega, 2006a], where n-alkanes are modeled as homonuclear chainlike molecules, composed of  $m$  Lennard-Jones segments of equal diameter  $\sigma$  and the same dispersive energy  $\epsilon$ , bonded tangentially to form the chain [Chapman, 1989]. According to Llovel and Vega [Llovel and Vega, 2006b] these three molecular parameters plus the crossover parameters  $\phi$  and  $L$ , are enough to describe all thermodynamic properties because no association parameters are needed in this case. The molecular parameters fitted to vapor liquid equilibria data are used in a transferable manner for the interfacial property calculations, i.e. no additional fitting is needed to obtain these parameters [See Table 4.5]. To calculate interfacial properties with DGT, the influence parameter is required. As for previously presented compounds, this parameter is fitted for each pure compound using interfacial tension experimental data from the triple up to the critical point [Landolt-Börnstein; NIST]. The resulting values are given in Table 4.6.

**Table 4.5.** Molecular parameters for the light alkanes studied in this work.

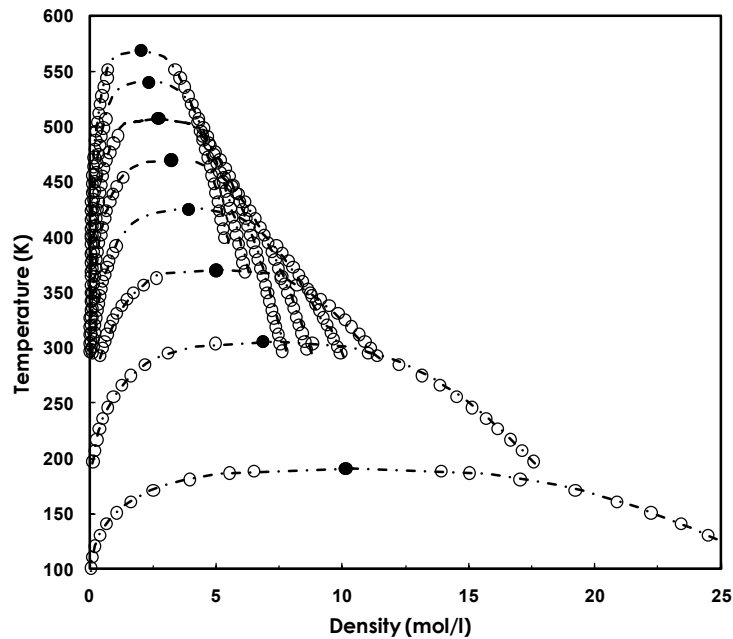
[Llovel et al. 2004]

COMPOUND	M	$\sigma(\text{\AA})$	$\varepsilon/k_B(\text{K})$	$\phi$	L/ $\sigma$
methane	1.000	3.741	151.1	5.50	1.04
ethane	1.392	3.770	207.5	6.20	1.10
propane	1.776	3.831	225.8	6.75	1.16
n-butane	2.134	3.866	240.3	7.25	1.22
n-pentane	2.497	3.887	250.2	7.57	1.27
n-hexane	2.832	3.920	259.8	7.84	1.33
n-heptane	3.169	3.937	266.0	8.15	1.38
n-octane	3.522	3.949	271.0	8.30	1.43

**Table 4.6.** Optimized influence parameters for the light alkanes studied in this work.

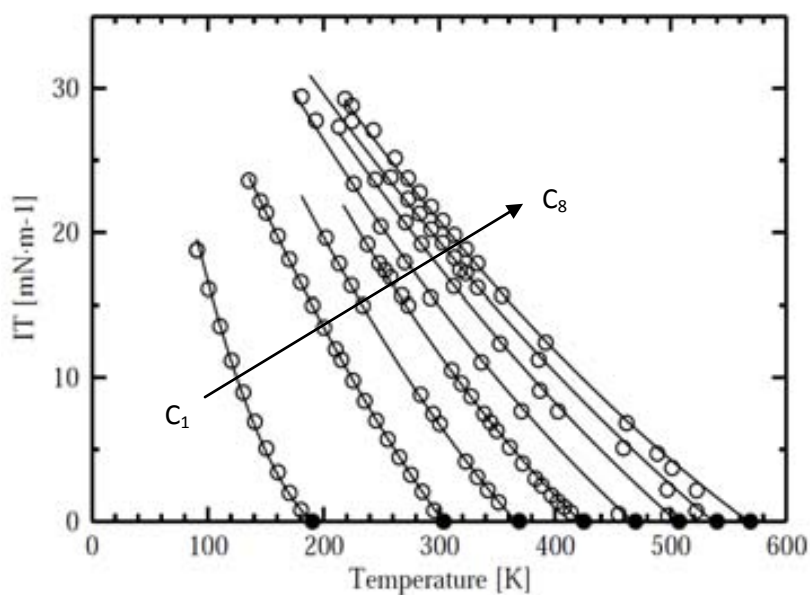
COMPOUND	$10^{19} c$ (J m <sup>5</sup> mol <sup>-2</sup> )
Methane	0.2522
Ethane	0.5999
Propane	1.142
n-butane	1.821
n-pentane	2.558
n-hexane	3.556
n-heptane	4.585
n-octane	5.728

In Figure 4.12 results obtained with soft-SAFT for the vapor-liquid equilibria of pure alkanes are shown. Calculations have been done for the first eight members of the n-alkanes family, from methane to n-octane. It can be observed that an excellent agreement between experimental data and the soft-SAFT predictions are obtained in all cases.



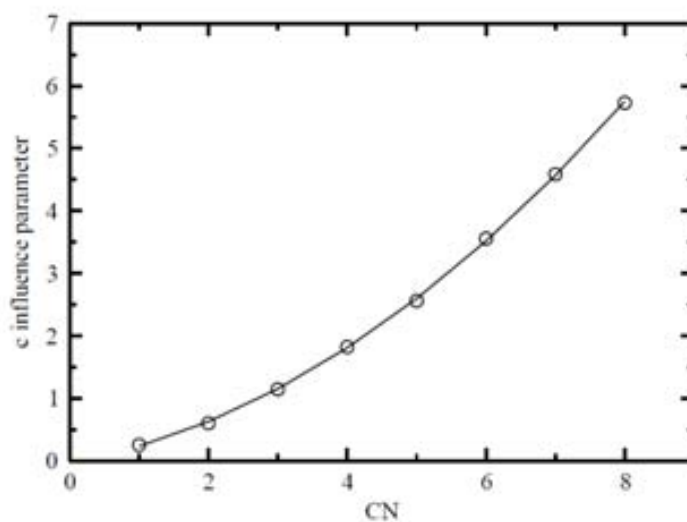
**Figure 4.12:** Vapor-liquid equilibria of *n*-alkanes, from methane to *n*-octane (from left to right). Symbols are experimental data from references [Landolt-Börnstein; NIST] and the dashed and dotted lines correspond to the crossover soft-SAFT combined with the DGT calculations.

Results concerning the vapor liquid interfacial tension for the *n*-alkanes series as obtained by crossover soft-SAFT and its combination with DGT for the interfacial properties are presented in Figure 4.13, together with the available experimental data [NIST; Landolt-Börnstein], obtaining an overall excellent agreement between experimental data and the description with crossover soft-SAFT is reached in all cases. The incorporation of the crossover treatment allows an accurate description of the interfacial tension for the whole range of temperatures, including the critical region.



**Figure 4.13:** Vapor-liquid interfacial tensions of *n*-alkanes, from methane to *n*-octane (from left to right). Symbols are experimental data from references [NIST; Landolt-Börnstein] and the full lines correspond to the predictions of the crossover soft-SAFT+DGT approach.

It has been observed that, as it happens with other molecular parameters for regular chemical families, the influence parameter for the light *n*-alkane series can be correlated with respect to the carbon number of the chain (or molecular weight of the molecules).



**Figure 4.14:** Optimized influence parameter for the light members of the *n*-alkane (circles) series versus the carbon number. Lines correspond to the values obtained from Equation 4.4.

As happened when compared to simulation data, a parabolic function is found to represent the influence parameter against the carbon number.

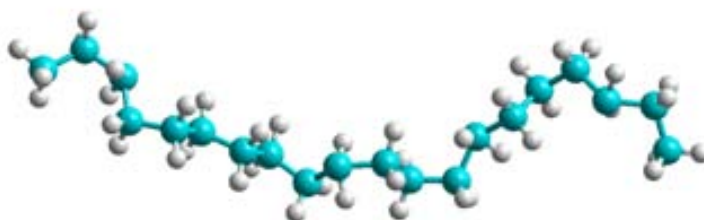
$$10^{19} c_{n \text{ alkanes}} = 0.0658 CN^2 + 0.1962 CN - 0.0908 [Jm^5 mol^{-2}] \quad (4.4)$$

This correlation is been plotted in Figure 4.14 together with the tabulated values provided in Table 4.6. It allows obtaining the interfacial behavior of heavier compounds of the series not included in the fitting procedure as well as the behavior of mixtures formed by these compounds, expanding the predictive capabilities of the equation (see section 4.3.1.1). This is a clear advantage of using a molecular-based equation of state such as the one used in this work versus other classical approaches.

### 4.2.1.3. Heavy n-Alkanes

Heavy n-alkanes are key compounds with a very little amount of experimental data concerning the phase equilibria of the pure fluids as well as binary mixtures, with even more scarce data on ternary mixtures. Some experimental data is also available for the surface tension of pure compounds, but more data on interfacial properties of heavy compounds is needed as well as for binary mixtures; as interfacial properties rule out important phenomena dealing with phase separation, adsorption, wetting, etc,

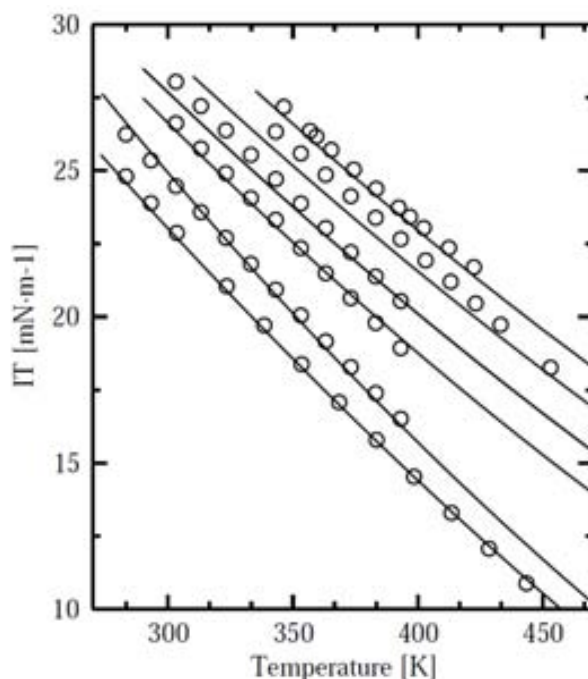
The main problem with heavy n-alkanes measurements is the fact that at high temperatures are difficult to hold, as they decompose above 600K. However, this data is needed for mixtures calculations, as models are based in data from pure compounds. Since most of the models available in the literature deal either with bulk phases or interfacial properties, it is desirable to have approaches able to simultaneously predict, with equal accuracy, phase and interfacial properties of these relevant industrial fluids.



**Figure 4.15:** Molecular 3D representation of *n*-eicosane (C=20).



Using the correlation provided in Equation (4.4) the vapor liquid interfacial tensions of several compounds which are not included in the series have been predicted, avoiding the need of additional fitting. As is stated, this is one of the main goals of the present Thesis work as it is important to keep a model with a high degree of transferability. Figure 4.16 depicts results obtained by soft-SAFT coupled with DGT for *n*-decane, *n*-dodecane, *n*-hexadecane, *n*-eicosane, *n*-hexacosane and *n*-dotriacontane as compared to available experimental data [Carvalho *et al.*, 2008; NIST]. The modeling approach provides excellent accuracy as compared to experimental data. The molecular parameters for these compounds were obtained from the correlation with the molecular weight presented in reference [Llovel *et al.*, 2004]. Note that these are pure predictions from the correlations, without any fitting, empowering the equation with predictive power for other members of the family for which experimental data is not available.



**Figure 4.16:** Predicted vapor-liquid interfacial tensions of heavy *n*-alkanes: *n*-C<sub>10</sub>, *n*-C<sub>12</sub>, *n*-C<sub>16</sub>, *n*-C<sub>20</sub>, *n*-C<sub>26</sub>, *n*-C<sub>32</sub> (from bottom to top). Symbols represent experimental data [NIST; Landolt-Börnstein] and lines correspond to the crossover soft-SAFT+DGT approach. See text for details.

## *Chapter 4*

Also note that classical modeling methods require knowledge of the critical point of the pure compounds which cannot be achieved experimentally for these systems, as they decompose before reaching the critical point. Hence, classical methods rely on correlations for critical points for obtaining this data, while our method only needs the correlation obtained from the lighter members of the series.

## 4.2.2. Associating compounds

The main distinguishable feature of the SAFT approach versus other modeling methods is the specific term for taking into account hydrogen-bonding and other associating interactions. In combination with the Density Gradient Theory, its capacity is extended to the calculation of the interfacial properties of associating compounds. In this section, some of the most common and representative industrial compounds are modeled: hydrogen sulfide, sulfur dioxide, ammonia, water, 1-alkanols, nitriles, refrigerants and, finally, ionic liquids are presented.

### 4.2.2.1. Hydrogen sulfide, ammonia and sulfur dioxide

Once again, to account on the different interaction sites a suitable model has to be proposed. A short description of all of these compounds and the results obtained are shown next.






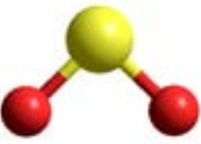
Hydrogen sulfide is a very challenging compound due to the delocalization of different associating interactions. A model with 3 associating sites is chosen: 2 for the sites of type *A* for the hydrogen atoms and 1 site of type *B* for the electronegativity of the sulfur, with only A-B interactions allowed. In Table 4.7a a molecular sketch of the model can be observed.

Sulfur dioxide is used in the wine industry, as a food additive, or as a bleaching agent [morethanorganic.com] but it is for the most part used for the production of sulfuric acid. This molecule is present in almost all flow rates in petrochemical industry and also used massively in the production of sulfuric acid. It is formed by two oxygens bonded to a sulfur atom, both presenting large polar activities. [Llovel *et al.*, 2012] It is a bent molecule surrounded by 4 electron pairs and can be described as a hypervalent molecule. There are three regions of electron density around the central sulphur atom. The SO<sub>2</sub> molecule is characterized by a relatively small polar moment, including dipolar and quadrupolar interactions. In this work we

have considered the dipole moment in an effective manner with two associating sites of different nature (1 positive and 1 negative). This approach has been followed for other polar molecules, such as HCl [Llovell *et al.*, 2007], obtaining a good representation of the phase diagram of the fluid. Hence, SO<sub>2</sub> is modeled as an associating molecule with two specific association sites, *A* and *B*, and only *AB* association interactions are allowed [Llovell *et al.*, 2012].

The first truly refrigerants like ammonia (R-717) were developed during the last part of the 19th century and during the first part of the 20<sup>th</sup> century. Today it is a very common fluid used in industry, from processing to refrigerating systems; this is a key compound nowadays. The ammonia is modeled with four sites; three associating sites of type A and one associating site of type B.

**Table 4.7** Molecular sketch for the compounds studied in this section.

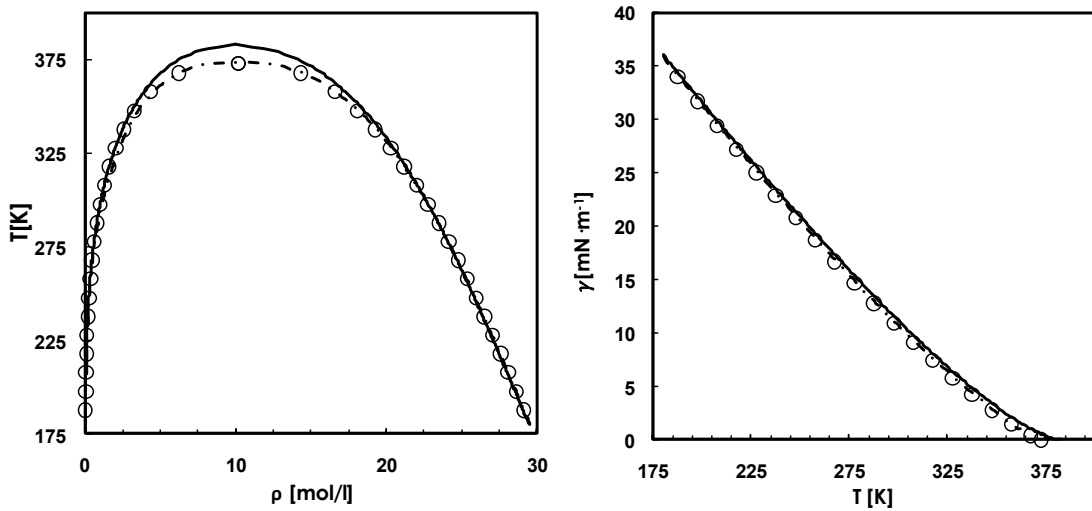
COMPOUND	COARSED GRAIN MODEL	ATOMISTIC MODEL	MOLECULAR MODEL
H <sub>2</sub> S			2A 1B
NH <sub>3</sub>			3A 1B
SO <sub>2</sub>			1A 1B

Once the model is chosen (see Table 4.7) we follow the same procedure as for the other compounds: molecular parameters are fitted to VLE and interfacial tension data to calculate the thermophysical properties of the selected compounds. The results are presented in Table 4.8.

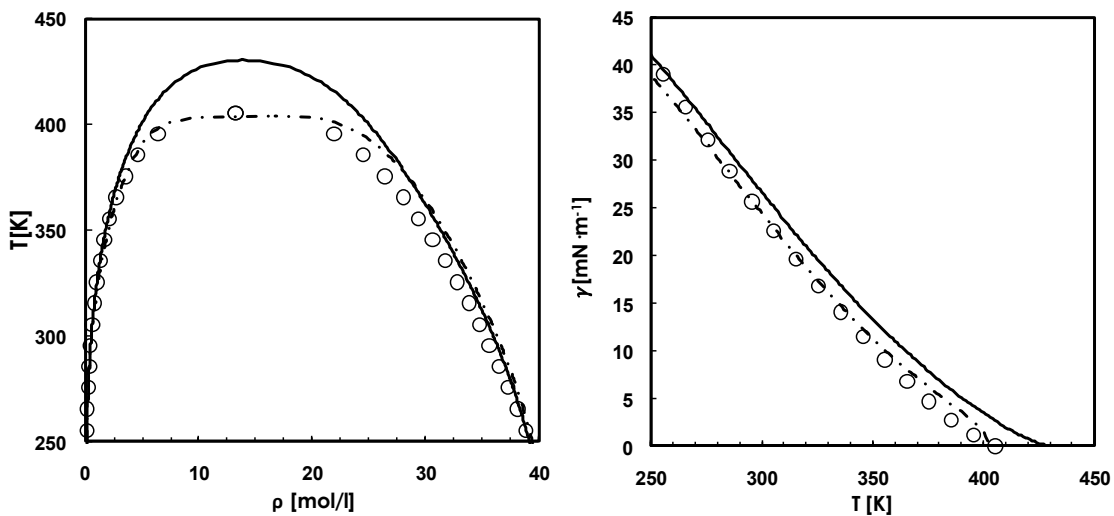
**Table 4.8.** Optimized parameters for the inorganic associating compounds.

COMPOUND	m	$\sigma(\text{\AA})$	$\epsilon/k_B(\text{K})$	$\phi$	$L/\sigma$	$\epsilon_{\text{HB}}/k_B(\text{K})$	$\square_{\text{HB}}(\text{\AA}^3)$	$10^{19} c$ ( $\text{J m}^5$ $\text{mol}^{-2}$ )	Reference
H <sub>2</sub> S	1.706	3.060	225.8	6.60	1.07	673.8	500.6	0.3550	Llovell <i>et al.</i> 2012
NH <sub>3</sub>	1.000	3.390	308.0	4.60	1.00	1851	555.0	0.1975	Llovell <i>et al.</i> 2012
SO <sub>2</sub>	2.444	2.861	228.3	7.10	1.18	1130	601.0	0.4650	Llovell <i>et al.</i> 2012

Results concerning the vapor liquid interfacial tension for hydrogen sulfide and ammonia as obtained by crossover soft-SAFT and its combination with DGT for the interfacial properties are presented in Figure 4.17 and Figure 4.18, together with the available experimental data [Landolt-Börnstein; NIST]. As can be observed in Figures, an overall excellent agreement between experimental data and the description with crossover soft-SAFT is reached in all cases. The incorporation of the crossover treatment allows an accurate description of the interfacial tension for the whole range of temperatures, including the critical region.



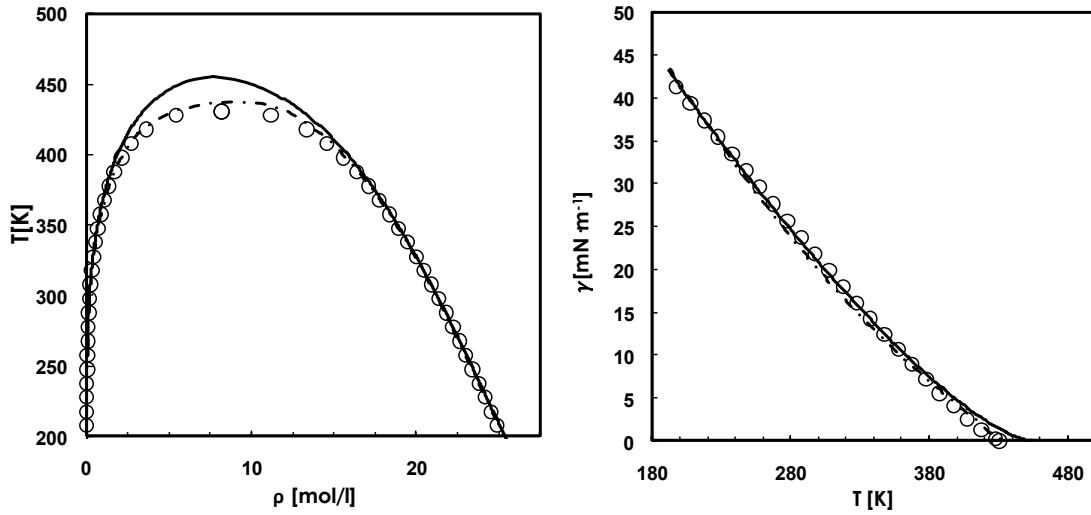
**Figure 4.17:** Vapor-liquid diagrams (left) and interfacial tensions (right) of hydrogen sulfide. Symbols represent experimental data [NIST] and solid line corresponds to the soft-SAFT+ DGT approach while the dashed and dotted line corresponds to the crossover soft-SAFT+DGT approach. See text for details



**Figure 4.18:** Predicted vapor-liquid diagrams (left) and interfacial tensions (right) of ammonia. Symbols represent experimental data [NIST] and solid line corresponds to the soft-SAFT+ DGT approach while the dashed and dotted line corresponds to the crossover soft-SAFT+DGT approach.

A comparison for the values obtained using the crossover or the original version of the soft-SAFT EoS are depicted in Figure 4.19. As can be observed, while noncrossover version does not capture the critical region, the equation including the crossover treatment is able to provide an excellent agreement in

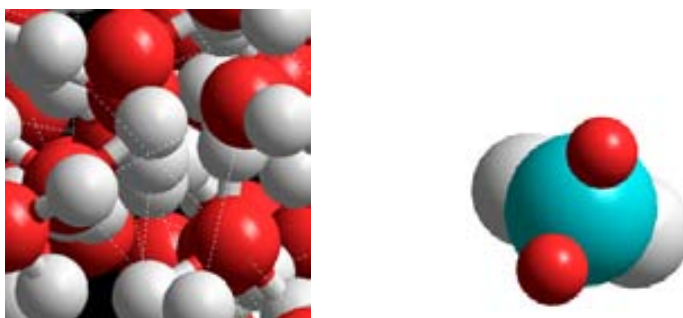
the whole temperature range, far from and close to the critical point. The interfacial tension of sulfur dioxide is also obtained, by means of the crossover and the noncrossover soft-SAFT combined with DGT and compared to available experimental data. As shown in the Figure, only the crossover version is able to capture the shape near the critical region, as expected.



**Figure 4.19:** Phase equilibria of sulfur dioxide. Symbols are experimental data from NIST solid lines are obtained with the soft-SAFT EoS +DGT and the dashed and dotted line are the predictions with the crossover soft-SAFT EoS + DGT. Temperature-density diagram (left) and Interfacial tension-temperature diagram (right).

### 4.2.2.2. Water<sup>7</sup>

Water is another fascinating compound: in spite of extensive studies about it, the available experimental data existing in the literature and its importance for our life as well as for several processes, this is one of the most challenging compounds from the modeling point of view. The main reason for this complexity is the associating nature of this compound – the anisotropic hydrogen bonding observed in H<sub>2</sub>O exerts an important influence on its thermophysical properties and phase behavior. Moreover it exhibits several particularities such as, for instance, a huge liquid density range with an unusual behavior at low temperatures exhibiting a density maximum in the liquid density at 277K. Hence, this compound is a very stringent test for any EoS. Here, the water molecules are modeled as a single spherical LJ core, accounting for the repulsive and dispersive forces between different molecules of the fluid, with four embedded off-center square well bonding sites. These four associating sites account for the two electron lone pairs and the two hydrogen sites of the water molecule. The four sites are represented by two A sites and two B sites, and only AB association is allowed between different molecules. This model has proved to give excellent results for pure water and also for water-hydrocarbon mixtures [Vega *et al.*, 2009].



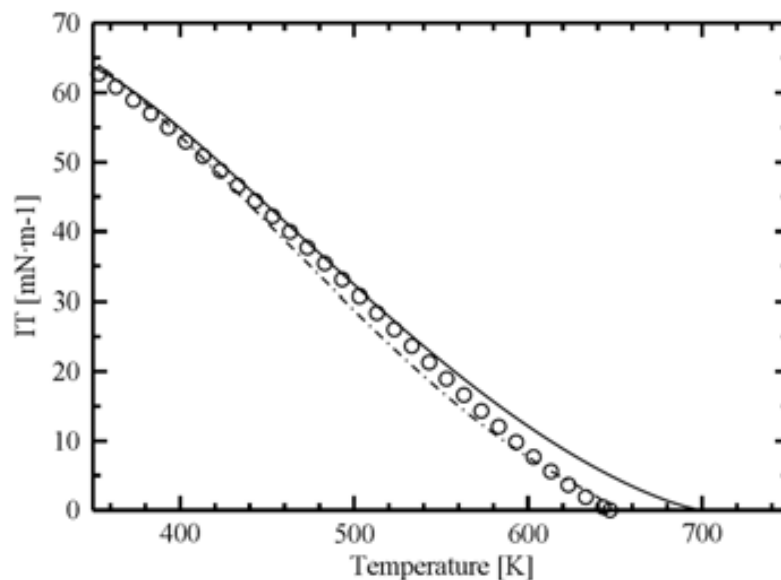
**Figure 4.20:** Representation of hydrogen bonding between water molecules and the chosen molecular model.

Hydrogen bonding interactions are included in the association term of the soft-SAFT equation, by means of the association volume and the association

<sup>7</sup> Part of this section has been published in Vilaseca, O. and Vega, L.F. Direct calculation of interfacial properties of fluids close to the critical region by a molecular-based equation of state. *Fluid Phase Equilib.* **2011**, 306, 4-14.



energy. Although water is also a polar molecule with dipole moment, polar effects are not explicitly considered and are somewhat effectively included in the association contribution. I have applied the soft-SAFT EoS, with and without crossover, coupled with DGT to water and results are shown in Figure 4.21 for vapor-liquid interfacial tensions, compared to experimental data.



**Figure 4.21:** Vapor-liquid interfacial tensions of water: original soft-SAFT + DGT, without the crossover term (solid line) and crossover soft-SAFT + DGT calculations (dotted and dashed line). Symbols represent experimental data from NIST database

Note the difference between the lines, while the critical point is overestimated with the classical soft-SAFT equation (solid line), the critical point is properly described if the crossover term is used (dotted and dashed line). The theory is also able to capture the S-shape (also observed in the previous section for ammonia) characteristic of the interfacial tension of water and, in general, strong hydrogen-bonding systems, difficult to achieve with most modeling approaches.

Some authors [Yang, Rowlinson] suggested that the S-shape of the surface tension curve was due to the surface entropy effects, though only this fact cannot explain the tendency of the surface tension but it can contribute on the understanding of other physicochemical properties of water. It has been demonstrated that far from the critical point both treatments provide quite similar results, but with the crossover term, the maximum  $-(d\sigma/dT)$  at about

473 K is described qualitatively. The deviations in this case are due to the chosen model from reference [Vega *et al.*, 2009] for the description of the water VLE (see the cited reference for more details on the water model).

The robustness of the soft-SAFT model is again revealed in this case; as no reparameterization is needed [See Table 4.9] and only the influence parameter has been fitted to experimental data from NIST database [See Table 4.10], to keep the model as predictive as possible.

**Table 4.9.** Molecular parameters for water (with and without crossover, together with the reference where the parameters were originally obtained).

COMPOUND	m	$\sigma(\text{\AA})$	$\epsilon/k_B(\text{K})$	$\phi$	L/ $\sigma$	$\epsilon_{\text{HB}}/k_B(\text{K})$	$\square_{\text{HB}}(\square^3)$	Reference
water with crossover	1.000	3.137	458.0	5.00	1.00	1037	2501	Vega <i>et al.</i> , 2009
water without crossover	1.000	3.137	480.0	-	-	923.2	2612	Vega <i>et al.</i> , 2009

**Table 4.10.** Optimized influence parameters for water.

COMPOUND	$10^{19} c (\text{J m}^5 \text{ mol}^{-2})$
water with crossover	0.0939
water without crossover	0.0803

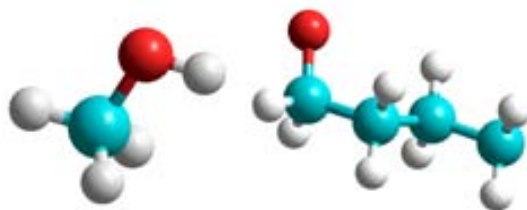
### 4.2.2.3. Light Alkanols<sup>8</sup>

The first alcohol (ethanol) was discovered by the Persian alchemist Al-Razi in the X<sup>th</sup> century. Nowadays these fluids play a key role in the medical area or in the production of alcoholic beverages. They are also employed in other industrial processes such as the manufacture of reagents, perfumes, cosmetics, solvents, medical drugs or vegetal essences such as vanilla, as well as bio-fuel which is in essence ethanol. The shortest alkanols (C<sub>1</sub>-C<sub>4</sub>) can be produced from the fermentation of glucose or by chemical reactions such as substitution, reduction of aldehydes or ketones, hydrolysis of alkanes, dehydration, oxidation or esterification among others.

From a molecular point of view alcohols are organic compounds characterized by the presence of hydroxyl group bounded to a carbon atom of an alkyl group or substituting an alkyl group on a bigger molecule. Due to the presence of the hydroxyl group their boiling points are higher than those of the equivalent n-alkanes having the same carbon number. Furthermore the shortest the alcohol the most soluble is in water due to its polarity. 1-alkanols are modeled as homonuclear chainlike molecules of equal diameter  $\sigma$  and the same dispersive energy  $\epsilon$ . The hydroxyl group in 1-alkanols is mimicked by two square-well sites embedded off-center in one of the LJ segments, with volume of association  $\kappa_{HB}$  and association energy  $\epsilon_{HB}$ . One site of *e* type corresponds to the lone pairs of electrons, and the other site is of type H corresponding to the hydrogen atom of the hydroxyl group (only *e*-H bonding is allowed). The pair of electrons is considered with only one site under the assumption that the structure of the molecule does not allow two hydrogen atoms to be associated at the same time due to sterical constraints, in accordance with the statements done by Pàmies, Vega and Llovel in their different works [Pàmies et al., 2001; Vega et al., 2005; Llovel et al., 2005], these five molecular plus the crossover parameters, are enough to describe all thermodynamic properties.

---

<sup>8</sup> Part of this section has been published in Vilaseca, O. and Vega, L.F. Direct calculation of interfacial properties of fluids close to the critical region by a molecular-based equation of state. *Fluid Phase Equilib.* **2011**, 306, 4-14.



**Figure 4.22:** Molecular 3D representation of 1-methanol and 1-butanol

The molecular parameters fitted to vapor liquid equilibria data are used in a transferable manner for the interfacial properties calculations, i.e. no additional fitting is needed to obtain these parameters [See Table 4.11]. As shown before, to calculate interfacial properties with DGT the influence parameter for each compound is required. In this work it has been optimized for each pure 1-alkanol using interfacial tension experimental data [Jasper, 1972; Landolt-Börnstein; NIST] from the triple to the critical point. The resulting values are given in Table 4.12.

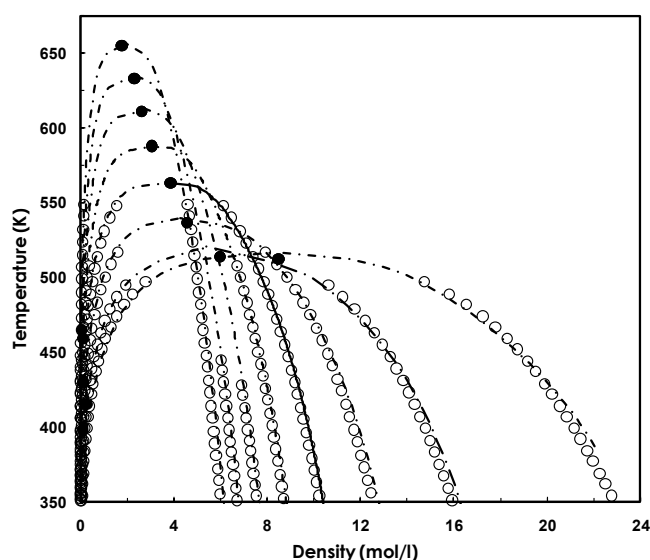
**Table 4.11.** Molecular parameters for the light alkanols studied in this work [Lovell et al. 2006]. See text for details.

COMPOUND	$m$	$\sigma(\text{\AA})$	$\epsilon/k_B(\text{K})$	$\phi$	$L/\sigma$	$\epsilon_{\text{HB}}/k_B(\text{K})$	$\square_{\text{HB}}(\square^3)$
methanol	1.481	3.390	227.4	7.70	1.390	3193	4907
ethanol	1.710	3.659	240.0	7.00	1.300	3470	2300
1-propanol	1.941	3.815	249.8	7.30	1.320	3600	2300
1-butanol	2.210	3.934	266.5	7.65	1.350	3600	2300
1-pentanol	2.470	4.020	279.5	7.83	1.370	3600	2300
1-hexanol	2.686	4.110	291.0	8.00	1.380	3600	2300
1-heptanol	2.920	4.170	299.5	8.10	1.390	3600	2300
1-octanol	3.148	4.212	306.0	8.25	1.395	3600	2300

**Table 4.12.** Optimized influence parameters for the light alkanols studied in this work.

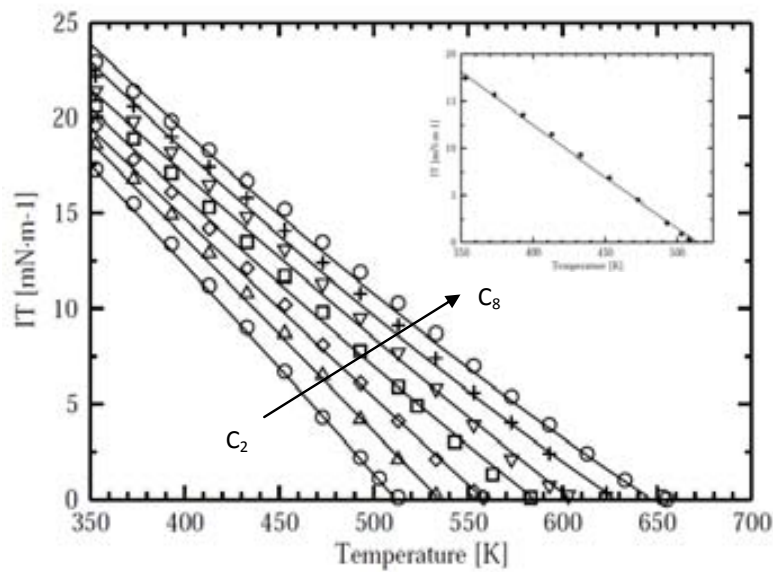
COMPOUND	$10^{19} c$ (J m <sup>5</sup> mol <sup>-2</sup> )
methanol	0.2556
ethanol	0.6278
1-propanol	1.1085
1-butanol	1.6586
1-pentanol	2.4285
1-hexanol	3.4870
1-heptanol	4.8157
1-octanol	6.2932

In Figure 4.23, results obtained with soft-SAFT for the vapor-liquid equilibria of 1-alkanols are shown. Calculations have been done for the first members of the 1-alkanols family, from methanol to 1-octanol. It can be observed that a satisfactory agreement between experimental data and the soft-SAFT predictions are obtained in all cases.



**Figure 4.23:** Vapor-liquid equilibria of light alkanols from ethanol to 1-octanol (from left to right). Symbols represent experimental data [NIST] and dashed and dotted lines correspond to the crossover soft-SAFT+DGT approach.

Results concerning the vapor liquid interfacial tension for the 1-alkanols series as obtained by crossover soft-SAFT and its combination with DGT for the interfacial properties are presented in Figure 4.24, together with the available experimental data [Jasper, 1972; Landolt-Börnstein; NIST]. As can be observed in the Figure, an overall excellent agreement between experimental data and the description with crossover soft-SAFT is reached in all cases. The incorporation of the crossover treatment allows an accurate description of the interfacial tension for the whole range of temperatures, including the critical region.

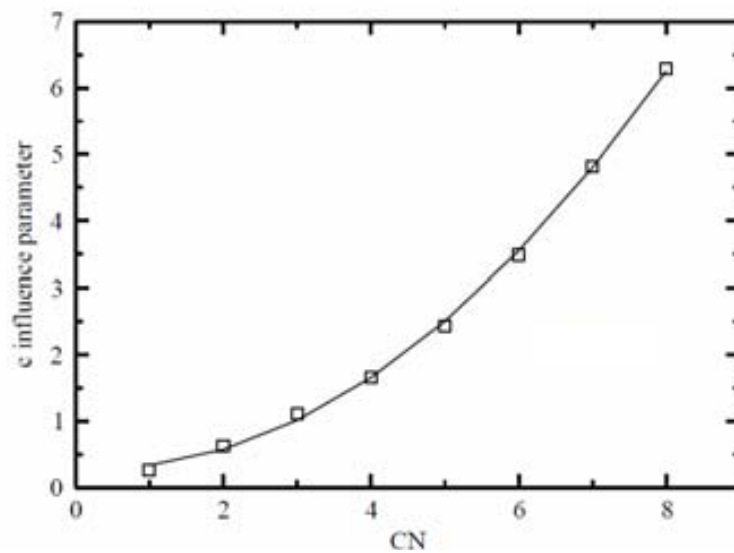


**Figure 4.24:** Vapor-liquid interfacial tensions of light alkanols from ethanol to 1-octanol (from left to right). For clarity methanol is shown separately in the inset. Symbols represent experimental data [Jasper, 1972; Landolt-Börnstein; NIST] and dotted lines correspond to the crossover soft-SAFT+DGT approach

We have observed that, as it happens with other molecular parameters for regular chemical families, the influence parameter for the light 1-alkanols series can be correlated with respect to the carbon number of the chain (or molecular weight of the molecules). The following parabolic function has been obtained in this work:

$$10^{19} c_{1 \text{ alkanols}} = 0.1016 CN^2 - 0.0681 CN + 0.2996 \text{ [Jm}^5 \text{mol}^{-2}] \quad (4.5)$$

This correlation is plotted together (see Figure 4.25) with the tabulated values in Table 4.11. As for n-alkanes, it allows obtaining the interfacial behavior of heavier compounds of the series not included in the fitting procedure as well as the behavior of mixtures formed by these compounds, expanding the predictive capabilities of the equation.



**Figure 4.25:** Optimized influence parameter for the light members of the light alkanols (squares) series versus the carbon number. Lines correspond to the values obtained from equation 4.5.

#### 4.2.2.4. Refrigerants<sup>9</sup>

Refrigeration is “the process of removing heat from an enclosed space that is to be maintained at a lower temperature than the surroundings” [Evans, 1942]. Hence, from this definition the word “refrigerant” is used to define the substance employed to remove this heat. During many centuries, the natural refrigerants used to preserve food, before mechanical refrigeration systems were introduced, were snow and ice. It was not until the 18th and the 19th centuries when several refrigeration machines were designed for practical applications, such as brewing or meatpacking industries, food transport or air-conditioning in hospitals, among others.

The development of mechanical refrigeration has been parallel to that of refrigerants. First reported refrigerants (1830s) [Radermacher *et al.*, 2005] were caoutchoucine, a distillate of Indian rubber and ethyl ether. Other substances were also in use until carbon dioxide and chemogene (a ternary mixture of petrol, ether and naphtha) were first used as refrigerants in 1866. The first truly refrigerants like ammonia (R-717) were developed during the last part of the 19<sup>th</sup> century and the first part of the 20<sup>th</sup>. It was not until the decade of 40s when chlorofluorocarbons (CFCs) were spread out. Since CFCs were suspected of causing the destruction of the stratospheric ozone [Molina and Rowland, 1974], the manufacturers replaced their use following the “Montreal Protocol (1987) to reduce substances that deplete the ozone layer”. Soon after, the treaty was amended and the production of Ozone Depleting Substances (ODS) was banned in 1995, five years after it was first established.

Following the aforementioned regulation, the traditional chlorofluorocarbon (CFC) and hydrochlorofluorocarbon (HCFC) refrigerants have been or must be phased out in the refrigeration industry because of their ozone depletion potentials (ODPs) and global warming potentials (GWPs). On account of the fluorocarbon industry, alternative compounds need to be designed. HCFCs, which had been commonly used in refrigerants, aerosols, blowing agents, solvents and sterility gases were only an interim solution until the new

---

<sup>9</sup> Part of this section has been published in Vilaseca, O.; Llovell, F.; Yustos, J.; Marcos, R.M.; Vega, L.F. Phase equilibria, surface tensions and heat capacities of hydrofluorocarbons and their mixtures including the critical region. *J. Supercrit. Fluids*, **2010**, 55 (2), 755-768



generation of substances; based on hydrofluorocarbons (HFCs) came into use. HFCs were introduced as ozone friendly alternatives to chlorofluorocarbons because they do not participate in chlorine or bromine catalytic cycles that deplete stratospheric ozone [WMO, 2009]. However, the problem is still far from being solved. Most HFCs are still potent greenhouse gases and their atmospheric concentrations are increasing rapidly; estimated 2050 global emissions are equivalent to 9-19% of projected global CO<sub>2</sub> emissions in business-as-usual scenarios [Velders *et al.*, 2009].

Hence, research based on the selection of friendly alternative refrigerants has become one of the most important tasks nowadays. Molecular constraints imposed on HFCs alternatives by environmental and final use performance requirements limit the number of replacement options. The selection of the best environmental solution not only depends on the greenhouse gas potential of the material itself, but also on the energy efficiency over the expected life of the system [Shankland, 2009]. All studies performed indicate the difficulty in finding a pure substance with the capabilities of classical refrigerants able to meet the current environmental requirements, and mixtures of some compounds appear as a suitable attractive option. Hence, although there is a search for replacing HFCs in the long term by other compounds with lower global warming potentials, these compounds are still present in thousands of industrial applications and will remain for some more years. As an example, HFC-134a (1,1,1,2-tetrafluoroethane) is widely used for refrigeration, air conditioning, and thermal insulating foam, but its largest and most emissive application is for mobile automobile air conditioners (MACs), used in more than 80% of passenger cars and commercial vehicles worldwide [Velders *et al.*, 2009].

The characterization and optimization of thermodynamic and transport properties of refrigerants, such as density, vapor pressure, solubility of components, interfacial properties, viscosity, heat capacity, etc., represent a key part of both the theoretical and the experimental work needed before they are put into their final use. Within this context, the complexity of the compounds and the vast amount of them exceeds the applicability of classical thermodynamic methods and therefore, molecular based equations of state appear as an excellent tool to explore the behavior of these mixtures from a modeling perspective.

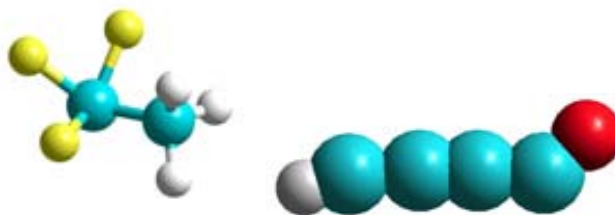
Hydrofluorocarbons (HFCs) are partially fluorinated alkanes in which some hydrogen atoms have been replaced by fluorine. The numbering code of the American Society of Heating, Refrigeration, and Air-conditioning Engineers (ASHRAE) is employed for the designation of these compounds. A total of fifteen HFCs, for which enough experimental data is available [NIST], are evaluated in this work. They are listed in Table 4.13.

**Table 4.13.** Name, code and structure of the refrigerants studied in this section.

Name (formula)	Code	Structure	Name (formula)	Code	Structure
Fluoromethane (CH <sub>3</sub> F)	R41		1,1,1,3,3-Pentafluoropropane (CF <sub>3</sub> -CH <sub>2</sub> -CHF <sub>2</sub> )	R245fa	
Diffuoromethane (CH <sub>2</sub> F <sub>2</sub> )	R32		1,1,2,2,3-Pentafluoropropane (CHF <sub>2</sub> -CF <sub>2</sub> -CHF <sub>2</sub> )	R245ca	
Trifluoromethane (CHF <sub>3</sub> )	R23		1,1,1,3,3,3-Hexafluoropropane (CF <sub>3</sub> -CH <sub>2</sub> -CF <sub>3</sub> )	R236fa	
1,1-Difluoroethane (CHF <sub>2</sub> -CH <sub>3</sub> )	R152a		1,1,1,2,2,3-Hexafluoropropane (CF <sub>3</sub> -CHF-CHF <sub>2</sub> )	R236ea	
1,1,1-Trifluoroethane (CF <sub>3</sub> -CH <sub>3</sub> )	R143a		1,1,1,2,2,3,3-Heptafluoropropane (CF <sub>3</sub> -CHF-CF <sub>3</sub> )	R227ea	
1,1,1,2-Tetrafluoroethane (CF <sub>3</sub> -CHF <sub>2</sub> )	R134a		1,1,1,3,3-Pentafluorobutane (CF <sub>3</sub> -CH <sub>2</sub> -CF <sub>2</sub> -CH <sub>3</sub> )	R365mfc	
Pentafluoroethane (CF <sub>3</sub> -CHF <sub>2</sub> )	R125		1,1,1,2,2,3,3,4-Octafluorobutane (CF <sub>3</sub> -CF <sub>2</sub> -CF <sub>2</sub> -CHF <sub>2</sub> )	R338mccq	
Fluoroethane (CH <sub>3</sub> F-CH <sub>3</sub> )	R161				

In the context of soft-SAFT, HFCs are described as homonuclear chainlike molecules, modeled as  $m$  Lennard-Jones segments of equal diameter  $\sigma$ , and the same dispersive energy  $\varepsilon$ , bonded to form the chain. Due to the electronegativity of fluorine, these molecules show a high dipole moment. The dipolar interactions can be modeled by the association term of the soft-SAFT equation, and thus, two additional parameters are needed: the energy and the volume of the associating sites  $\epsilon_{ij}$  and  $k_{ij}$ , represented from now on by  $\epsilon_{HB}$  and  $k_{HB}$  for simplicity and consistency with other compounds modeled in this Thesis work. The number of association sites for each HFC molecule, as well as the allowed interactions among the sites, has to be specified within the model. Although an individual fitting of all parameters could be done for each individual molecule, we will try to make the model as general as possible, seeking the transferability and prediction capacity of the method. Since the associating interactions are due to the permanent dipoles, the directional forces between opposite partial charges can be easily understood considering

two sites that interact one to the other. This is therefore the general model applied to all the series of HFC molecules and it is illustrated in this caption.



**Figure 4.26:** Schematic representation of a hydrofluorocarbon.

The fitting of the molecular parameters is done as in previous cases, fitting to experimental vapor pressure and saturated liquid density data. However, given the nature of the equation, physical information can be used in order to minimize the number of parameters to be optimized. As done in a previous work with *n*-perfluoroalkanes [Llovel *et al.*, 2007; Dias *et al.*, 2004a,b; 2006;2009] we set the values of the *m* parameter for each group of HFC molecules with the same number of carbon atoms equal to those optimized for the related *n*-alkanes [Pàmies and Vega, 2001; Pàmies, 2003]. This approximation is based on experimental studies that indicate that C-C bond lengths for crystalline poly(tetrafluoroethylene) and polyethylene are equivalent [Pàmies, 2003]. Furthermore, taking into account that the length of the molecular chain should not affect the strength of the association bonds and leads to a higher transferability of the set of parameters, the association parameter  $K_{HB}$  that accounts for the volume of the association site is fixed to a constant value for all the HFCs. The rest of the molecular parameters of the model are calculated by fitting to available experimental data [NIST] and are listed in Table 4.14. The thermodynamic range of data used goes approximately from a reduced temperature  $T/T_c \approx 0.7$  till the critical temperature.

In the present work, there are some particularities to be mentioned, which enhance the transferability of the model. First, due to the transfer of the parameter *m* from the *n*-alkanes, it is possible to use the value from one chemical family to the other in a purely predictive manner, but, as a result, the correlation of *m* with the molecular weight of the new compounds is not

allowed, as HFC molecules with the same number of carbon atoms, and therefore equal  $m$ , have different molecular weights than the homologous  $n$ -alkanes.

The combination of  $m$  and  $\sigma^3$  gives an estimation of the volume of the molecules [Pàmies and Vega, 2001; Pàmies, 2003]. This product can correlate with the molecular weight of the different compounds. As  $m$  is already transferred from the  $n$ -alkanes, the value of  $\sigma$  can be directly obtained in this manner, empowering the equation with predictive capabilities. Several linear relationships are proposed in this work according to the carbon number:

$$\text{- for fluoromethanes,} \quad m^3 = 0.3223 M_w + 45.01 \quad (4.6a)$$

$$\text{- for fluoroethanes,} \quad m^3 = 0.3670 M_w + 63.21 \quad (4.6b)$$

$$\text{- for fluoropropanes,} \quad m^3 = 0.3603 M_w + 81.15 \quad (4.6c)$$

$$\text{- for fluorobutanes,} \quad m^3 = 0.3417 M_w + 105.51 \quad (4.6d)$$

Units of  $\sigma$  and  $M_w$  are Å and g/mol, respectively. These equations and also the following are represented graphically in Figure 4.27.

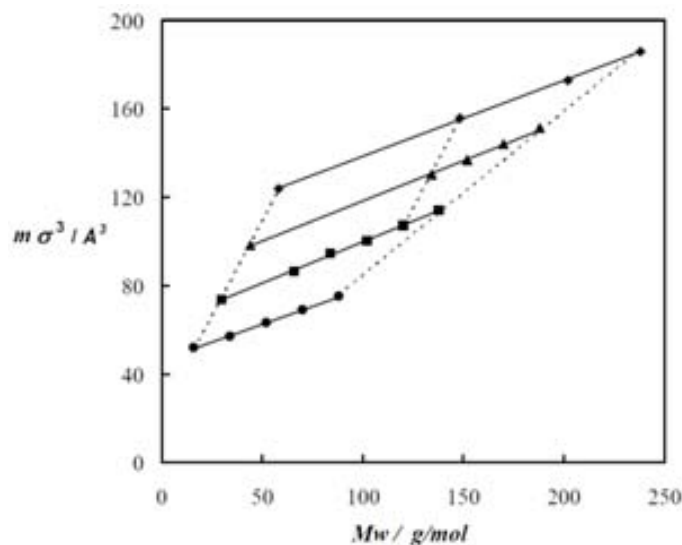
$$\text{- for } n\text{-alkanes [Pàmies and Vega,2001],} \quad m^3 = 1.73 M_w + 22.8 \quad (4.6e)$$

$$\text{- for } n\text{-perfluoroalkanes [Dias } et \text{ al.,2009],} \quad m^3 = 0.7105 M_w + 15.28 \quad (4.6f)$$

$$\text{- for pentafluoroalkanes,} \quad m^3 = 1.8558 M_w - 117.90 \quad (4.6g)$$

The regression coefficient for all the lines is about 0.999 in almost all cases, indicating the reliability for the extrapolation and prediction of this parameter. Additionally, as presented in Equation (4.6g) for the pentafluoroalkanes, it is shown that for HFC molecules from different groups (i.e. with different number of carbon atoms) but with the same number of

fluorine atoms,  $m\sigma^3$  and  $M_w$  can also be linearly correlated. These features show the consistency of the correlations and the transferability of this parameter to any type of HFC not included in this work.



**Figure 4.27:** Correlations of  $m\sigma^3$  with  $M_w$  for the HFC molecules (equations (4.6a-4.6d), continuous lines): fluoromethanes ( $\square$ ), fluoroethanes ( $\square$ ), fluoropropanes ( $\Delta$ ), fluorobutanes ( $\diamond$ ); and other series of molecules (equations 4.6e-4.6g), dashed lines): *n*-alkanes, *n*-perfluoroalkanes and pentafluoroalkanes.

Secondly, the parameters  $\varepsilon$  and  $\varepsilon_{HB}$  need to be optimized individually for each HFC molecule, while the parameter of association  $\kappa_{HB}$  is fixed to a constant value of  $24050 \text{ \AA}^3$ , which is an average optimized value for the whole series that can be transferred for any HFC molecule. The parameter  $\varepsilon$  could not be correlated with  $M_w$  as it had been done with other families of compounds (alkanes, perfluoroalkanes, 1-alkanols) studied with the soft-SAFT equation. A possible explanation could be the highly heteronuclearity of the HFC families in which not only the number of segments is increased, but also the type of functional groups that conforms the molecules are different.

**Table 4.14.** Optimized molecular parameters for the refrigerants studied in this work.

HFC	Formula	T range (K)	$m$	$\sigma$ (Å)	$\epsilon / k_B$ (K)	$\epsilon_{HB} / k_B$ (K)	$\phi$	$c \cdot 10^{19}$ ( $J \cdot m / mol^5$ )
R41	CH <sub>3</sub> F	180-317.6	1.000	3.810	139.1	1545	9.00	0.3992
R32	CH <sub>2</sub> F <sub>2</sub>	180-350.5	1.000	3.912	145.7	1830	8.50	0.6995
R23	CHF <sub>3</sub>	150-301.0	1.000	4.060	126.2	1544	9.50	0.8596
R152a	CHF <sub>2</sub> -CH <sub>3</sub>	155-385.6	1.392	3.968	163.3	1919	8.50	1.146
R143a	CF <sub>3</sub> -CH <sub>3</sub>	140-352.8	1.392	4.103	149.0	1717	8.60	1.155
R134a	CF <sub>3</sub> -CH <sub>2</sub> F	170-376.5	1.392	4.163	165.6	1887	8.10	1.482
R125	CF <sub>3</sub> -CHF <sub>2</sub>	173-339.5	1.392	4.242	150.8	1685	8.40	1.498
R245fa	CF <sub>3</sub> -CH <sub>2</sub> -CHF <sub>2</sub>	200-429.5	1.776	4.162	186.2	2095	8.00	2.487
R245ca	CHF <sub>2</sub> -CF <sub>2</sub> -CH <sub>2</sub> F	200-449.0	1.776	4.162	199.3	2122	8.00	2.487
R236fa	CF <sub>3</sub> -CH <sub>2</sub> -CF <sub>3</sub>	180-399.3	1.776	4.241	171.7	1986	8.00	2.487
R236ea	CF <sub>3</sub> -CHF-CHF <sub>2</sub>	180-415.5	1.776	4.241	187.6	1951	8.00	2.487
R227ea	CF <sub>3</sub> -CHF-CF <sub>3</sub>	160-375.4	1.776	4.315	167.6	1806	8.00	2.487
R365mfc	CF <sub>3</sub> -CH <sub>2</sub> -CF <sub>2</sub> - CH <sub>3</sub>	220-464.6	2.134	4.202	207.1	2086	8.00	-
R338mccq	CF <sub>3</sub> -CF <sub>2</sub> -CF <sub>2</sub> - CH <sub>2</sub> F	220-434.5	2.134	4.328	191.8	2019	8.00	-

Notes: The volume of association was considered a constant value for all hydrofluorocarbons and was optimized to a value of  $24050 \text{ \AA}^3$ .

The crossover parameter  $L/\sigma$  was set to a constant value of 1.25 for all compounds.

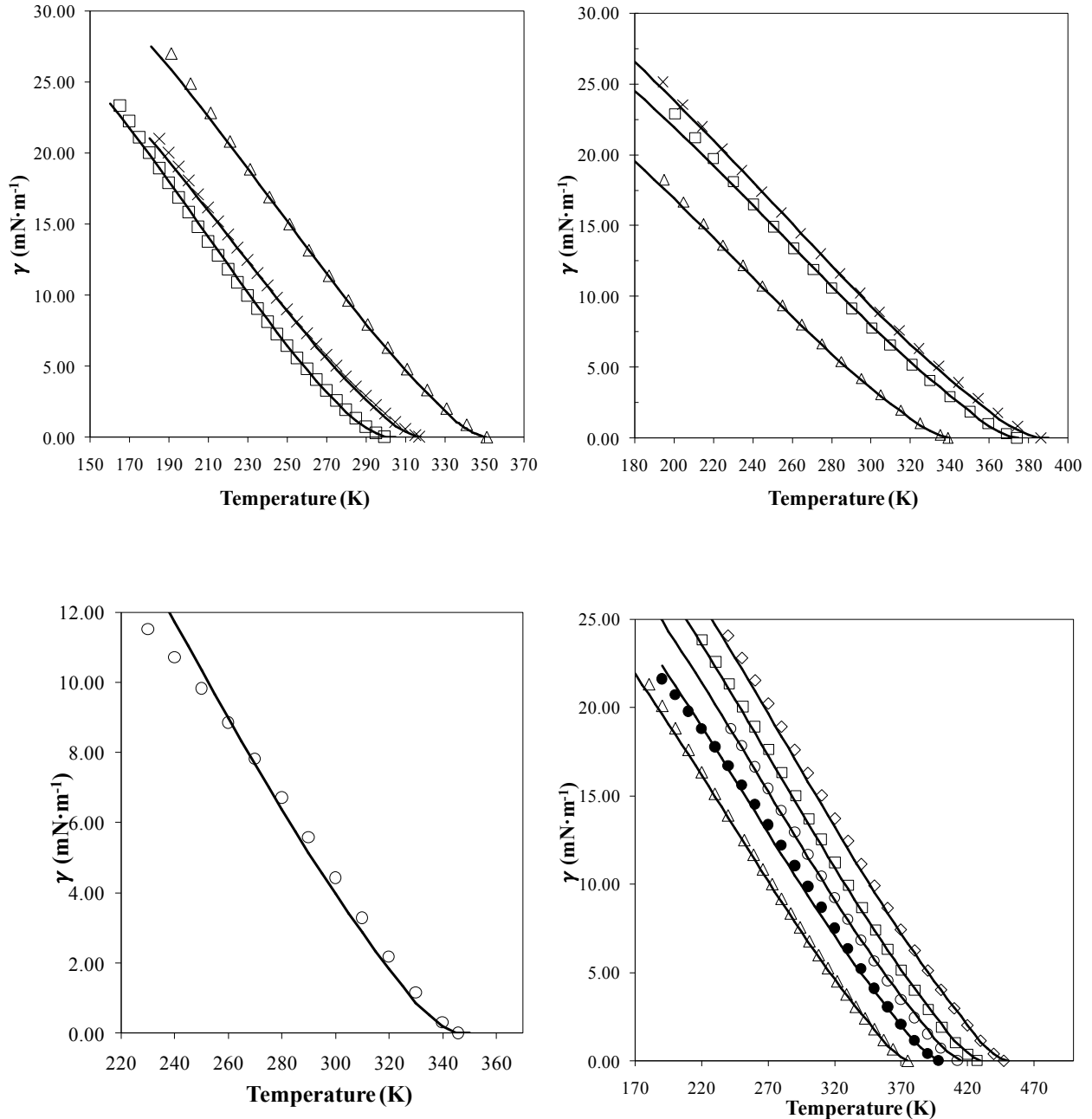
The results for interfacial tension of the selected HFCs obtained by the crossover soft-SAFT and its combination with DGT for the interfacial properties are presented in Figures 4.28a-d, together with the available experimental data [NIST]. As can be observed, an excellent agreement between experimental data and the description with crossover soft-SAFT is reached in all cases. The incorporation of the crossover treatment allows an accurate description of both, the liquid density and the vapor density far from and close to the critical point, as well as the interfacial tension for the whole range of temperatures, including the critical region, where classical equations fail.

Concerning the influence parameter  $c$  (see Table 4.14), it has been observed than in the case of compounds with short chain length, up to R143a, the

c

d

influence parameter increases proportionally to their molecular weight, remaining constant for the heavier compounds. This dependence becomes especially useful for predictive purposes.



**Figure 4.28:** Vapor-liquid interfacial tension for (a) R23( $\square$ ), R32( $\Delta$ ) and R41(+); (b) R125( $\Delta$ ), R152a(+), R134a ( $\square$ ); (c) R143a( $\square$ ); (d) R227 ( $\Delta$ ), R236fa (+), R236ea ( $\square$ ), R245fa ( $\square$ ) and R245ca ( $\diamond$ ). Symbols represent the experimental data [NIST] while the lines correspond to the soft-SAFT + DGT modeling.

### 4.2.2.5. Nitriles<sup>10</sup>

Under the definition of the IUPAC a nitrile is any organic compound that has a  $-C\equiv N$  functional group. This group is accounted within the soft-SAFT approach with the association term explicitly considered for this family. Nitriles are polar molecules modeled as chains with a single association site located on the CN group, representing the dipolar moment [Belkadi *et al.*, 2010]. Hence, although the dipolar moment is not explicitly taken into account its effect is implicitly considered in the association parameters. Some of the well known applications of the nitriles are the super-glue, latex free laboratory and medical gloves or several pharmaceutical products, to mention common examples [Pollard and Woodley, 2006].



**Figure 4.29:** Molecular 3D representation propionitrile.

We have followed the same process to obtain the interfacial properties of another interesting family of compounds from the industrial perspective, the *n*-nitriles family; results are presented in Figure 4.30a,b. The soft-SAFT parameters were taken from [Belkadi *et al.*, 2010] and are given in Table 4.15.

**Table 4.15.** Molecular parameters for the nitriles studied in this work, together with the references where the parameters were originally obtained.

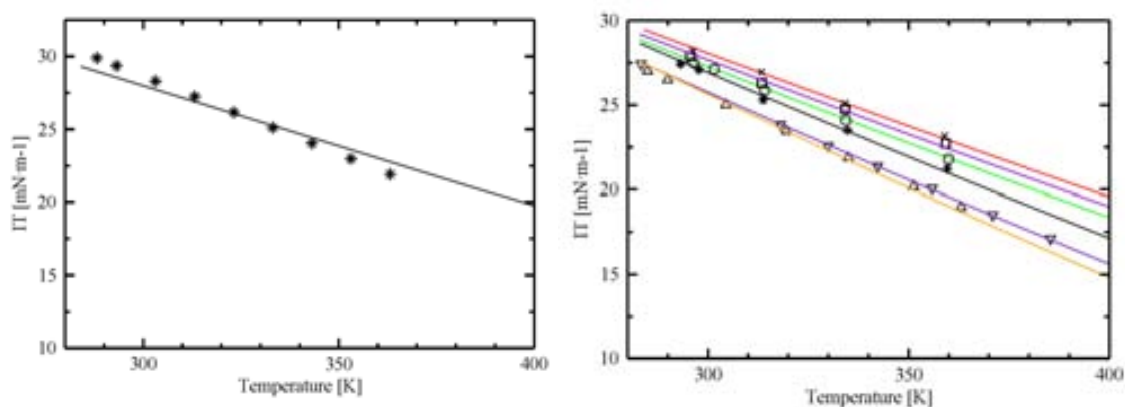
COMPOUND	$m$	$\sigma(\text{\AA})$	$\varepsilon/k_B(K)$	$\phi$	$L/\sigma$	$\varepsilon_{HB}/k_B(K)$	$\square_{HB}(\square^3)$	Reference
acetonitrile	1.450	3.700	268.0	8.47	1.25	8425	69	Belkadi <i>et al.</i> , 2010
propionitrile	1.570	3.980	274.0	8.57	1.27	8425	49	Belkadi <i>et al.</i> , 2010

<sup>10</sup> Part of this section has been published in Vilaseca, O. and Vega, L.F. Direct calculation of interfacial properties of fluids close to the critical region by a molecular-based equation of state. *Fluid Phase Equilib.* **2011**, 306, 4-14.



n-butyronitrile	1.660	4.250	280.0	8.75	1.28	8425	49	Belkadi <i>et al</i> , 2010
Valeronitrile	1.800	4.480	286.3	8.80	1.34	8425	49	Belkadi <i>et al</i> , 2010
hexanenitrile	1.920	4.760	291.1	8.91	1.37	8425	49	Belkadi <i>et al</i> , 2010

Figure 4.30a depicts the surface tension of acetonitrile ( $\text{CH}_3\text{CN}$ ) as compared to experimental data whereas results obtained from soft-SAFT + DGT for the rest of the *n*-nitriles compounds, from  $\text{C}_2\text{H}_5\text{CN}$  to  $\text{C}_8\text{H}_{17}\text{CN}$ , are presented in Figure 4.30b, as compared to experimental data [Landolt-Börnstein]. As observed in the Figure, the agreement between the calculations and the experimental data is excellent for the whole range of conditions. The representation of  $\text{C}_6\text{H}_{13}\text{CN}$  has been omitted in the Figure for clarity of the plot; results are at the same level of agreement as the rest of the family. It should be noted that, as the available experimental data is far away from the critical region, no crossover was considered in this case, in order to save computational effort.



**Figure 4.30:** Vapor-liquid interfacial tensions of *n*-nitriles. a) Acetonitrile ( $\text{CH}_3\text{CN}$ ), b) from propionitrile ( $\text{C}_2\text{H}_5\text{CN}$ ) to nonanenitrile ( $\text{C}_8\text{H}_{17}\text{CN}$ ), from left to right. Symbols are experimental data from [Landolt-Börnstein] and the full lines correspond to the soft-SAFT+DGT approach.

Finally we have tried to use the same procedure than with the alkanes and 1-alkanols to establish a correlation for the *c* parameter for the *n*-nitriles series; however, at this time it was not possible to find an accurate correlation as a function of the carbon number. As the value of the *c* parameter is very

sensitive to small variations [see Table 4.16], the inability to obtain this correlation may be due to the different sources of the experimental data (see *Landolt-Börnstein* references therein) for each one of the compounds. In addition, the peculiar behavior of these compounds with a very high dipole, due to the presence of the  $-\text{CN}$  group, may also affect the different behavior at the interface, hence precluding a regular behavior.

**Table 4.16.** *Optimized influence parameters for the nitriles studied in this work.*

COMPOUND	$10^{19} c$ ( $\text{J m}^5 \text{mol}^{-2}$ )
acetonitrile	0.9163
propionitrile	1.5729
<i>n</i> -butyronitrile	2.8824
valeronitrile	5.3316
hexanenitrile	9.9741
heptanenitrile	10.846
octanenitrile	18.266
nonanenitrile	18.911

#### 4.2.2.6. Ionic liquids<sup>11,12</sup>

Ionic liquids, also known as liquid electrolytes, ionic melts, ionic fluids, liquid salts, or ionic glasses, is a term generally used to refer to salts that form stable liquids. Nowadays it is considered that any organic salt that is liquid below 100°C falls into this category. They are usually formed by a large organic cation like quaternary ammonium, imidazolium or pyridinium ions combined with an anion of smaller size and more symmetrical shape such as [Cl]<sup>-</sup>, [Br]<sup>-</sup>, [I]<sup>-</sup>, [BF<sub>4</sub>]<sup>-</sup>, [PF<sub>6</sub>]<sup>-</sup>, [Tf<sub>2</sub>N]<sup>-</sup>, etc, although some symmetric cations are also combined with asymmetric anions to form ionic liquids. In spite of their strong charges, their asymmetry frustrates them from being solid below 100°C and this is why they remain liquid at these low temperatures.

It is believed that the first synthesized ionic liquid reported in the literature is ethanolanmonium nitrate, published by Gabriel in 1888 [Gabriel *et al.*, 2006]. However, one of the earlier known truly room temperature ionic liquids was [EtNH<sub>3</sub>]<sup>+</sup>[NO<sub>3</sub>]<sup>-</sup>, the synthesis of which was published in 1914 [Walden, 1914; Sugden *et al.*, 1929]. Much later, different ionic liquids based on mixtures of 1,3-dialkylimidazolium or 1-alkylpyridinium halides and trihalogenoaluminates, initially developed for their use as electrolytes, were to follow [Chum *et al.*, 1975; Wilkes *et al.*, 1982]. Ionic liquids remained unused for years, mostly because of their moisture sensitivity and their acidity/basicity (the latter can sometimes be used to an advantage). However, when in 1992, Wilkes and Zawarotko reported the preparation of ionic liquids with a new set of alternative, 'neutral', weakly coordinating anions such as hexafluorophosphate ([PF<sub>6</sub>]<sup>-</sup>) and tetrafluoroborate ([BF<sub>4</sub>]<sup>-</sup>) [Wilkes and Zawarotko, 1992], a much wider range of applications for ionic liquids were envisioned, and this has been a field of continuous growth since then.

---

<sup>11</sup> Part of this section has been published in Vega, L.F.; Vilaseca, O.; Llovel F.; Andreu, J.S. Modeling ionic liquids and the solubility of gases in them: Recent advances and perspectives. *Fluid Phase Equilib.* **2010**, *294*, 15-30.

<sup>12</sup>Part of this section has been published in Vilaseca, O. and Vega, L.F.; Critical, interfacial and surface properties of ionic liquids by a molecular-based equation of state. Submitted (2012).

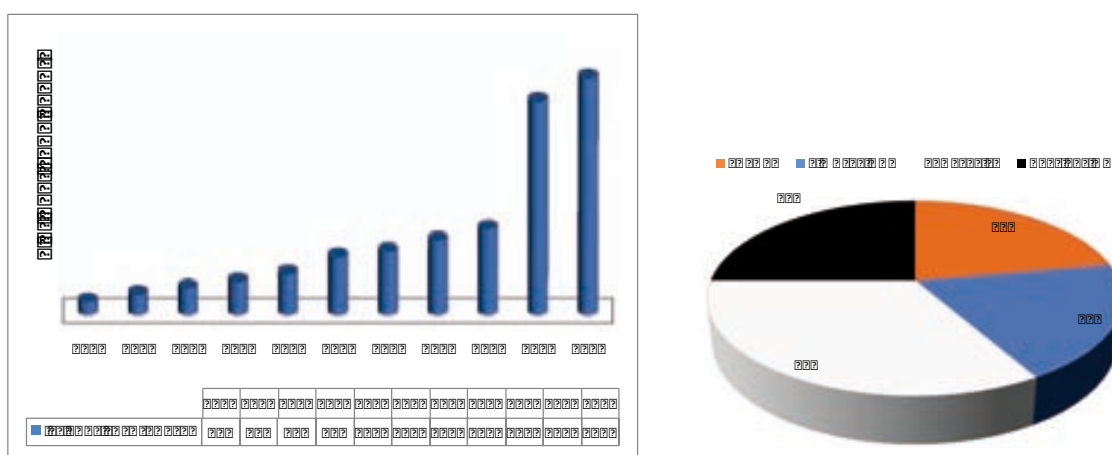
There are some key properties of these compounds that make them particularly attractive for different applications: in fact, their extremely low volatility has become one of their most important benefits compared to volatile organic solvents used as traditional industrial solvents. High thermal and electronic stability, high ionic conductivity, a wide liquid temperature and good solubility characteristics complete the list of advantages versus other traditional compounds for different applications.

As already mentioned, a huge amount of different ionic liquids can be synthesized through the combination of an organic or inorganic anion and an organic (or inorganic) cation, and the number of new synthesized ionic liquids continues to grow incessantly. For instance, just regarding the imidazolium family, there are over 30,000 1,3-functionalized entries recorded in the CAS database. Further scope for derivatization beyond ramification of linear alkyl-substituents, for example with branched, chiral, fluorinated, or an active-functionality, can yield further useful materials. The degree and type of substitution renders the salts low melting, largely by reducing cation-anion Coulombic interactions and disrupting ion-ion packing [Easteal *et al.*, 1970]. In this way, the specific properties of an ionic liquid can be almost selected ad-hoc, in order to have compound with the most appropriate characteristics for a specific application.

Among an uncountable amount of different possibilities [Holbrey *et al.*, 2004], the use of ionic liquids as media for CO<sub>2</sub>/gas separations appears especially promising, as CO<sub>2</sub> is more highly soluble than the rest of the gases. Process temperature and the chemical structures of the cation and the anion have significant impacts on gas solubility and gas pair selectivity. In addition to their role as a physical solvent, ionic liquids might also be used in supported ionic liquid membranes as a highly permeable and selective transport medium. Overall, they are considered environmentally friendly compounds (even if it depends on the selection of the cation and the anion) that can be used in catalytic reactions [Wasserscheid *et al.*, 2000], gas and liquid separations, cleaning operations, electrolyte or fuel cells or even as lubricants and heat transfer fluids [Welton, 1999; Brennecke and Maginn, 2001]. A summary of capabilities and limitations of ionic liquids in CO<sub>2</sub> based

separations respect to a variety of materials is provided in a very recent and detailed contribution by Bara and co-authors [Bara *et al.*, 2009].

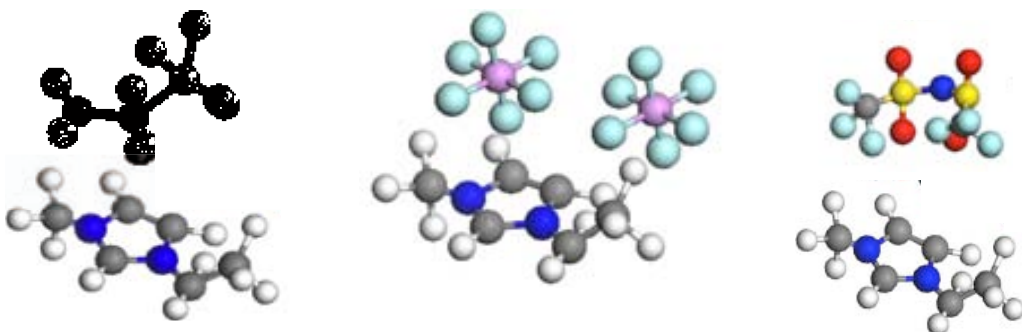
As an example of the growing interest in this field, Figure 4.31.(left) depicts the number of contributions in scientific Journals included in the Web of Science related to ionic liquids is plotted versus the year of publication in the last decade. The blooming of publications in ionic liquids in the last years is due, in part, to the popularization of these compounds done by Rogers and Seddon [Rogers and Seddon, 2003] and the review paper published by Welton some years ago [Welton, 1999]. It should be mentioned that, in spite of their potential for several industrial applications, the list of published works is more related to synthesis, characterization and modeling of these materials, than to applications, being the list of industrial applications still very short. As an example of the distribution of works:



**Figure 4.31:** (Left) Number of publications about ionic liquids published in journals included in the Web of Science List, year by year in the last decade. (Right) Distribution of topics related to the presentations about ionic liquids at the 17th International Symposium on Thermophysical Properties. See text for details.

Figure 4.31. (right) shows the allocation of topics devoted to different aspects of ionic liquids presented in the last International Symposium on Thermophysical Properties [2009]. As observed in the Figure, 42% of the presentations were dedicated to modeling (22% to theory and 20% to molecular simulations), while 33% of the contributions dealt with the measurement of some specific properties and the remaining 25% dealt with applications. This average share of topics is also found in other similar conferences and in the open literature.

Following the methodology of our previous works [Vilaseca and Vega, 2011; Vilaseca *et al.*, 2010; Lovell *et al.*, 2012], the vapor-liquid interfacial tensions for the  $[C_n\text{-mim}][\text{PF}_6]$ ,  $[C_n\text{-mim}][\text{BF}_4]$  and  $[C_n\text{-mim}][\text{Tf}_2\text{N}]$ . The model used here is based on the previous work [Andreu and Vega, 2008] and is intended to build a simplified coarse-grained model for these molecules, trying to keep their main physical features. Following the previous work  $[C_n\text{-mim}][\text{Tf}_2\text{N}]$  ILs are modeled as homonuclear chainlike molecules with three associating sites mimicking the strong interactions between the anion and the cation. The number of associating sites is chosen based on the delocalization of the anion electric charge due the oxygen groups, enhancing the possibility of interaction with the surrounding cations through them. As a consequence, one associating A type site represents the nitrogen atom interactions with the cation, while two B sites represent the delocalized charge due the oxygen molecules on the anion, allowing only AB interactions between different IL molecules. A sketch of the model is presented in Figure 4.32. For more details, the reader is referred to reference [Andreu and Vega, 2008].

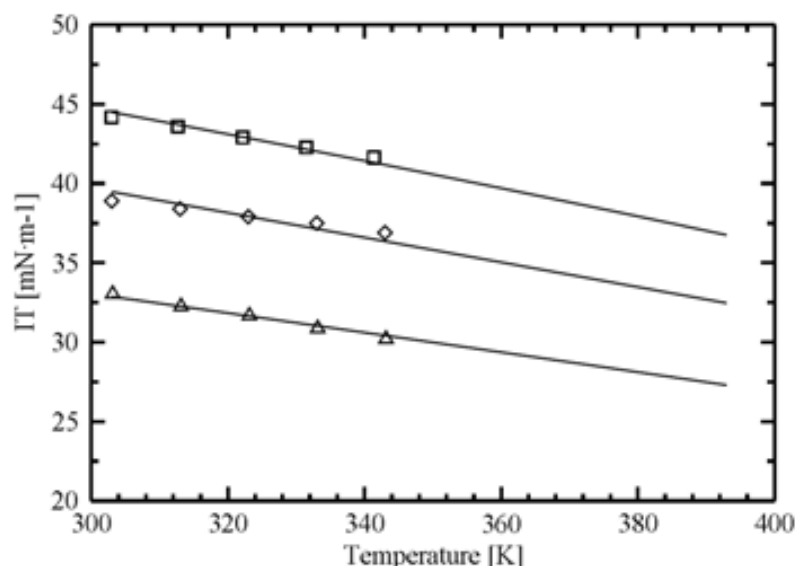


**Figure 4.32:** Representation of ionic liquids molecules  $[C_n\text{-mim}][\text{BF}_4]$ ,  $[C_n\text{-mim}][\text{PF}_6]$  and  $[C_n\text{-mim}][\text{Tf}_2\text{N}]$ .

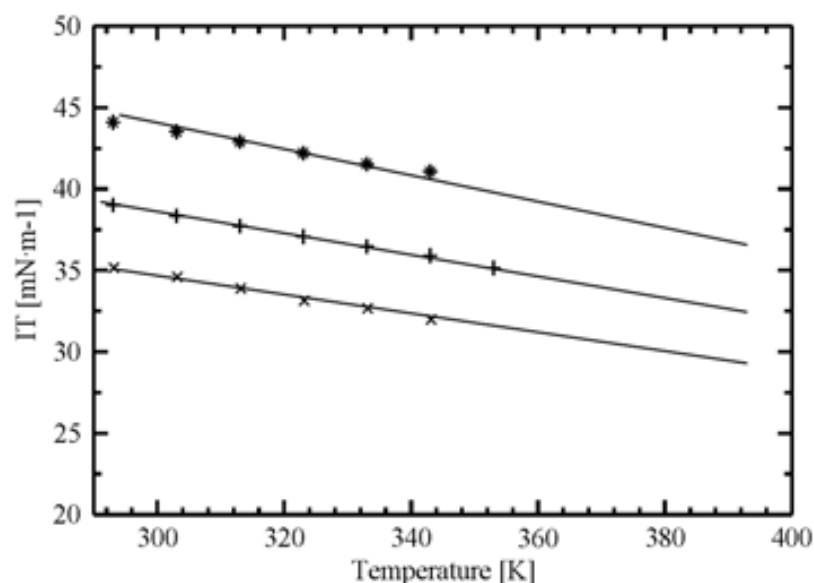
$[\text{BF}_4]^-$  and  $[\text{PF}_6]^-$  imidazolium ionic liquids were modeled in previous work [Andreu and Vega, 2007; Vega *et al.*, 2010] as Lennard Jones chains with one associating site in each molecule. This assumption was based on results obtained from molecular dynamics simulations [Urahata *et al.*, 2004; Del Popolo *et al.*, 2004; Morrow and Maginn, 2002] showing the ion pairing of these systems. This model mimics the neutral pairs (anion plus cation) as a

single chain molecule with this association site describing the specific interactions because of the charges and the asymmetry. For more details, the reader is referred to the original references [Andreu and Vega, 2008; Vega *et al.*, 2010].

These compounds are very challenging systems from the modeling point of view, as they are highly asymmetric and charged. Although using a simple model, as it is shown in Figures 4.33 and 4.34, for the  $[C_n\text{-mim}][\text{PF}_6]$  and  $[C_n\text{-mim}][\text{BF}_4]$  family very good results are found when compared to experimental data [Freire *et al.*, 2007; Gathe *et al.*, 2008; Landolt-Börnstein] with an AAD% lower than 0.60% in all cases. We have used the same molecular model and parameters obtained from our previous work [Andreu and Vega, 2007; 2008] and applied them here in a transferable manner. As shown in Figure 4.33 the theory is able to provide accurate results for this system, obtaining greater deviations with respect to experimental data for the lighter member studied ( $[\text{C}_4\text{-mim}][\text{PF}_6]$ ). Note that given the particular characteristics of the ionic liquids, the influence parameter value (see table 4.17) is one order of magnitude higher than for the more regular compounds, giving an idea of the high inhomogeneity of these systems.



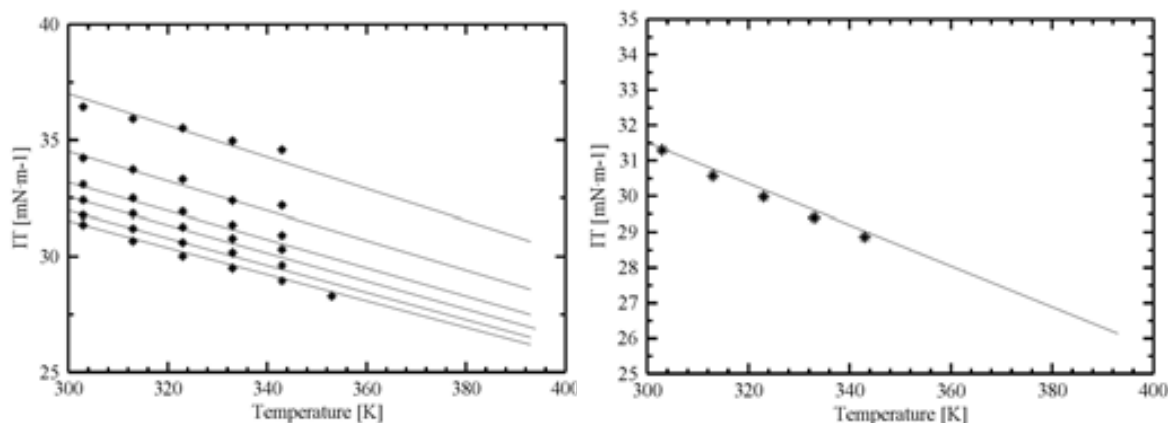
**Figure 4.33:** Interfacial tension as a function of temperature for the ionic liquid family 1,3-methyl-imidazolium tetrafluoroborate  $[C_n\text{-mim}][\text{BF}_4]$  as a function of temperature. Symbols:  $[\text{C}_2\text{-mim}][\text{BF}_4]$  (squares),  $[\text{C}_6\text{-mim}][\text{BF}_4]$  (diamonds) and  $[\text{C}_8\text{-mim}][\text{BF}_4]$  (triangles) represent experimental data [Freire *et al.*, 2007; Gathe *et al.*, 2008] and lines correspond to the soft-SAFT+DGT approach.



**Figure 4.34:** Interfacial tension as a function of temperature for the ionic liquid family 1,3-methyl-imidazolium hexafluorophosphate  $[C_n\text{-mim}][\text{PF}_6]$  as a function of temperature. Symbols:  $[C_2\text{-mim}][\text{PF}_6]$  (asterisks),  $[C_6\text{-mim}][\text{PF}_6]$  (pluses) and  $[C_8\text{-mim}][\text{PF}_6]$  (crosses) represent experimental data [Freire *et al.*, 2007] and lines correspond to the soft-SAFT+DGT approach.

Finally, results for the interfacial tension of eight members of the  $[C_n\text{-mim}][\text{Tf}_2\text{N}]$  family are presented in Figures 4.35a and 4.35b. Lines represent soft-SAFT + DGT calculations while the symbols represent experimental data [Carvalho *et al.*, 2008]. The molecular model and parameters for these ionic liquids were also taken from [Andreu and Vega, 2007;2008; Vega *et al.*, 2010]. As in the case of the  $[C_n\text{-mim}][\text{PF}_6]$  family, the interfacial tension trend with temperature is well reproduced, with an AAD% lower than 0.60% in all cases, especially as the chain length of the alkyl group increases, in spite of the greater asymmetry and non-ideality of these systems. Note that the value of the interfacial tension diminishes as the alkyl chain length increases, contrarily to other known organic compounds' behavior [Panayiotou, 2002]. A reasonable explanation for these high surface tensions are the vdW forces and the hydrogen bonds that exist between the cations, and the anions and cations, that increase the interactions between the ions leading to enhanced values of surface tension [Freire *et al.*, 2007].





**Figure 4.35:** Left) Vapor-liquid interfacial tensions of the ionic liquid family 1-alkyl-3-methyl-imidazolium bis(trifluoromethylsulfonyl)imide as a function of temperature [ $C_2\text{-mim}][\text{Tf}_2\text{N}]$ , [ $C_3\text{-mim}][\text{Tf}_2\text{N}]$ , [ $C_4\text{-mim}][\text{Tf}_2\text{N}]$ , [ $C_5\text{-mim}][\text{Tf}_2\text{N}]$ , [ $C_6\text{-mim}][\text{Tf}_2\text{N}]$  and [ $C_7\text{-mim}][\text{Tf}_2\text{N}]$ ] (from top to bottom). Right) [ $C_8\text{-mim}][\text{Tf}_2\text{N}]$ . Symbols represent experimental data [Carvalho *et al.*, 2008] and lines correspond to the soft-SAFT+DGT calculations.

As previously obtained for the  $n$ -alkanes and 1-alkanols [Vilaseca and Vega, 2011] or the perfluoroalkanes series [Dias *et al.*, 2009], the influence parameter can be correlated with respect to the carbon number of the alkyl chain for the case of the ionic liquids with  $[\text{Tf}_2\text{N}]$ . No correlations for the [ $C_n\text{-mim}][\text{PF}_6]$  and for the [ $C_n\text{-mim}][\text{BF}_4]$  family are proposed due to the lack of experimental data, with only three members for whom experimental data is available, and the different sources of experimental data.

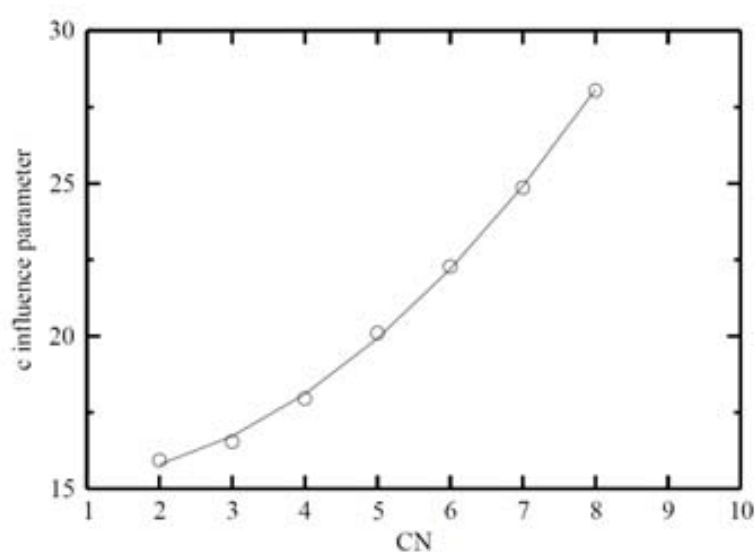
**Table 4.17.** Optimized influence parameters for the ionic liquids studied in this work. See text for details.

COMPOUND	$10^{19} c$ (J m <sup>5</sup> mol <sup>-2</sup> )	COMPOUND	$10^{19} c$ (J m <sup>5</sup> mol <sup>-2</sup> )
[ $C_4\text{-mim}][\text{BF}_4]$	13.468	[ $C_2\text{-mim}][\text{Tf}_2\text{N}]$	15.932
[ $C_6\text{-mim}][\text{BF}_4]$	15.034	[ $C_3\text{-mim}][\text{Tf}_2\text{N}]$	16.540
[ $C_8\text{-mim}][\text{BF}_4]$	14.067	[ $C_4\text{-mim}][\text{Tf}_2\text{N}]$	17.952
[ $C_4\text{-mim}][\text{PF}_6]$	17.682	[ $C_5\text{-mim}][\text{Tf}_2\text{N}]$	20.100
[ $C_6\text{-mim}][\text{PF}_6]$	18.545	[ $C_6\text{-mim}][\text{Tf}_2\text{N}]$	22.278
[ $C_8\text{-mim}][\text{PF}_6]$	19.573	[ $C_7\text{-mim}][\text{Tf}_2\text{N}]$	24.857
		[ $C_8\text{-mim}][\text{Tf}_2\text{N}]$	28.037

The following parabolic function has been obtained by fitting the ionic liquid members of the  $[C_n\text{-mim}][\text{Tf}_2\text{N}]$  family with the alkyl chain length ranging from  $C_2$  to  $C_8$ :

$$10^{19} c_{\text{Tf}_2\text{N}} = 0.2233 \text{ CN}^2 - 0.1872 \text{ CN} + 15.275 \text{ [Jm}^5\text{mol}^{-2}] \quad (4.7)$$

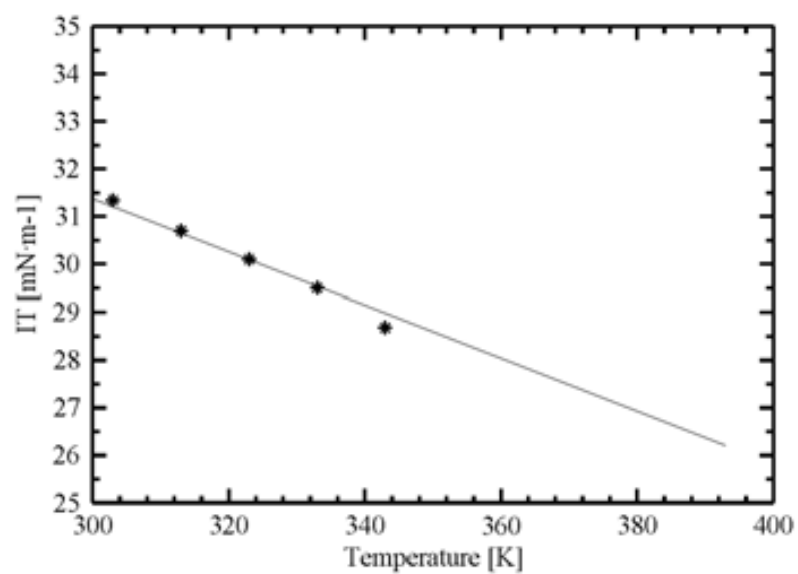
This correlation is plotted together with the tabulated fitted values in Figure 4.36.



**Figure 4.36:** Optimized influence parameter for the light members of the *n*-alkyl-3-methyl-imidazolium bis(trifluoromethylsulfonyl)imide:  $[C_n\text{-mim}][\text{Tf}_2\text{N}]$ , versus the carbon number. Solid line corresponds to the values obtained from equation (4.7).

Using the previous correlation, the predictive interfacial tension for  $[C_{10}\text{-mim}][\text{Tf}_2\text{N}]$ , with the  $c$  parameter calculated from Equation (4.7) is presented in Figure 4.37 with excellent agreement when compared to experimental data [Carvalho *et al.*, 2008] with an AAD% lower than 0.20% for all points. Some authors (Santos and Coutinho for instance) have explained the disruptions beyond  $C_6$ , on the values of some physical chemical properties as the calorific capacity or the interfacial tension. We have denoted that the shift in the interfacial tension values for the long members is not as big as in the case of the short compounds for the same family. With our model we have also

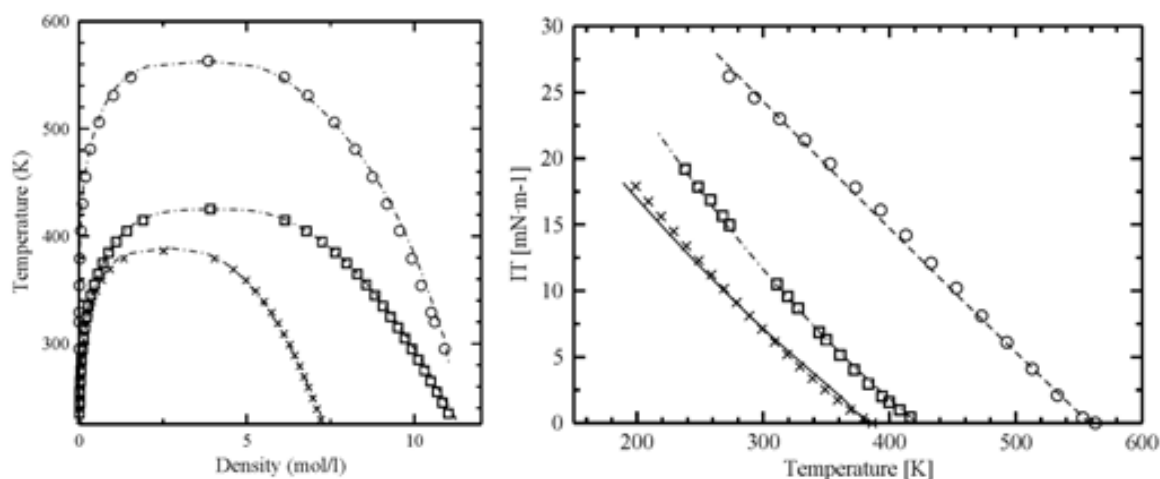
captured the disruption in the value of the interfacial tension for the compounds having more than six carbon molecules.



**Figure 4.37:** Predictions for the vapor-liquid interfacial tensions of  $[C_{10}\text{-mim}][Tf_2N]$ . Symbols represent experimental data [Carvalho et al., 2008] and lines correspond to the soft-SAFT+DGT predictions.

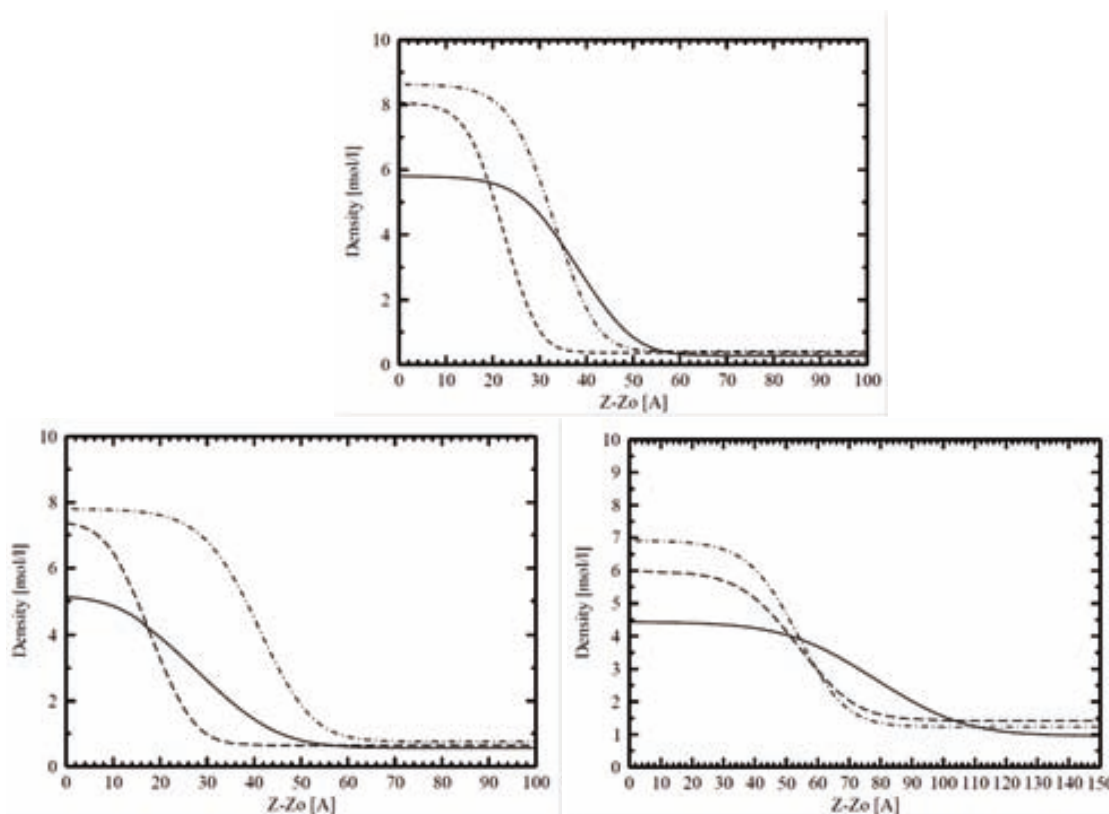
### 4.2.3. Comparison between organic families

One of the main advantages of using a molecular-based equation of state is that it can be used to compare the behavior of different compounds under the same or similar conditions. For instance, we present in Figure 4.38a comparison between a selected member (with four carbons, C<sub>4</sub>) of three homologous chemical families, the *n*-alkanes, and perfluoroalkanes or 1-alkanol families. Results from crossover soft-SAFT vapor-liquid equilibria for butane, perfluorobutane and 1-butanol [Llovell *et al.*, 2004; Dias *et al.*, 2006; Llovell, 2006] are presented in Figure 4.38a, together with experimental data [Landolt-Börnstein, NIST], while the interfacial tensions of these three compounds obtained by combining crossover soft-SAFT with DGT are presented in Figure 4.38b. Two comments are in order: first, the agreement between the theory and the experiments is excellent for the three compounds and for the two properties studied, and secondly, the plots clearly show the fascinating behavior of the perfluoroalkanes, than in spite of being very similar to the corresponding alkanes and with equilibria vapor densities very similar, except in the near critical region, their equilibria liquid densities are very different, hence presenting lower interfacial tensions.



**Figure 4.38:** Comparison of phase and interfacial properties of a C<sub>4</sub> compound from the three homologous chemical families: butane (squares), perfluorobutane (crosses) and butanol (circles). a) vapor-liquid equilibria phase diagram, b) interfacial tensions as a function of temperature. Symbols represent the experimental data [[Landolt-Börnstein, NIST] while the lines correspond to the crossover soft-SAFT+DGT approach.

Additional information about the interfacial behavior of these three compounds can be obtained by calculating the density profiles at different temperatures. We have employed a transformation from location space to density space [Poser and Sanchez, 1981], the integration of which provides a way to calculate density profiles (Equation 3.3), which are depicted in Figure 4.39 for three reduced temperatures,  $T_r=T/T_c$ , 0.84, 0.91 and 0.97. The overall behavior of the three compounds with respect to temperature is as expected; the interfacial density profile becomes wider and smoother as the critical temperature is approached. More interesting is to observe the behavior of the perfluoroalkane compound, compared to the other two compounds with the same number of carbon atoms, as at the same reduced temperature shows a wider and smoother profile, indicating that the molecules prefer to stay at the interface instead of at the two bulk phases.



**Figure 4.39:** Comparison of the density profiles of butane (dotted and dashed lines), butanol (dashed lines) and perfluorobutane (solid lines) as predicted from crossover-soft-SAFT + DGT at three reduced temperatures a)  $T_r=0.84$ , b)  $T_r=0.91$  and c)  $T_r= 0.97$ . See text for details.

## 4.3. Modeling of binary mixtures

### 4.3.1. Nonassociating mixtures<sup>13</sup>

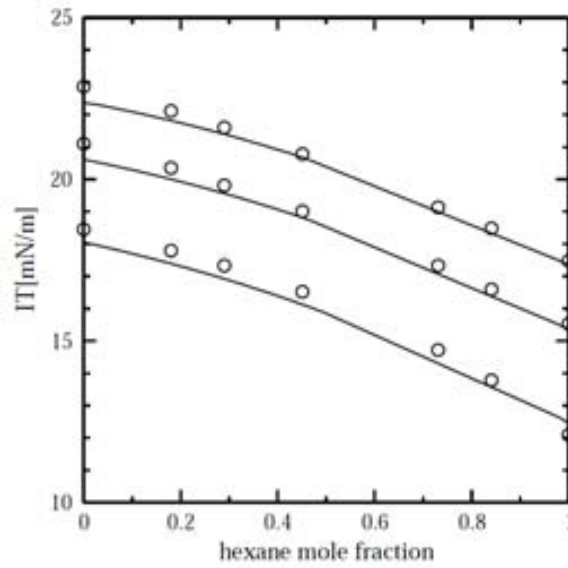
The first mixtures chosen on this PhD thesis are systems composed of mixtures of hydrocarbons such as *n*-alkanes with carbon dioxide. On one hand, these mixtures are very frequent in a wide variety of industrial processes and it is important to have a quantitative model able accurate thermophysical properties. On the other hand, they can be used as a first test to check the performance of the approach for the simultaneous calculation of the vapor liquid equilibria and the interfacial tension of simple and nonassociating mixtures.

#### 4.3.1.1. Hydrocarbon mixtures

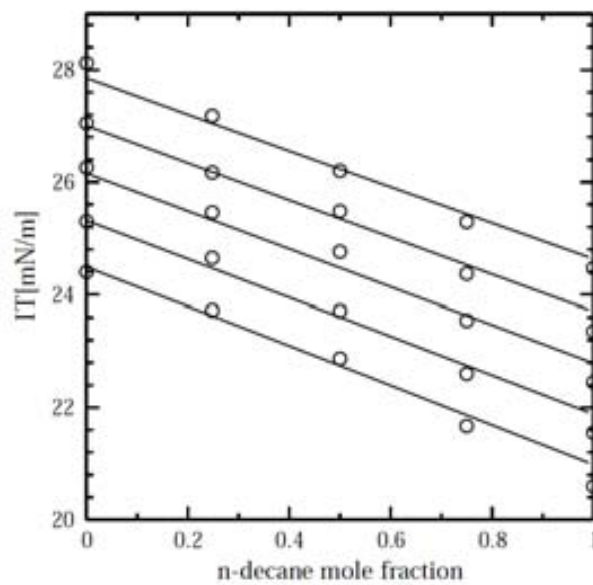
We present next predictive results for selected *n*-alkane mixtures to show some few examples of the performance of the approach for mixtures. Figures 4.40, 4.41 and 4.42 show predictions for the interfacial tensions of the mixtures *n*-hexane + *n*-decane, *n*-decane + *n*-hexadecane and *n*-hexadecane + *n*-eicosane, respectively, at different isotherms. The molecular parameters of the compounds were obtained from the correlations of reference [Pàmies and Vega, 2001] and there is no fitting to mixture data ( $\eta=\xi=\beta=1$ ), hence, results are entirely predictive. Results obtained from soft-SAFT + DGT are compared with available experimental data in all cases [Landolt-Börnstein, Carvalho *et al.*, 2008; Rolo *et al.*, 2002]. The crossover version of the equation was used for the *n*-hexane + *n*-decane mixture, as the temperatures are close to the critical temperature, while no-crossover was needed for the other two mixtures. Considering the scatter of the experimental data, predictions are in very good agreement with experimental data, showing the robustness of the approach. Slight deviations observed in the interfacial tension of the pure components may be due to the fact that experimental data come from different sources; a comparison of literature values can be found in reference [Rolo *et al.*, 2002].

---

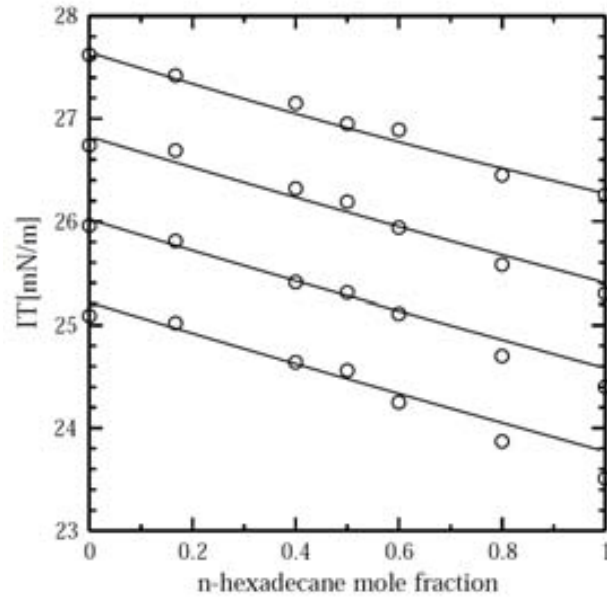
<sup>13</sup> Part of this section has been published in Vilaseca, O. and Vega, L.F. Direct calculation of interfacial properties of fluids close to the critical region by a molecular-based equation of state. *Fluid Phase Equilib.* **2011**, 306, 4-14.



**Figure 4.40:** Predictions for the vapor-liquid interfacial tensions of the *n*-hexane + *n*-decane mixture at: 303.15, 323.15, and 353.15 K (from top to bottom). Circles represent experimental data [Landolt-Börnstein] and lines correspond to the crossover soft-SAFT+DGT predictions.



**Figure 4.41:** Predictions for the vapor-liquid interfacial tensions of the *n*-decane + *n*-hexadecane mixture at: 293.15, 303.15, 313.15, 323.15 and 333.15 K (from top to bottom). Circles are experimental [Landolt-Börnstein] and lines correspond to the soft-SAFT+DGT approach.

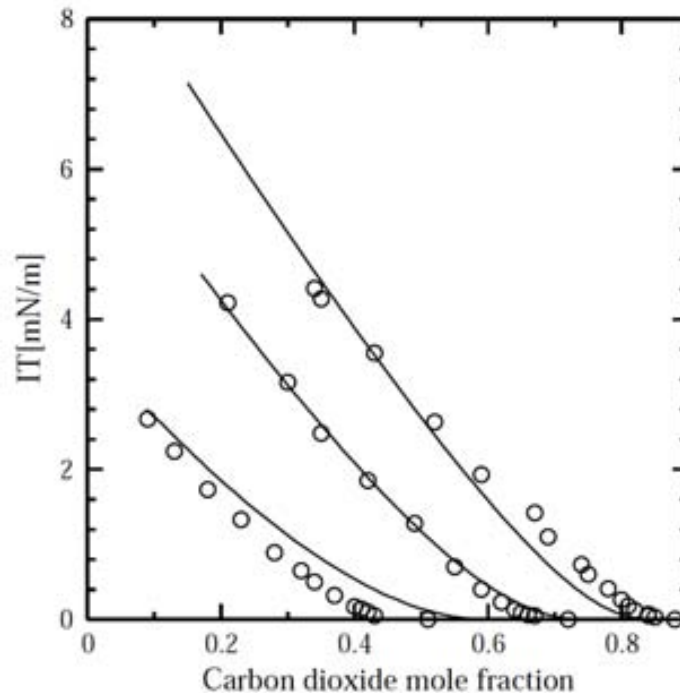


**Figure 4.42:** Predictions for the vapor-liquid interfacial tensions of the n-hexadecane + n-eicosane mixture at: 313.15, 323.15, 333.15 and 343.15 K (from top to bottom). Circles are experimental data [Landolt-Börnstein] and lines correspond to the soft-SAFT+DGT approach.



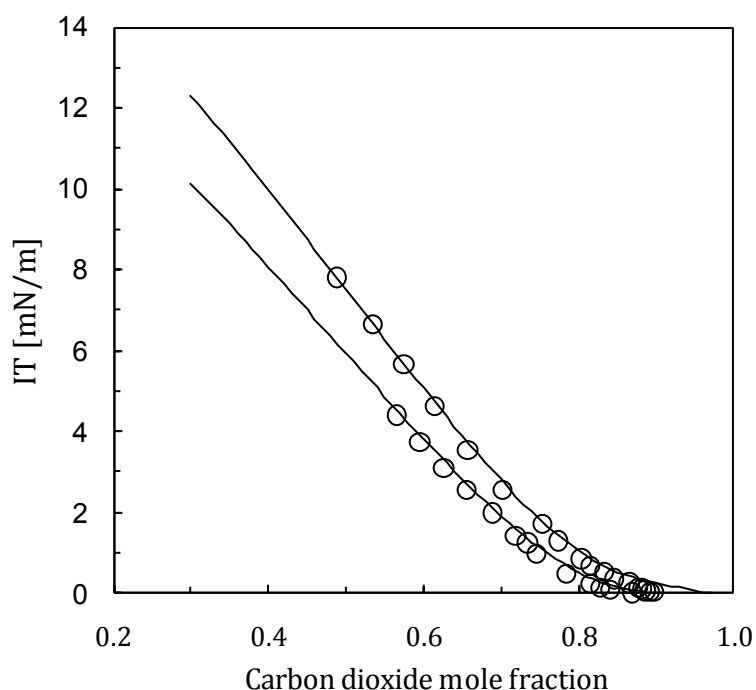
### 4.3.1.2. Carbon dioxide mixtures

The interfacial tensions of a couple of carbon dioxide + n-alkane mixtures are shown here. First of all, the interfacial tensions of carbon dioxide + n-butane mixture at three temperatures are plotted in Figure 4.43. The experimental data was taken from reference [Hsu *et al.*, 1985]. This mixture had already been studied using DGT coupled to different equations by other authors [Cornelisse, 1997; Miqueu, 2000;2001;2003; Pàmies, 2003], and parachor methods, and it is interesting to compare here the performance of soft-SAFT + DGT with the other approaches. The binary parameters  $\chi$  and  $\psi$  were adjusted to bulk vapor-liquid equilibrium data and the interfacial tension was then predicted using the same parameters. The crossed influence parameter  $\hat{a}$  was set to unity. Good overall results are obtained at all temperatures in the whole range of compositions, in closer agreement to experimental data.



**Figure 4.43:** Vapor-liquid interfacial tensions of the carbon dioxide + n-butane mixture at: 319.3, 344.3 and 377.6 K (from left to right). Symbols represent experimental data [Hsu *et al.*, 1985] and lines are calculations from the crossover soft-SAFT+DGT approach with two binary parameters ( $\chi = 1.025, \psi = 0.98$ ).

Following the same procedure, the carbon dioxide + n-decane mixture at two temperatures are plotted in Figure 4.44. Again, binary parameters fitted to VLE data were used ( $\delta = 1.010$ ,  $\delta = 0.935$ ) and the interfacial tension was obtained using  $\delta = 1$ . Good overall results are also obtained in this case for the two temperatures for which experimental data is available [Nagarajan et Robinson, 1986].



**Figure 4.44:** Vapor-liquid interfacial tensions of the carbon dioxide + n-decane mixture at: 344.3 and 377.6 K (from right to left). Symbols represent experimental data [Nagarajan et Robinson., 1986] and lines are calculations from the crossover soft-SAFT+DGT approach with two binary parameters, ( $\delta = 1.010$ ,  $\delta = 0.935$ ).

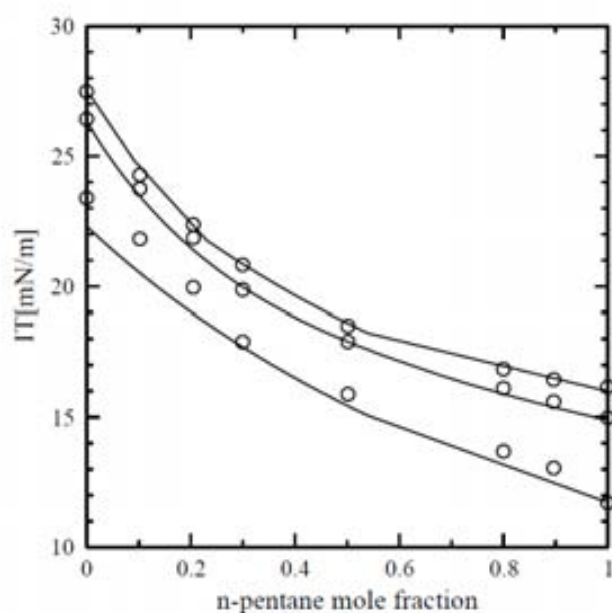
It is remarkable that the inclusion of the crossover term for the calculation of these mixtures, derives in a good description of the critical region, making a step forward in the existing works that did not employ a crossover treatment to account on the density fluctuations while approaching the critical region.

### 4.3.2. Associating mixtures

In this section, self-associating mixtures and cross-associating mixtures results are presented. This is a breakthrough in the calculation of binary mixtures by means of the DGT combined with an equation of state. Until the present work the most of the papers have dealt with nonassociating mixtures leaving apart the field of associating compounds especially close to the critical region.

#### 4.3.2.1. n-Alkane + Nitrile mixtures<sup>14</sup>

Here, results for the interfacial tension of the mixture butanenitrile + pentane are depicted in Figure 4.45. Lines correspond to soft-SAFT calculations while experimental data at three different temperatures,  $T = 293$ , 303 and 333K, was taken from [Landolt-Börnstein]. No binary parameters were used, being the theoretical calculations purely predictive.



**Figure 4.45:** Vapor-liquid interfacial tensions of the butanenitrile + pentane mixture at: 293, 303 and 333 K (from top to bottom). Symbols represent experimental data [Landolt-Börnstein] and lines are predictions from the soft-SAFT+DGT approach.

<sup>14</sup> Part of this section has been published in Vilaseca, O. and Vega, L.F. Direct calculation of interfacial properties of fluids close to the critical region by a molecular-based equation of state. *Fluid Phase Equilib.* **2011**, 306, 4-14.

As in the previous cases, the agreement between the equation and the experimental results is outstanding. It is remarkable that the agreement is excellent in the high temperatures and notable for the lowest studied temperature.

### 4.3.2.2. Refrigerants mixtures<sup>15</sup>

The proposed model and the fitted parameters for HFC can be further tested by studying the behavior of mixtures as compared to experimental data. We have selected several mixtures of HFCs for which experimental data is available in the open literature and have compared the soft-SAFT predictions with them, finding good agreement in most of the cases. As refrigerants are modeled as associating compounds, cross-association plays an important role in those predictions.

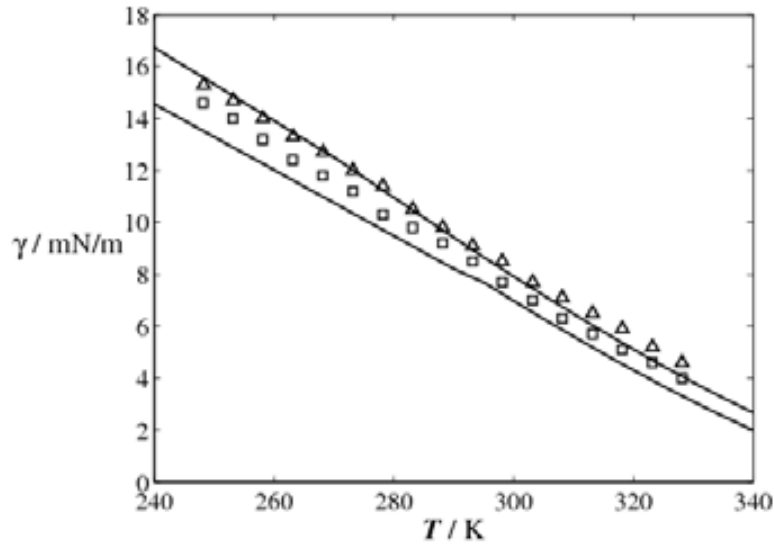
Binary mixtures of refrigerants have been modeled considering that the two associating sites of each refrigerant have a different nature (one type  $A$  and one type  $B$ ). If we consider refrigerant 1 has association sites  $A$  and  $B$  and refrigerant 2 has association sites  $A'$  and  $B'$ , then two types of association are possible: self-association (interaction  $AB$  in one refrigerant, or  $A'B'$  in the other) and cross-association (interaction  $AB'$  and  $A'B$  between two refrigerants). All the other possible interactions have been set to zero. The values of the volume and energy of the cross-association interactions are directly obtained following the classical Lorentz-Berthelot combining rules for the volume and the energy of association, respectively. Note that in the case of  $\kappa_{HB}$ , the cross-interaction values will have the same value than the self-interactions, as we have used a constant value for all the refrigerants studied in this work. All the cross-association values have been considered to be equal ( $AB' = A'B$ ).

Even if some mixtures of refrigerants are asymmetric, it is expected that the interactions in the mixture will be captured by this simple associating model. As we are looking for the predictive capability of the equation, the two binary interaction parameters  $\eta$  and  $\xi$  of the generalized Lorentz-Berthelot combining

---

<sup>15</sup> Part of this section has been published in Vilaseca, O.; Llovel, F.; Yustos, J.; Marcos, R.M.; Vega, L.F. Phase equilibria, surface tensions and heat capacities of hydrofluorocarbons and their mixtures including the critical region. *J. Supercrit. Fluids*, **2010**, 55 (2), 755-768

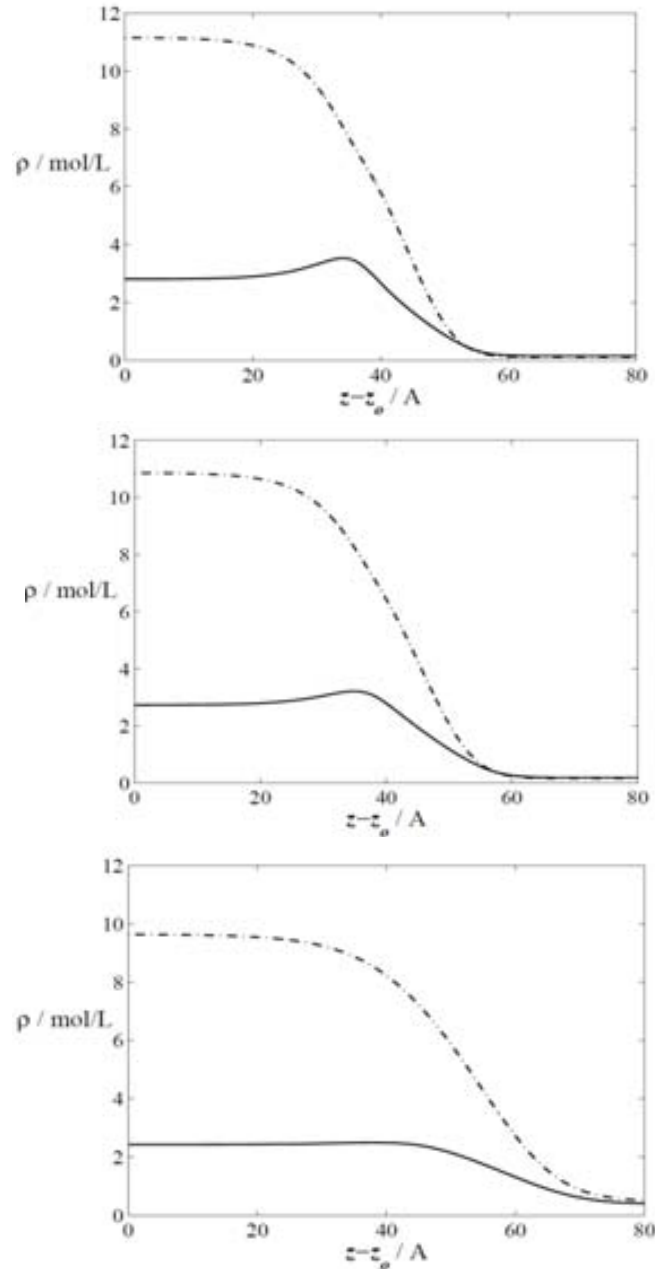
rules have been set to 1, i.e. they have not been used. Hence, results presented here for mixtures of HFCs are purely predictive.



**Figure 4.46:** Interfacial properties of the systems propane + R152a mixture (a) Interfacial tension for a mass composition fraction  $w_1=0.2008$  ( $\Delta$ ) and  $w_1=0.4922$  ( $\square$ ). Symbols represent the experimental data [Zhao et al., 2010] while the lines correspond to the soft-SAFT modeling.

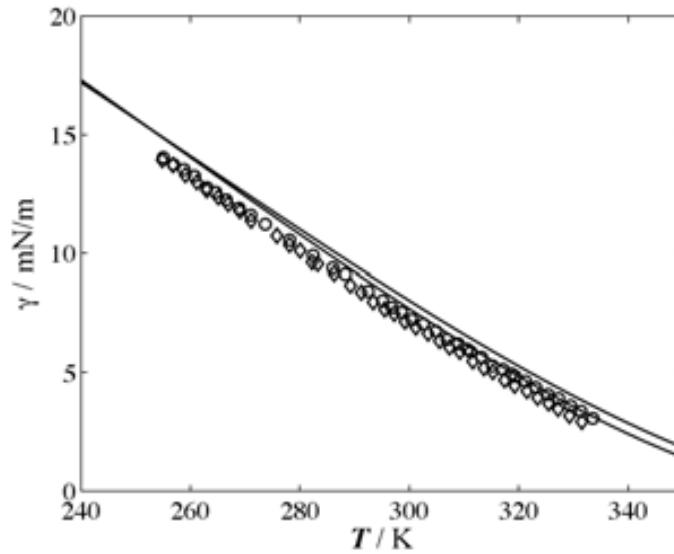
Efficient design of mechanical refrigerators requires the knowledge of several thermophysical properties. The interfacial tension of the mixtures plays an important role, as it could potentially be used in vapor compression cycles. In Figure 4.46, an example of the system propane (R290) (1) and R152a (2) is presented at a mass fraction  $w_1=0.2008$  and  $w_1=0.4922$ , as a function of temperature. Experimental data (symbols) were taken from literature [Zhao et al., 2010] while the solid lines represent the crossover soft-SAFT + DGT calculations. Moreover no binary interaction parameters have been used in this case ( $\eta = \xi = 1.000$ ). As explained, in addition to interfacial tensions, the density gradient theory of van der Waals also allows the calculation of interfacial density profiles. They provide information about the concentration behavior of the mixture, as well as any preferential adsorption, at the interface. As an example we have chosen the mixture presented in Figure 4.47, propane (R290) and R152a, and calculated the density profiles of both components along the interface, for the mass fraction  $w_1=0.2008$  and three

different temperatures, using crossover soft-SAFT coupled with DGT. Results are depicted in Figure 4.47. Interestingly it is observed that propane exhibits a positive surface activity (or absolute adsorption,  $d\rho_1/dz=0$ ;  $d^2\rho_1/dz^2 < 0$  in the interfacial region), which is a function of temperature, disappearing at the highest temperature investigated.



**Figure 4.47:**  $\rho_1$ - $z$  and  $\rho_2$ - $z$  density profiles for the mixture propane + R152a at a fixed mass composition fraction  $w_1=0.2008$  and three temperatures  $T=270\text{K}$ ,  $295\text{K}$  and  $315\text{K}$ . The full line represents the propane density profile while the dotted-dash line represents the R152a density profile along the interface.

Finally, a second example is given with the prediction of the mixture R32-R134, a common blend used in refrigerators. This is a stringent test to the model as several interactions are present in this kind of mixtures form by two associating compounds. As can be observed in Figure 4.48, an excellent agreement is found between experimental data and the calculations performed by the soft-SAFT combined with the DGT.



**Figure 4.48:** Interfacial properties of the systems R32 + R134 mixture (a) Interfacial tension for a mass composition fraction  $w_1=0.2379$  ( $\Delta$ ) and  $w_1=0.4017$  ( $\square$ ). Symbols represent the experimental data [Yuan-Yuan et al., 2003] while the lines correspond to the soft-SAFT modeling.

### 4.3.2.3. Water + Alkanol mixtures

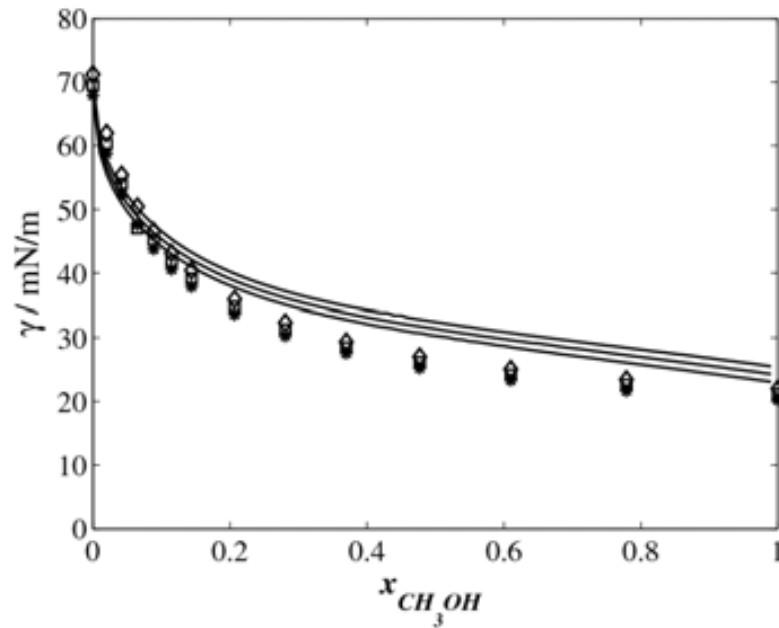
Historically, the thermodynamics modeling of mixtures containing components with highly directional attractive molecular interactions has been a challenge, as classical equations of state do not explicitly consider those interactions in their models. In the case where more than one compound in the mixture is able to associate and form cross associates, the strong and directional nature of the association bonds has a large impact on their phase behavior, and their description with classical approaches is generally poor, with high deviations from the experimental measurements. Among these systems, we mention aqueous mixtures with alcohols. These mixtures are present in many industrial applications: antifreeze, forced induction internal combustion engines increasing, reagents, solvents, antiseptic and preservative for specimens.

It has been proved that in order to have an accurate model for the estimation of the thermophysical properties of these systems, it is necessary to consider self and cross-association when building the theory. As the model for mixtures used here explicitly considers these associations from its inception, it allows the self-association of the molecules described in previous paragraphs, as well the cross-association between the electron pair of water and hydrogen of the hydroxyl group of the 1-alkanol, and the hydrogen of water and the oxygen of the hydroxyl group of the 1-alkanol.

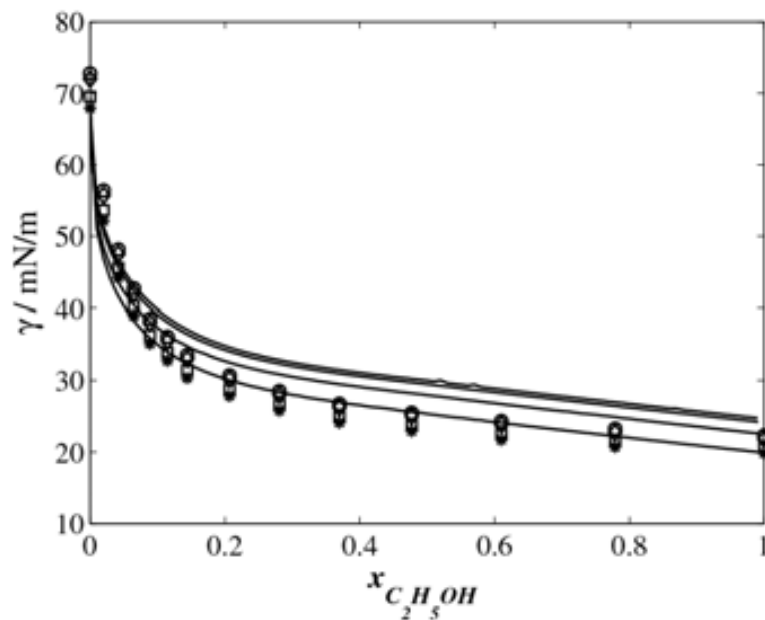
The model is tested also to reproduce the vapor-liquid and liquid-liquid equilibria of several mixtures of water and 1-alkanols. The binary parameters  $\eta$  and  $\xi$  are fitted to mixture VLE data and, from there, the interfacial tension is evaluated (note that the crossed influence parameter  $\beta$  is still 1) with no further fitting, in a predictive manner.

In Figure 4.49 and 4.50, the interfacial tensions at different temperatures of the water + methanol and water + ethanol mixtures are shown.





**Figure 4.49:** Vapor-liquid interfacial tensions of the water-methanol mixture at: 303, 313 and 323 K (from top to bottom). Symbols represent experimental data [Gonzalo et al., 1995; Landolt-Börnstein] and lines are the soft-SAFT + DGT predictions.



**Figure 4.50:** Vapor-liquid interfacial tensions of the water-ethanol mixture at: 293, 298, 313 and 323 K (from top to bottom). Symbols represent experimental data [Gonzalo et al., 1995; Landolt-Börnstein] and lines are predictions from the soft-SAFT+DGT approach. See text for details.

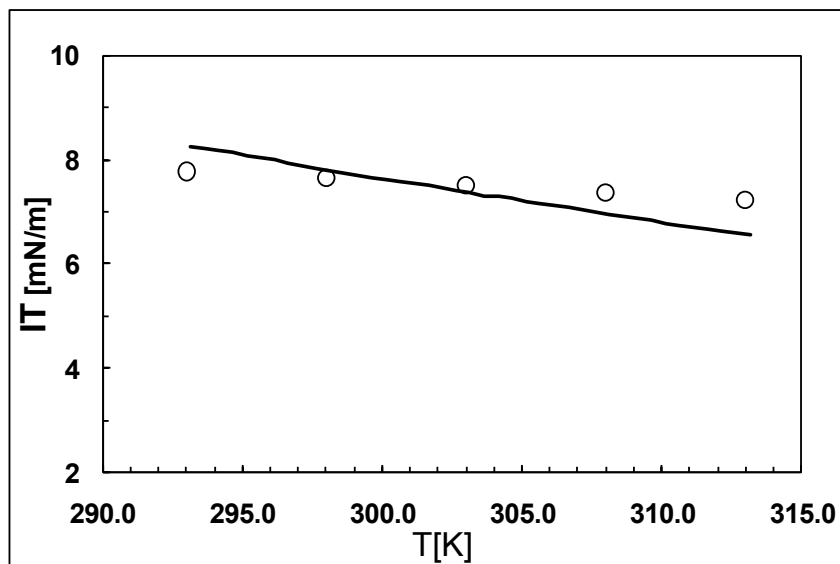
In general, good agreement is obtained between experimental data and the predictions with the soft-SAFT calculations combined with the DGT in the whole range of compositions. This confirms the capability of the model to transfer the parameters obtained for the pure compounds while applying a realistic associating model.

#### 4.3.2.4. Ionic liquid + n-Alkane mixtures

We have also considered in this PhD thesis the challenging mixture composed by ionic liquid and n-alkanes. To our knowledge, there are no modeling works of the interfacial properties of these systems published in literature. In fact, these systems are difficult to model, as liquid-liquid equilibrium is involved. The original DGT theory was conceived for an accurate description of the vapor-liquid interface; hence, care must be taken when applying it to the calculation of liquid-liquid interfacial tensions.

For modeling purposes it is important to recall here that the n-alkanes are considered as Lennard-Jones chains with no associating sites, while ionic liquids are modeled as an ionic pair where the cation and anion are forming a chain, with a specific number of associating sites mimicking the cation-anion interaction between different pairs.

Results for the interfacial properties of  $[C_4mim][Tf_2N]$  + n-hexane as obtained from soft-SAFT are compared to experimental data in Figure 4.51. The rest of the compounds are included for completeness. The calculations are done by fitting the binary parameters using interfacial tension data.



**Figure 4.51:** Vapor-liquid interfacial tensions for the  $[C_4mim][Tf_2N]$  + n-hexane mixture from 293 to 313 K. Symbols represent experimental data [Gardas et al., 2010] and lines are predictions from the soft-SAFT+DGT approach.

## Chapter 4

These preliminary results prove that the approach can be used to accurately model these extremely challenging mixtures. The Soft-SAFT + DGT approach correctly gives the value of the interfacial but it is unable to provide the correct tendency as a function of temperature. It has to be considered that it could be corrected by using a  $\beta \neq 1$  or by having a wider range of temperatures for the interfacial tension experimental data.

## **4.4. Surface and critical properties of ionic liquids**<sup>16</sup>

Precise measurements of ionic liquids (IL) physical properties near the critical point are an unexplored field. Experimental data at these extreme conditions is very difficult to achieve due to the low vapor pressures of these compounds and also because thermal degradation occurs well before the critical region is reached. However, in order to design thermally stable ILs information about the critical region is a requirement. Hence, the need of reliable predictions of the critical properties of ionic liquids has pushed the development of theoretical methods physically sounded. We present here the application of the soft-SAFT EoS coupled with DGT to obtain surface tensions as well as the critical temperature, pressure and density estimations, for three different imidazolium ionic liquid families. Surface thermodynamic properties are also derived from the temperature dependence of the surface tension values, and compared with those obtained with Guggenheim's (Gug) and Eötvös (Eöt) empirical equations. Qualitative agreement with available experimental and simulation data is obtained, reinforcing the value of using molecular based equations of state with sound parameters and predictive capabilities.

In the particular case of ionic liquids different approaches have been used to describe the surface and the critical properties of the ionic liquids which are at this moment an unexplored field. Given the importance of these fluids at the present time, as possible new green solvents and for other applications, we should establish a systematic methodology to evaluate the physical properties as this is one of the existing barriers to be overcome prior to their industrial and commercial development.

The surface entropy and the surface enthalpy values have demonstrated that these compounds have a high ordered surface as the prior studies of Watson and Law had enounced. For the study of these molecules we have also used

---

<sup>16</sup> Part of this section is going to be published in Vilaseca, O. and Vega, L.F.; Critical, interfacial and surface properties of ionic liquids by a molecular-based equation of state. In preparation (2012).

the Principle of Corresponding States proposed by van der Waals in 1880 and developed by Guggenheim in 1947.

Following the methodology of our previous works [Vilaseca and Vega, 2011; Vilaseca *et al.*, 2010; Llovel *et al.*, 2012], the vapor-liquid interfacial tensions have been calculated and shown in Section 4.2.2.6. After that, the soft-SAFT approach is also used to calculate the critical properties of these families of ILs, in a similar manner as done for simple fluids. In addition, we have also calculated the surface entropy  $S^\square$  and surface enthalpy,  $H^\square$ , using  $\square$  as obtained from soft-SAFT + DGT and its dependency with temperature, far from the critical point.

### 4.4.1. Critical Properties

The critical temperature,  $T_c$ , the critical pressure,  $P_c$ , and the critical density,  $\rho_c$ , have been estimated by direct calculations of the vapor-liquid equilibria with soft-SAFT equation of state combined with the DGT, assuming that the interfacial tension value vanishes at the critical point and, the results (see Table 4.18) are compared to those obtained by Rebelo *et al.* [2005] and the group of Coutinho [2007; 2008] where they adopted the Guggenheim (Gug) and Eötvös (Eöt) approaches to treat their interfacial tension experimental data.

$$\gamma = K \left( 1 - \left( \frac{T}{T_c} \right) \right)^{\frac{11}{9}} \quad \text{(Gug)} \quad (4.8)$$

$$\gamma \left( \frac{M}{\rho} \right)^{\frac{2}{3}} = K(T_c - T) \quad \text{(Eöt)} \quad (4.9)$$

The critical density obtained by means of our calculations with the soft-SAFT equation of state, have been compared with those obtained by Weiss *et al.* [2010a,b] using the Cailletet-Mathias linear-diameter rule for the coexistence curve following the correlation and results presented in Table 4.18.

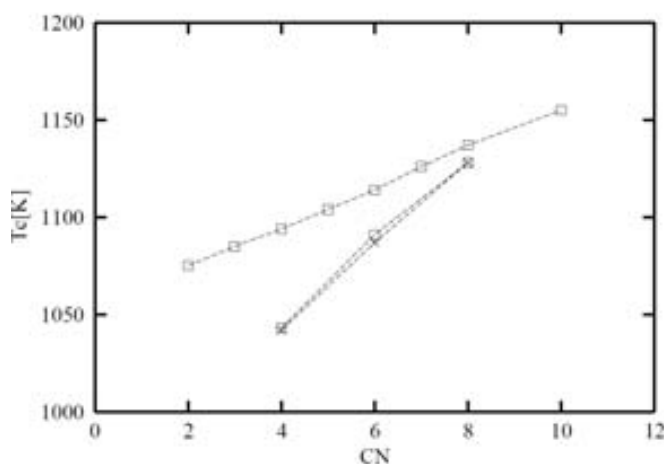
$$\rho_c = mT_c + h \quad (4.10)$$

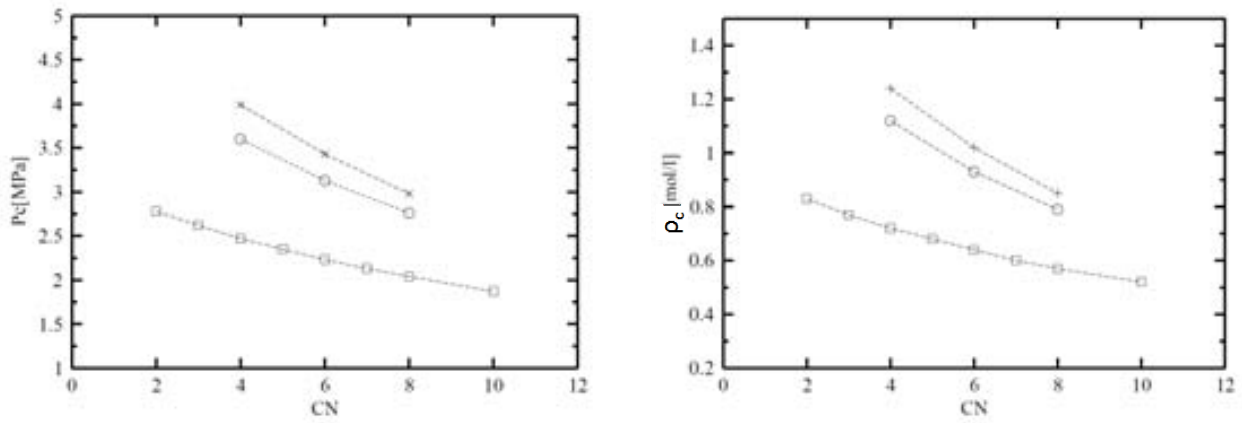
a)

*Results and discussion*

$T_c$  is the critical temperature in K, and  $\rho_c$  is the critical density in  $\text{g cm}^{-3}$  and  $m$  and  $h$  are the coefficients for the correlation, in  $\text{g cm}^{-3}$  and  $\text{g cm}^{-3} \text{K}^{-1}$  respectively. This equation was used in Weiss' previous work to compile the best estimated values from different experimental and simulation data (see [Weiss *et al.*, 2010a, b] and the references therein for details).

An average for the critical temperature between  $T_c = 1000 \pm 50 \text{ K}$  and  $T_c = 1100 \pm 50 \text{ K}$  (see Table 4.18) has been found in accordance with the values reported in the literature [Freire *et al.*, 2007; Carvalho *et al.*, 2008; Gathe *et al.* 2008], where the empirical approaches based on the corresponding states correlations, proposed by Guggenheim (Gug) [Guggenheim, 1945] and Eötvös (Eöt) [Shereshefsky, 1931] were adopted to obtain the critical properties from experimental measurements. It can be seen that the imidazolium ionic liquids with  $[\text{BF}_4]^-$  and  $[\text{PF}_6]^-$  exhibit the almost the same value for the critical temperature for the same alkyl chain length, while the imidazolium  $[\text{Tf}_2\text{N}]$  ionic liquids shows critical temperature about 15%-20% higher for corresponding alkyl chain length. As is can be observed in Figure 4.52a the longer the alkyl chain length is the higher the critical temperature is and, as expected, the lower the critical density (Figure 4.52b) and the critical pressure (Figure 4.52c) are. The estimated critical densities for the  $[\text{C}_n\text{-mim}][\text{Tf}_2\text{N}]$  compounds have been compared with those obtained by Weiss *et al.* [2010] and a very good agreement is found for short and long chains. This can be considered as a first approximation since the approach is still being tested for these ionic families.





**Figure 4.52:** Critical properties for the light members of the [C<sub>n</sub>-mim][BF<sub>4</sub>] (circles), [C<sub>n</sub>-mim][PF<sub>6</sub>] (diamonds) and [C<sub>n</sub>-mim][Tf<sub>2</sub>N] (squares) ionic liquids, versus the carbon number. a) Critical Temperature b) Critical Pressure c) Critical density.

It can be seen that [C<sub>n</sub>-mim][BF<sub>4</sub>] and [C<sub>n</sub>-mim][PF<sub>6</sub>] exhibit the almost the same value for the critical density and pressure for the same alkyl chain length, while the [C<sub>n</sub>-mim][Tf<sub>2</sub>N]<sup>-</sup> shows critical temperature about 20%-30% lower for corresponding alkyl chain length. The tendency of results obtained for the critical temperature is opposed to those obtained by empirical approaches. Nevertheless, as proposed by Weiss *et al.* [2010] the corresponding states method not seems to be the better approach to calculate the critical properties of these particular fluids, being the atomistic and molecular simulations followed by molecular based equations of state, the most suitable methods to estimate critical properties.

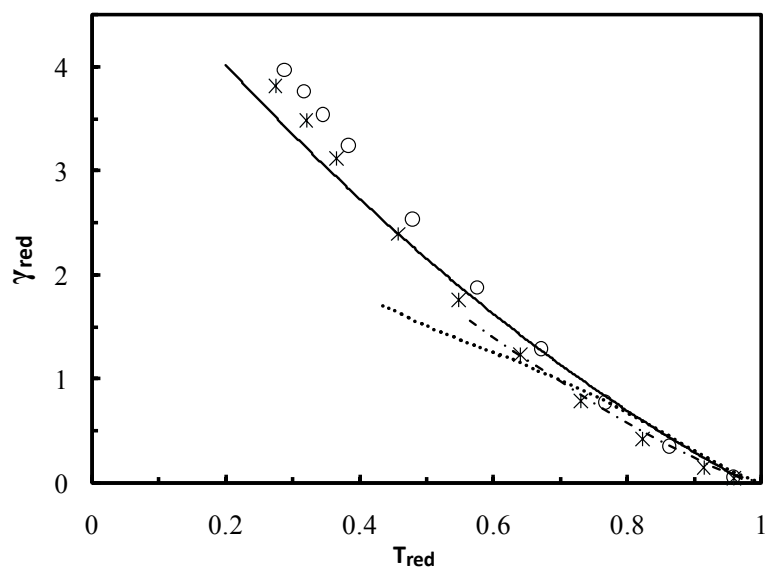
On the framework of the corresponding states method we have analyzed the interfacial tension data, correlating the reduced interfacial tension  $\gamma_{red}$  with the reduced temperature  $T/T_c = T_{red}$  according to:

$$\gamma_{red} = c' \frac{\gamma}{T_c} \left( \frac{T}{T_c} \right)^{2/3} \quad (4.11)$$

where  $c'$  is a constant that equals  $1/(10^7 k_B/N_A)^{2/3} \approx 1.016 \text{ J}^{-1} \text{ K mol}^{2/3}$  if  $\gamma$  is measured in  $\text{mN}\cdot\text{m}^{-1}$ ,  $T_c$  in K, and  $\rho_c$  in  $\text{g cm}^{-3}$ ; here,  $k_B$  denotes Boltzmann's constant and  $N_A$  Avogadro's number. Figure 4.53 shows the corresponding surface tension  $\gamma_{red}$  as a function of the reduced temperature  $T_{red}$  as defined in



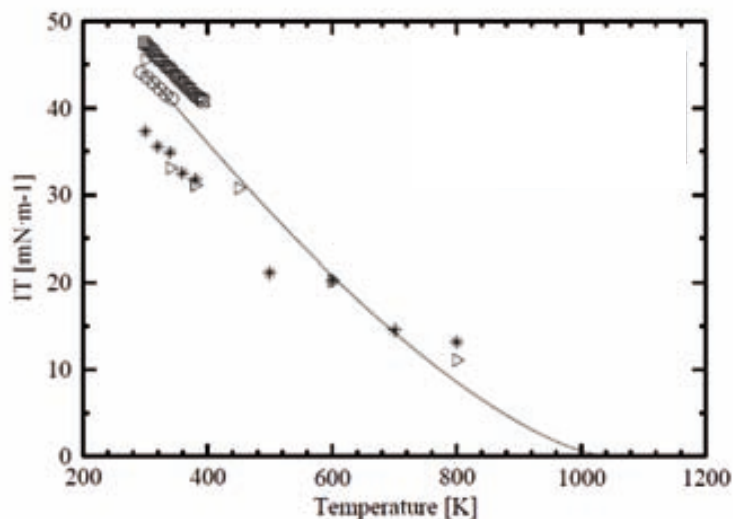
Equation (4.11) for argon, for R32 and for ethanol indicating the range of nonpolar to moderate polar fluids. Results from soft-SAFT + DGT calculations for two ionic liquids,  $[C_4\text{-mim}][PF_6]$  and  $[C_4\text{-mim}][Tf_2N]$  are represented up to the critical point. No inflexion point has been found in any ionic liquid, in this comparison, only moderate polar fluids like methanol shows an inflexion point around  $\gamma_{red} = 0.7$ . However, it is important to highlight that the ionic liquids studied in this contribution deviate from the master curve at low temperatures, while at high temperatures they are between the ranges of nonpolar to moderate polar fluids. In hence, in accordance with the conclusions obtained by Weiss *et al.* [2010], there are significant contributions to the thermodynamic behavior of ionic liquids beyond the Columbic forces governing at low temperatures, such as van der Waals forces, specific interactions, hydrogen bonding or the formation of short-lived ion pairs [Law and Watson, 2001; Zhao *et al.*, 2010], which reduced the ionic character of the fluid.



**Figure 4.53:** Corresponding states surface tension  $\gamma_{red}$  as a function of the reduced temperature  $T_{red}$ . Experimental data [Landolt-Börnstein] for argon (dashed line) and for R32 (solid line) and ethanol (dotted line). Results from soft-SAFT + DGT calculations for two ionic liquids  $[C_4\text{-mim}][PF_6]$  (circles) and  $[C_4\text{-mim}][Tf_2N]$ (stars) are represented.

### 4.4.2. Interfacial thermodynamic properties

$[C_4\text{-mim}][PF_6]$  is a representative member of the imidazolium  $[BF_4]$ , and, as such it has been investigated by different authors. In Figure 4.54 a comparison among the published interfacial tension data is represented, including experimental data from different sources, simulation data obtained with different packages (symbols), and the soft-SAFT calculations performed in this work, represented by a solid line. Qualitative agreement is found between the experimental data [Freire *et al.*, 2007; Carvalho *et al.*, 2008; Gathee *et al.* 2008] and the simulation results reported by Weiss *et al.* [2010a,b] using the Gromacs Simulation Package, while in the other cases significant deviations are found, especially in the case of the YASP results, unable to describe the behavior of the interfacial phenomena at low temperatures. Contrarily, it is remarkable to say that our simple model is able to accurately describe the interfacial tension at high temperatures with a good agreement with the first simulation data reported in the literature with both commercial packages. In fact, this approach can be used as a first test for both experimental and simulation data.



**Figure 4.54:** Interfacial tension as a function of temperature for  $[C_4\text{-mim}][PF_6]$ . Symbols represent simulation data YASP (stars) and GROMACS (triangles up) [Weiss *et al.*, 2010a,b], and experimental data from Freire *et al.*, [2007] (circles) and Gathee *et al.*, [2008] (squares), while the solid line represents the soft-SAFT+DGT calculations.

### 4.4.3. Surface thermodynamic properties

The surface entropy,  $S^\gamma$ , may be obtained by approximating the quasi-linear interfacial tension variation with temperature. Far enough from the critical point, the surface entropy,  $S^\gamma$ , can be obtained from:

$$S^\gamma = -\left(\frac{d\gamma}{dT}\right) \quad (4.12)$$

being  $\gamma$  the interfacial tension. In a similar manner, the surface enthalpy,  $H^\gamma$ , can be obtained from the following expression:

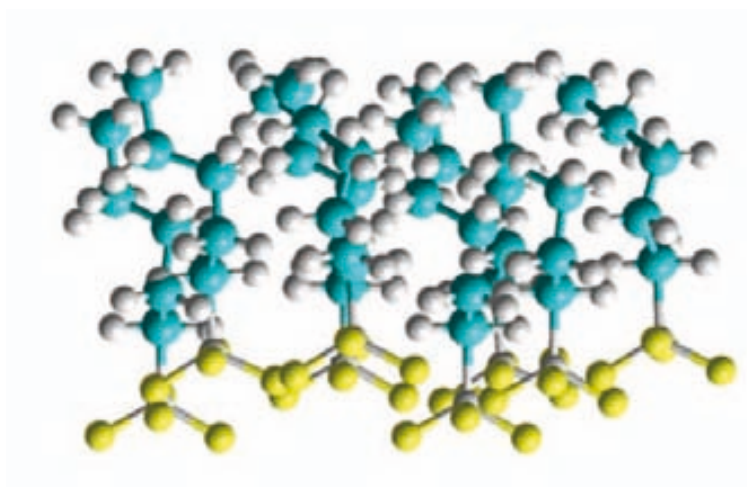
$$H^\gamma = \gamma - T\left(\frac{d\gamma}{dT}\right) \quad (4.13)$$

Results obtained for these properties by applying soft-SAFT are presented in Table 4.19, where the comparison with results published by other authors is also shown.

A high ordered surface is expected in the case of ionic liquids in consonance with the simulations done by Linden-Bell (2006) and the surface studies of Law and Watson [2001]; the surface entropies are more influence by the anion type than by the cation chain length [Freire *et al.*, 2007]. This can be inferred from the results presented here since  $[C_n\text{mim}][\text{BF}_4]$  and  $[C_n\text{mim}][\text{PF}_6]$  exhibit almost the same value for the interfacial tension at a given temperature for the same alkyl chain length, while the  $[C_n\text{mim}][\text{Tf}_2\text{N}]$  ionic liquids show an interfacial tension value about 15%-20% lower at the same temperature conditions, making the solubility of a given substance in these ionic liquids higher. Hence, the smaller surface tension is the most favorable the solubility of two given compounds is, due to the lower inhomogeneity of the system.

The energies for both  $[C_n\text{mim}][\text{BF}_4]$  and  $[C_n\text{mim}][\text{PF}_6]$  have almost the same value while in the case of the  $[C_n\text{mim}][\text{Tf}_2\text{N}]$  the values are lower, indicating a higher value of the cohesive forces and the microscopic ordering of surface molecules. In all cases, the calculated values of the surface entropy indicate a significant degree of surface ordering, decreasing its value with the cation length and the anion type. A schematic representation of the surface ordering

of some  $[\text{C}_5\text{-mim}][\text{Tf}_2\text{N}]$  molecules in a planar surface is presented in Figure 4.55.



**Figure 4.55:** Representation of an ionic liquid in a planar interface. See text for details.

The results obtained with the soft-SAFT+DGT approach for the entropy and enthalpy of surface are presented in Table 4.19, compared with those reported in the literature by other authors [Rebelo *et al.*, 2005; Gathe, 2008; Carvalho *et al.*, 2008]. The tendency of both, the entropy and the enthalpy of surface, is to diminish as the alkyl chain-length increases, in accordance to the results reported in the literature. The long range interactions and the specific anion-cation interactions roughly considered in our simple model, could explain the deviations in the results obtained for the short alkyl chains. Nevertheless, an overall agreement is reached with our simple model with little computational cost, even for the shortest chains.

Results and discussion

**Table 4.18.** Critical properties for the compounds studied in this work. See text for details.

	This work T <sub>c</sub> (K)	Coutinho <i>et al.</i> ,2008. T <sub>c</sub> (K)		Rebello <i>et al.</i> 2008. T <sub>c</sub> (K)		This work P <sub>c</sub> (MPa)	This work ρ <sub>c</sub> (mol·l <sup>-1</sup> )	Weiss ρ <sub>c</sub> (mol·l <sup>-1</sup> )	RD* (%)
	soft-SAFT	(Eöt)	(Gug)	(Eöt)	(Gug)	soft-SAFT	soft-SAFT	Sim. data	
		RD* (%)	RD* (%)	RD* (%)	RD* (%)				RD* (%)
[C <sub>4</sub> -mim]-[BF <sub>4</sub> ]	<b>1042</b>	-13.53%	-6.81%	-19.00%	-11.13%	<b>3.99</b>	<b>1.24</b>	-	-
[C <sub>6</sub> -mim]-[BF <sub>4</sub> ]	<b>1085</b>	-	-	-	-	<b>3.43</b>	<b>1.02</b>	-	-
[C <sub>8</sub> -mim]-[BF <sub>4</sub> ]	<b>1128</b>	22.87%	22.61%	8.95%	12.23%	<b>2.98</b>	<b>0.85</b>	-	-
[C <sub>4</sub> -mim]-[PF <sub>6</sub> ]	<b>1043</b>	6.33%	8.15%	-13.81%	-5.66%	<b>3.60</b>	<b>1.12</b>	<b>1.23</b>	-9.06%
[C <sub>6</sub> -mim]-[PF <sub>6</sub> ]	<b>1091</b>	-2.29%	4.77%	-6.33%	-0.67%	<b>3.13</b>	<b>0.93</b>	-	-
[C <sub>8</sub> -mim]-[PF <sub>6</sub> ]	<b>1128</b>	13.39%	15.07%	11.61%	13.83%	<b>2.76</b>	<b>0.79</b>	-	-
[C <sub>2</sub> -mim]-[Tf <sub>2</sub> N]	<b>1075</b>	3.35%	-14.98%	-12.47%	-2.33%	<b>2.78</b>	<b>0.83</b>	<b>0.66</b>	20.26%
[C <sub>3</sub> -mim]-[Tf <sub>2</sub> N]	<b>1085</b>	-14.19%	-2.21%	-	-	<b>2.62</b>	<b>0.77</b>		
[C <sub>4</sub> -mim]-[Tf <sub>2</sub> N]	<b>1094</b>	-1.46%	5.67%	1.55%	7.50%	<b>2.47</b>	<b>0.72</b>	<b>0.81</b>	-12.61%
[C <sub>5</sub> -mim]-[Tf <sub>2</sub> N]	<b>1104</b>	-3.80%	4.71%	-	-	<b>2.35</b>	<b>0.68</b>	-	-
[C <sub>6</sub> -mim]-[Tf <sub>2</sub> N]	<b>1114</b>	1.44%	8.35%	13.20%	16.34%	<b>2.23</b>	<b>0.64</b>	<b>0.72</b>	-13.16%
[C <sub>7</sub> -mim]-[Tf <sub>2</sub> N]	<b>1126</b>	13.06%	17.23%	-	-	<b>2.13</b>	<b>0.60</b>	-	-
[C <sub>8</sub> -mim]-[Tf <sub>2</sub> N]	<b>1137</b>	14.60%	19.26%	-	-	<b>2.04</b>	<b>0.57</b>	<b>0.78</b>	-36.15%
[C <sub>10</sub> -mim]-[Tf <sub>2</sub> N]	<b>1155</b>	22.51%	24.68%	31.00%	30.74%	<b>1.87</b>	<b>0.52</b>	-	-

\*The relative deviation is calculated from the central value reported in the references.

**Table 4.19.** Surface properties for the compounds studied in this work. See text for details.

	This work (S <sup>□</sup> ) 10 <sup>-5</sup> (J m <sup>-2</sup> K <sup>-1</sup> )	Coutinho <i>et al.</i> , 2008 (S <sup>□</sup> ) 10 <sup>-5</sup> (J m <sup>-2</sup> K <sup>-1</sup> )	RD* (%)	Gathee <i>et al.</i> , 2008. (S <sup>□</sup> ) 10 <sup>-5</sup> (J m <sup>-2</sup> K <sup>-1</sup> )	RD (%)	This work (H <sup>□</sup> ) 10 <sup>-2</sup> (J m <sup>-2</sup> )	Coutinho <i>et al.</i> 2008 (H <sup>□</sup> ) 10 <sup>-2</sup> (J m <sup>-2</sup> )	RD* (%)
[C <sub>4</sub> -mim]-[BF <sub>4</sub> ]	<b>8.11</b>	6.4	21.70%	5.62	30.70%	<b>6.87</b>	6.34	7.71%
[C <sub>6</sub> -mim]-[BF <sub>4</sub> ]	<b>6.86</b>	-	-	5.07	26.09%	<b>5.91</b>	-	-
[C <sub>8</sub> -mim]-[BF <sub>4</sub> ]	<b>5.46</b>	7.1	30.04%	4.87	10.81%	<b>4.91</b>	5.44	10.79%
[C <sub>4</sub> -mim]-[PF <sub>6</sub> ]	<b>8.07</b>	6.2	23.17%	7.24	10.29%	<b>6.70</b>	6.23	7.01%
[C <sub>6</sub> -mim]-[PF <sub>6</sub> ]	<b>6.64</b>	6.3	4.52%	7.07	-6.48%	<b>5.86</b>	5.76	1.65%
[C <sub>8</sub> -mim]-[PF <sub>6</sub> ]	<b>5.78</b>	6.7	15.92%	-	-	<b>5.18</b>	5.49	-5.98%
[C <sub>2</sub> -mim]-[Tf <sub>2</sub> N]	<b>6.14</b>	4.8	21.82%	-	-	<b>5.55</b>	5.09	7.49%
[C <sub>3</sub> -mim]-[Tf <sub>2</sub> N]	<b>5.91</b>	5.2	12.01%	-	-	<b>5.21</b>	5.00	3.55%
[C <sub>4</sub> -mim]-[Tf <sub>2</sub> N]	<b>5.64</b>	5.5	2.48%	-	-	<b>5.00</b>	4.97	0.48%
[C <sub>5</sub> -mim]-[Tf <sub>2</sub> N]	<b>5.78</b>	5.3	8.30%	-	-	<b>4.98</b>	4.83	2.60%
[C <sub>6</sub> -mim]-[Tf <sub>2</sub> N]	<b>5.54</b>	5.4	2.53%	-	-	<b>4.85</b>	4.81	0.72%
[C <sub>7</sub> -mim]-[Tf <sub>2</sub> N]	<b>5.57</b>	6.1	-9.52%	-	-	<b>4.81</b>	4.98	-3.05%
[C <sub>8</sub> -mim]-[Tf <sub>2</sub> N]	<b>5.76</b>	6.2	-7.64%	-	-	<b>4.88</b>	5.00	-2.08%
[C <sub>10</sub> -mim]-[Tf <sub>2</sub> N]	<b>5.56</b>	5.9	-6.12%	-	-	<b>4.81</b>	4.93	-2.16%

## 4.5. References

- Andreu, J.S.; Vega, L.F. *J. Phys. Chem. C* **111**, 16028 (2007).
- Andreu, J.S.; Vega, L.F. *J. Phys. Chem. B* **112**, 15398 (2008).
- Bara, J.E.; Carlisle, T.K.; Gabriel, C.J.; Camper, D.; Finotello, A.; Gin, D.L.; Noble, R. *Ind. Eng. Chem. Res.* **48**, 2739 (2009).
- Blas, F.J.; Martín del Río, E.; de Miguel, E.; Jackson, G. *Molec. Phys.* **99** (2001).
- Belkadi A., Llovel, F.; Gerbaud, V.; Vega, L.F. *Fluid Phase Equilib.* **266**,154 (2008).
- Belkadi A., Llovel, F.; Gerbaud, V.; Vega, L.F. *Fluid Phase Equilib.* **289**,191 (2010).
- Blas, F.J.; Vega, L.F.; *Ind. Eng. Chem. Res.* **37**, 660 (1998).
- Blas, F.J.; Vega, L.F. *Mol. Phys.* **92**, 135 (1997).
- Blas, F.J.; Martín del Río, E.; de Miguel, E.; Jackson, G. *Molec. Phys.* **99** (2001).
- Bongiorno, V.; Scriven, L.E.; Davis, H.T. *J. Colloid Interface Sci.* **57** ,462 (1976).
- Bongiorno, V.; Davis, H. T. *Phys.Rev. A* **12**, 2213 (1975).
- Brennecke, J.F. ; Maginn, E.J. *AIChE J.* **47**, 2384 (2001).
- Cahn, J.W.; Hilliard, J.E. *J. Chem. Phys.* **28**, 258 (1958).
- Carey, B.S.; Striven, L.E.; Davis, H.T. *AIChE J.* **24**, 1076 (1978).
- Carey, B.S.; Striven, L.E.; Davis, H.T. *J. Chem. Phys.* **69**, 5040 (1978).
- Carey, B.S.; Striven, L.E.; Davis, H.T. *AIChE J.* **26**, 705 (1980).
- Chapman, W.G. *PhD Thesis*, Cornell University, Ithaca, NY, USA, 1988.
- Chum, H.L.; Koch,V.R.; Miller,L.L.;Osteryoung, R.A. *J. Am. Chem. Soc.* **97**, 3264 (1975).
- Cornelisse, P.M.W. *PhD Thesis*, Delft University of Technology, Netherlands,1997.

- Cornelisse, P.M.W.; Peters, C.J.; de Swaan Arons, J. *Fluid Phase Equilib.* **82**,109 (1993).
- Cornelisse, P.M.W.; Peters, C.J.; de Swaan Arons, J. *Fluid Phase Equilib.* **117**, 312 (1996).
- Davis, H.; Scriven, L.E. T. *Adv. Chem. Phys.* **49** , 357 (1982).
- Del Popolo, M.G.; Voth, G.A. *J. Phys. Chem. B.* **108**, 1744 (2004).
- Dias, A.M.A; Pàmies, J.C.; Coutinho, J.A.P; Marrucho, I.M., Vega, L.F. *J. Phys. Chem. B* **108**, 1450 (2004).
- Dias, A.M.A.; Carrier, H.; Daridon, J.L.;Pàmies, J.C.; Vega, L.F.; Coutinho, J.A.P.; Marrucho, I.M. *Ind. Eng. Chem. Res.* **45**, 2341 (2006).
- Dias, A.M.A; Llovel, F.; Coutinho, J.A.P; Marrucho, I.M., Vega, L.F. *Fluid Phase Equilib.* **286**, 134 (2009).
- Duque,D.; Vega, L.F. *J. Chem. Phys.* **121**, 17 (2004).
- Duque,D.; Pàmies, J.C.; Vega, L.F. *J. Chem. Phys.* **121**, 11395 (2004).
- Easteal, E.J.; Angell,C.A. *J. Phys. Chem.* **74**, 3987(1970).
- Enders S; Kahl, H.; Winkelmann, J. *Fluid Phase Equilib.* **228-229**, 511(2005).
- Escobedo, F.A.; De Pablo, J.J. *Mol. Phys.* **87** (2), 347(1996).
- Escobedo, J; Mansoori, G.A. *AIChE J.*, **42**(5),1425(1996).
- Evans, W.V. *J. Chem. Educ.* **19** ,539 (1942).
- Galliero,G. *J. Chem. Phys.* **133**, 074705(2010).
- Gil-Villegas, A.; Galindo, A.; Whitehand, P.J.; Mills, S.J.; Jackson, G. *J. Chem. Phys.* **106**, 4168. (1997)
- Gloor, G.J.; Blas, F.J; Martín del Río, E.; de Miguel, E.; Jackson, G *Fluid Phase Equilib.* **521**, 194 (2002).
- Gabriel, S; Weiner, J. *Ber. Dtsch. Chem. Ges.* **21**, 2669 (2006).
- Gross, J.; Sadowski, G. *Ind. Eng. Chem. Res.* **40**, 1244 (2001).
- Guggenheim, E.A. *J. Chem. Phys.* **13**, 253 (1945).



- Heintz, A; Kulikov, D.V; Verevkin, S.P. *J. Chem. Eng. Data* **46** (6), 1526 (2001).
- Holbrey, J.D. *Chim. Oggi* **22**, 35 (2004).
- Hsu, J.J.-C.; Nagarajan, N.; Robinson, Jr., *J. Chem. Eng. Data* **30**, 485 (1985).
- Iglesia, E. *Appl Catal A-Gen* 61(1-2), 59 (1997).
- Jasper, J. J., *J. Phys. Chem. Ref. Data* **1**, 841, (1972).
- Johnson, J.K.;Müller, E.A.; Gubbins, K.E. *J. Phys. Chem.* **98**, 6413 (1994).
- Karl Westberg, K.; Cohen, N.; Wilson, K. W. *Science* **171**, 1013 (1971).
- Kahl, H.; Enders S. *Fluid Phase Equilib.* 263, 160 (2008).
- Kahl, H.; Enders, S. *Phys. Chem.Phys.* 4, 931 (2002).
- Kahl, H.; Enders, S.*Fluid Phase Equilib.* 172, 27 (2000).
- Kahl, H.; Enders, S.*Fluid Phase Equilib.* **172**, 27 (2000).
- Kahl, H.; Enders, S. *Phys. Chem.Phys.* **4**, 931 (2002).
- Kahl, H.; Enders S. *Fluid Phase Equilib.* **263**, 160 (2008).
- Landolt-Börnstein, *Numerical Data and Functional Relationships in Science and Technology, New Series / Editor in Chief: W. Martienssen Group IV: Physical Chemistry, Volume 16, Surface Tension of Pure Liquids and Binary Liquid Mixtures.* Editor: M.D. Lechner, Authors: Ch. Wohlfarth and B. Wohlfarth. 1997.
- Landolt-Börnstein, *Numerical Data and Functional Relationships in Science and Technology, New Series / Editor in Chief: W. Martienssen Group IV: Physical Chemistry, Volume 24, Surface Tension of Pure Liquids and Binary Liquid Mixtures. Supplement to IV/16.* Editor: M.D. Lechner, Authors: Ch. Wohlfarth.2010.
- Lide, D. R. *CRC Handbook of chemistry and physics.* CRC Press, 83 edition, (2002).
- Llovell,F.; Pàmies J.C.; Vega.L.F. *J. Chem. Phys.* **121**, 21 (2004).
- Llovell,F.; Vega, L.F. *J. Phys. Chem.* **110**, 1350 (2006)a.

- Llovell, F.; Vega, L.F. *J. Phys. Chem. B* **110**, 11427 (2006)b.
- Llovell, F.; Florusse, L.J.; Peters, C.J.; Vega, L.F. *J. Phys. Chem. B* **111**, 10180-10188 (2007).
- Llovell, F.; Marcos, R.M.; MacDowell, N.; Vega, L.F. *J. Phys. Chem. B*, dx.doi.org/10.1021/jp303344f (2012).
- Lotfi, A.; Vrabec, J.; Fischer, J. *Mol. Phys.* **76**(6), 1319 (1992).
- MacDowell, L.G.; Blas, F.J. *J. Chem. Phys.* **131**, 074705 (2009).
- MacDowell, N.; Llovell, F.; Adjiman, C.S.; Jackson, G.; Galindo, A. *Ind. Eng. Chem. Res.* **49**, 1883 (2010).
- McCoy, B.F.; Davis, H.T. *Phys. Rev. A* **20**, 1201 (1979).
- Mejía, A.; Pàmies, J.C.; Duque, D.; Segura, H.; Vega, L.F. *J. Chem. Phys.* **123**, 034505.1 (2005).
- Mejía, A.; Vega, L.F. *J. Chem. Phys.* **124**, 244505 (2006).
- Miqueu, C. *PhD Thesis*, Université de Pau et des Pays de l'Adour, France. 2001.
- Miqueu, C.; Broseta, D.; Satherley, J.; Mendiboure, B.; Lachaise, J.; Graciaa, A. *Fluid Phase Equilib.* **172**, 169 (2000).
- Miqueu, C.; Mendiboure, B.; Graciaa, A.; Lachaise, J. *Fluid Phase Equilib.* **207**, 225 (2003).
- Molina, M.J.; Rowland, F.S. *Nature* **249**, (1974).
- Morrow, T. I.; Maginn, E. J. *J. Chem. Phys. B* **106**, 12807 (2002).
- Muller, E.; Gubbins, K.E. *Ind. Eng. Chem. Res.* **40**, 2193 (2001).
- Müller, E.; Mejía, A. *Fluid Phase Equilibria* **282**, 68 (2009).
- Nagarajan, N.; Robinson, Jr., R. L. *J. Chem. Eng. Data* **31**, 168 (1986).
- Niño Amezquita, O.G.; Enders, S.; Jaeger, P.T.; Eggers R. *Ind. Eng. Chem. Res.* **49**, 592 (2010).
- Niño Amezquita, O.G.; Enders, S.; Jaeger, P.T.; Eggers R. *J. Supercrit. Fluids* **55**, 724 (2010).
- NIST Chemistry Web book; <http://webbook.nist.gov/chemistry>.

- Oliveira, M.B.; Marrucho, I. M.; Coutinho, J.A.P.; Queimada, A.J. *Fluid Phase Equilib.* **267**, 93 (2008).
- Pàmies, J.C.; Vega, L. F., *Ind. Eng. Chem. Res.* **40**, 2532 (2001).
- Pàmies, J.C.; Vega, L. F., *Mol. Phys.* **100**, 2519 (2002).
- Pàmies, J.C. *Ph. D. Thesis*, Universitat Rovira i Virgili, Tarragona, 2003.
- Pollard, D.J.; Woodley, J.M. *Trends Biotechnol* **25** (2), 66 (2006).
- Panayiotou, C. *Langmuir* **18**, 8841 (2002).
- Proceedings of the 17th Symposium on Thermophysical Properties, Boulder, CO (USA), June 21-26 (2009).
- Queimada, A. J.; Marrucho, I. M.; Coutinho, J. A. P. *Fluid Phase Equilib.* **183-184**, 229 (2001).
- Queimada, A. J.; Marrucho, I. M.; Coutinho, J. A. P.; Stenby, E.H. *Int. J. of Thermophys.* **26**, 47 (2005)
- Queimada, A.J.; Rolo, L.I.; Caço, A.I.; Marrucho, I.M.; Stenby, E.H. Coutinho, J.A.P. *Fuel* **85**, 874 (2006).
- Rai, N ; Maginn, E. *J. Phys. Chem. Lett.* **2**, 1439 (2011).
- Radermacher, R.; Hwang, Y. *Vapor compression heat pumps with refrigerant mixtures, in: Handbook of Chemistry and Physics*, CRC Press, Florida, 2005.
- Rogers,R.D.; Seddon,K.R. *Science* **302** 792 (2003).
- Rowlinson, J. S. and Widom, B., *Molecular Theory of Capillarity*. Oxford University Press, Oxford, UK, 1982.
- Rowlinson, J. S. *J. Stat. Phys.* **20**, 197 (1979).
- Salvino, L.W.; White, J.A. *J. Chem. Phys.* **96** ,4559 (1992).
- Segura, C.J.; Chapman, W.G.; Shukla, K.P. *Molec. Phys.* **90**, 759 (1990).
- Shankland, I. *Low global warming working fluids – the frying pan or the fire?* Touloukian Award Lecture of the 17th Symposium on Thermophysical Properties, 2009.
- Shereshefsky, J.L. *J. Phys. Chem.* **35**, 1712 (1931).
- Stell, G.; Rasaiah, J. C.; Narang, H. *Mol. Phys.* **27**, 1393 (1974).

Sugden, S. *J. Chem. Soc.* **125**, 32 (1924).

Sugden, S.; Wilkins, H. *J. Chem. Soc.* 1291 (1929).

Sunley, G.J.; Watson, D.J. *Catal Today* **58**(4), 293 (2000).

Urahata, S. R.; Ribeiro, M. C. C. *J. Chem. Phys.* **120** (4), 1855 (2004).

van der Waals, J. D. *Over de Continuïet Van Den Gas- En Vloeistof-Toestand (On the Continuity of the Gaseous and Liquid States); Translation by J. S. Rowlinson.* PhD thesis, University of Leiden, 1873.

van der Waals, J. D. Ph.D. Thesis, University of Leiden, Netherlands, 1873.

van der Waals, J. D. *Z. Phys. Chem.* **13**, 657 (1894).

Vargas, A. S. Ph.D. Thesis, University of Minnesota, USA, 1976.

Vega, L.F.; Llovel, F.; Blas, F.J. *J. Phys. Chem. B* **113**, 7621 (2009).

Velders, G.J.M.; Fahey, D.W.; Daniel, J.S.; McFarland, M.; Andersen, S.O. *Proceedings of the National Academy of Sciences of the United States of America* **106**, 10949(2009).

Vilaseca, O.; Llovel, F.; Yustos, J.; Marcos, R.M.; Vega, L.F. *J. Supercrit. Fluids* **55**, 755 (2010).

Vilaseca, O.; Vega, L.F. *Fluid Phase Equilib.* **306**, 4 (2011).

Vilaseca, O.; Vega, L.F. In preparation.

Walden, P. *Bull. Acad. Imper. Sci. (St. Petersburg)* 1800 (1914).

Wasserscheid, P.; Keim, W. *Angew. Chem. Int. Ed. Engl.* **39**, 3772 (2000).

Weiss, V.C.; Heggen, B.; Müller-Plathe, F. *J. Phys. Chem. C* **114**, 3599 (2010)a.

Weiss, V.C. *J. Phys. Chem. B* **114**(28), 9183 (2010)b.

Welton, T. *Chem. Rev.* **99**, 2071(1999).

Wilkes, J.S.; Levisky, J.A.; Wilson, R.A.; Hussey, C.L. *Inorg. Chem.* **21**, 1263 (1982).

Wilkes, J.S.; Zaworotko, M.J. *Chem. Commun.* 965 (1992).

*Results and discussion*

World Meteorological Organization, *Scientific Assessment of Ozone Depletion: 2006, Global Ozone Research and Monitoring Project Report No. 50*, Geneva, Switzerland, 2007.

Yuan-Yuan, D.; Hong, L.; Zhong-Wei, W. *J.Chem.Eng. Data* **48**, 1068 (2003).

Zhao,G; Bi, S.; Wu,J; Zhigang, L. *J. Chem. Eng. Data* **55** (9), 3077 (2010).

Zuo, Y.-X; Stenby, E.H. *Can. J. Chem. Eng.* **75**, 1130 (1997).

<http://www.co2now.org>

<http://www.morethanorganic.com>

*United States Patent 5294261*



# 5. Conclusions and Future Work

*“The ignorant says, the wise hesitates and reflects”*

*Aristotle (384 BC – 322 BC); Greek philosopher and Scientist*

## Conclusions and Future Work

This PhD Thesis has been devoted to a methodological study of the application of the crossover soft-SAFT equation coupled with DGT, for the simultaneous prediction of phase and interface properties of all type of compounds and mixtures of them. Results have been discussed and compared to available experimental or simulation data, obtaining an excellent agreement both, far from the critical point and close to the critical region, thanks to the use of the crossover approach in combination with DGT. The results presented here represent a step forward versus existing works in the literature, in which the description of interfacial tensions near the critical point was not as accurate, as a consequence of the classical formulation of the chosen Equation of State. It has been demonstrated that, the combination of the right terms in a molecular-based approach to calculate the interfacial properties provide additional insights, for instance: density profiles, orientation, interfacial thickness, surface ordering among others, only available by advanced modeling techniques.

It has been found that within this approach, the use of a constant (temperature independent) influence parameter provides accurate interfacial properties for pure systems and mixtures in the whole thermodynamic range. The influence parameter for the *n*-alkane, 1-alkanol and [C<sub>n</sub>mim][Tf<sub>2</sub>N] series presents a parabolic dependence with the carbon number of the chain, as previously observed for the perfluoroalkanes family. Taking advantage of this, accurately predicted interfacial tensions of compound not included in the series and mixtures of them have been reported here, in excellent agreement with available experimental data, making the model as robust and predictive as possible. In this sense, accurate descriptions were also obtained for the other investigated systems, including nitriles, refrigerants, neutral and acid gases, carbon dioxide and water. In fact, the equation was even able to capture the S-shape of the interfacial tension of water as a function of temperature.



## *Conclusions and Future Work*

The same approach has been applied to three families of ionic liquids, of clear technological importance, but challenging systems from the modeling point of view. This is the first time that, an EoS is coupled to the DGT to simultaneously calculate the interfacial tension at elevated temperatures, while capturing the asymptotic behavior as the critical region is approached. Moreover, the critical temperatures, densities and pressures were estimated with a molecular based approach, founding a good agreement with the values reported in the literature from simulation and experimental extrapolations. Furthermore, the surface thermodynamic properties of these ionic liquids have been calculated, and results were compared with the values reported in the literature, being all of them within the same range.

In summary, this Thesis work reinforces the rigorous approach of combining molecular-based equations (such as SAFT-type) with other physically sound theories in order to expand the applications of the equation to the calculation of other properties, such as interfacial and critical properties, with the same approach and degree of accuracy for predictive purposes. In addition, the need to couple DGT with an accurate equation for the bulk in order to obtain both, phase and interfacial equilibria, with the same level of precision is also highlighted. Consequently, a precise description of the fluid macroscopic and microscopic behavior of experimental systems can be achieved by means of a molecular approach.

The availability of such predictive tools with little computational efforts is needed to accurately design some processes and products. It is intended that the obtained results from this PhD thesis would be used in industry for designing and optimization functions, saving time and money with a good reliability on the results; giving the hint to solve everyday industrial problems.

## **Future work**

After completing this work different applications and extensions to the approach can be done to further enhance its capabilities. I highly some of them here:

- The implementation of a methodology for the beta different than one would be useful to calculate the interfacial properties of some highly asymmetric mixtures, as seen in this thesis.
- To establish a truly molecular relation for the prediction of the influence parameter would be also engaging.
- An extension of the DGT to ternary mixtures is very appealing and also a challenge for the petroleum and the Enhanced Oil Recovery from reservoirs.
- Applying the same tools to other experimental challenging but relevant industrial systems such as amines, esters, acetones or polymers.
- Modeling some blends as water-alkanes, water with ionic liquids and carbon dioxide, alcohols with carbon dioxide or blends of ionic liquids would of practical use for the petrochemical industry.
- To perform molecular simulations, especially for a system which the soft-SAFT combined with the DGT gives poor results or the case of some complex associating mixtures. Also an implementation of the approach and its algorithm in some process simulator will enhanced the results of interfacial tension calculations, especially for the new and complex mixtures for which the classical approaches fail and there are neither correlations nor experimental data available in the literature.

## List of publications

The following publications have arisen from this thesis work:

### Research articles

- [1] Vega, L.F.; Vilaseca, O.; Llovel F.; Andreu, J.S. Modeling ionic liquids and the solubility of gases in them: Recent advances and perspectives. *Fluid Phase Equilib.* **2010**, *294*, 15-30.
- [2] Vilaseca, O.; Llovel, F.; Yustos, J.; Marcos, R.M.; Vega, L.F. Phase equilibria, surface tensions and heat capacities of hydrofluorocarbons and their mixtures including the critical region. *J. Supercrit. Fluids*, **2010**, *55* (2), 755-768.
- [3] Vilaseca, O. and Vega, L.F. Direct calculation of interfacial properties of fluids close to the critical region by a molecular-based equation of state. *Fluid Phase Equilib.* **2011**, *306*, 4-14.
- [4] Llovel,F.; Valente, E.; Vilaseca, O.; Vega, L. F. Modeling Complex Associating Mixtures with [Cn-mim][Tf2N] Ionic Liquids: Predictions from the Soft-SAFT Equation. *J. Physical Chemistry B* **2011**,*115* (15), 4387–4398.
- [5] Llovel,F.; Vilaseca, O.; Vega, L.F. Thermodynamic Modeling of Imidazolium-Based Ionic Liquids with the [PF6] anion by means of the soft-SAFT EoS. *Separation Sci. and Tech.*, **2012**, *47*(2), 399-410.
- [6] Vilaseca, O. and Vega, L.F.; Critical, interfacial and surface properties of ionic liquids by a molecular-based equation of state. In preparation 2012.
- [7] Llovel,F.; Vilaseca, O.; Jung, N.; Vega, L.F. Phase and interfacial properties of the water-alkanols family with the crossover soft-SAFT and the Density Gradient Theory. In preparation 2012.

### *List of publications*

- [8] Vilaseca, O.; Llovel, F.; Marcos, R.M; Vega, L.F. Modeling with the soft-SAFT combined with the DGT of amines with carbon dioxide for environmental purposes. In preparation 2012.

Number of published papers: 5 + 3 in preparation

Number of book chapters: 1

Number of citations: 71 (July 2012)

H factor: 5

#### *Book Chapters*

- [1] Vega, L.F.; Vilaseca, O.; Valente, E.; Andreu, J.S.; Llovel F.; Marcos, R.M.; *"Ionic Liquids, Theory and Applications" Chapter 13. Using Molecular Modelling Tools to Understand the Thermodynamic Behaviour of Ionic Liquids*, ISBN 978-953-307-349-1 Publisher: InTech, Publishing date: February 2011

#### *Conference Proceedings*

- [1] Vilaseca, O.; Llovel, F.; Marcos, R.M.; Vega, L.F. *Thermodynamic modeling of alternative refrigerants* 2011 9<sup>th</sup> Conference on supercritical fluids and their applications 8<sup>th</sup>-10<sup>th</sup> September 2010.Sorrento (Italy)
- [2] Dowell, N.M.; Hallett, J.P.; Vilaseca, O.; Llovel, F.; Vega, L.F. *Towards green bioprocessing: Ionic liquids for biomass deconstruction*. 2011 AIChE Annual Meeting, 16<sup>th</sup>-21<sup>st</sup> October 2011.Minneapolis (USA)
- [3] Llovel, F.; Belo, M.; Vilaseca, O.; Coutinho, J.A.P.; Vega L. F. *Thermodynamic Modeling of the Solubility of Supercritical CO<sub>2</sub> and Other Gases on Ionic Liquids with the soft-SAFT Equation of State*. ISSF 2012. 10th International Symposium on Supercritical Fluids. 13<sup>th</sup>-16<sup>st</sup> May 2012. San Francisco (USA)

#### *Others*

*Acting as a reviewer for Journal of Physical Chemistry (ACS Publications).*

## List of conference contributions

- [1] O. Vilaseca, R. M. Marcos, L.F.Vega *Applicability of the crossover soft-SAFT equation for alkanes and CO<sub>2</sub>*. XVI Congreso de Física Estadística (FisEs2009). 9<sup>th</sup>-11<sup>th</sup> September 2009 Huelva (Spain).

Type of presentation: Poster

- [2] L.F. Vega, A.Mejía, O.Vilaseca *Derivative properties of pure fluids and binary mixtures of n-alkane and 1-alkanols through a molecular-based equation of state*. 17th Symposium on Thermophysical Properties. Boulder (USA) 21<sup>st</sup>-26<sup>th</sup> June 2009.

Type of presentation: Oral

- [3] O. Vilaseca, L.F. Vega *Phase and interface behavior of pure compounds and binary mixtures with soft-SAFT*. II Jornadas de Jóvenes Investigadores en Física Atómica y Molecular. 21<sup>st</sup>-22<sup>nd</sup> January 2010. Barcelona (Spain)

Type of presentation: Oral

- [4] F. Llovell, O. Vilaseca, J. S. Andreu, E. Valente, R. M. Marcos, L. F.Vega *Molecular modeling of ionic liquids: theory and simulations*. 12th Internacional Conference on Properties and Phase Equilibria for Process and Product Design (PPEPPD) 16<sup>th</sup>-21<sup>st</sup> May 2010. Suzhou (China).

Type of presentation: Poster

- [5] F. Llovell, O. Vilaseca, R. M. Marcos, L. F. Vega *A statistical mechanics based equation of state for thermodynamic predictions: soft-SAFT*. XXVI Reunió Anual de la Xarxa de Referència de Química Teòrica i Computacional. 12<sup>nd</sup>-21<sup>th</sup> July 2010. Bellaterra, Barcelona (Spain).

Type of presentation: Oral

*List of contributions*

- [6] O. Vilaseca, L.F. Vega, R. M. Marcos *Prediction of interfacial properties: a comparison of theoretical approaches with experimental data.* International Soft Matter Conference 2010. 5<sup>th</sup>-8<sup>th</sup> July 2010. Granada, (Spain)  
Type of presentation: Poster
- [7] O. Vilaseca, F. Llovell, R. M. Marcos, L.F. Vega *Thermodynamic modeling of alternative refrigerants.* 9th Conference on Supercritical Fluids and Their Applications 5<sup>th</sup>-8<sup>th</sup> September 2010. Sorrento (Italy)  
Type of presentation: Poster
- [8] E. Valente, F. Llovell, O. Vilaseca, R.M. Marcos, L.F. Vega *Thermodynamic characterization of ionic liquids and their mixtures with supercritical carbon dioxide.* 9th Conference on Supercritical Fluids and Their Applications 5<sup>th</sup>-8<sup>th</sup> September 2010. Sorrento (Italy)  
Type of presentation: Poster
- [9] E. Valente, F. Llovell, O. Vilaseca, R.M. Marcos, L.F. Vega *Recent advances in the modeling of complex mixtures of ionic liquids with soft-SAFT combined with Density Gradient Theory.* 20 Years of the SAFT Equation: recent Advances and Challenges. 19<sup>th</sup>-21<sup>th</sup> September 2010. Bellaterra, Barcelona (Spain).  
Type of presentation: Poster
- [10] F. Llovell, O. Vilaseca, J. S. Andreu, E. Valente, R. M. Marcos, L.F.Vega *Molecular modeling of ionic liquids and their use as solvents for separation and extraction processes.* 2010 AIChE Conference 14<sup>th</sup>-19<sup>th</sup> November 2010. Salt Lake City (USA)  
Type of presentation: Oral
- [11] O. Vilaseca, F. Llovell, L.F. Vega *Critical, interfacial and surface properties of ionic liquids by a molecular-based equation of state.* XVII Congreso de Física Estadística (FisEs2011) 2<sup>nd</sup>-4<sup>th</sup> June 2011 Barcelona (Spain).  
Type of presentation: Poster

*List of contributions*

- [12] F. Llovell, O. Vilaseca, E. Valente, N. Jung, L.F. Vega *Thermodynamic modeling of cross-association systems with the soft-SAFT EoS*. 25<sup>th</sup> European Symposium on Applied Thermodynamics ESAT11. 24<sup>th</sup>-27<sup>th</sup> June 2011. Saint Petersburg (Russia)  
Type of presentation: Oral
- [13] O. Vilaseca, F. Llovell, R.M. Marcos, L.F. Vega *Thermodynamic modeling of alternative refrigerants*. 25<sup>th</sup> European Symposium on Applied Thermodynamics ESAT11. 24<sup>th</sup>-27<sup>th</sup> June 2011. Saint Petersburg (Russia)  
Type of presentation: Poster
- [14] F. Llovell, O. Vilaseca, E. Valente, L.F. Vega *Thermodynamic Study of Imidazolium Ionic Liquids with different anions using the soft-SAFT EoS*. 2<sup>nd</sup> Iberian Meeting on Ionic liquids. 20<sup>th</sup>-22<sup>nd</sup> July 2011. Santiago de Compostela- A Coruña (Spain)  
Type of presentation: Oral
- [15] O. Vilaseca, L.F. Vega *Modeling the critical, interfacial and surface properties of ionic liquids*. 2<sup>nd</sup> Iberian Meeting on Ionic liquids. 20<sup>th</sup>-22<sup>nd</sup> July 2011. Santiago de Compostela- A Coruña (Spain)  
Type of presentation: Oral
- [16] O. Vilaseca, F. Llovell, L.F. Vega *Physicochemical properties of ionic liquids by a molecular-based equation of state*. 1<sup>st</sup> International Conference on Ionic Liquids in Separation and Purification Technology. 4<sup>th</sup>-7<sup>th</sup> September 2011. Sitges-Barcelona (Spain)  
Type of presentation: Oral
- [17] N. MacDowell, J.P. Hallet, O. Vilaseca, F. Llovell, L.F. Vega *Towards Green Bioprocessing: Ionic Liquids for Biomass Deconstruction*. 2011 AIChE Meeting. 16<sup>th</sup>-21<sup>st</sup> October 2011. Minneapolis (USA)  
Type of presentation: Oral

*List of contributions*

- [18] O. Vilaseca, F. Llovell, L.F. Vega. *Critical, interfacial and derivative properties of ionic liquids by a molecular-based equation of state*. 2011 AIChE Meeting. 16<sup>th</sup>-21<sup>st</sup> October 2011. Minneapolis (USA) Type of presentation: Poster
- [19] F. Llovell, O. Vilaseca, L.F. Vega *Molecular modeling of aqueous systems using the soft-SAFT EoS*. SAFT2011 Workshop. 24<sup>th</sup>-25<sup>th</sup> October 2011. Pau (France)  
Type of presentation: Poster
- [20] F. Llovell, O. Vilaseca, L.F. Vega *Modeling Ionic Liquids with soft-SAFT: an exploration of critical, interfacial and derivative properties*. SAFT2011 Workshop. 24<sup>th</sup>-25<sup>th</sup> October 2011. Pau (France)  
Type of presentation: Poster
- [21] F. Llovell, O. Vilaseca, L.F. Vega *Thermodynamic modeling of ionic liquids for extraction and separation purposes*. 12<sup>th</sup> Mediterranean Conference on Chemical Engineering. 15<sup>th</sup>-18<sup>th</sup> November 2011. Barcelona (Spain)  
Type of presentation: Oral
- [22] R.M. Marcos, O. Vilaseca, F. Llovell, L.F. Vega *Characterization of thermophysical properties of blends of refrigerants using a molecular-based equation of state*. 12<sup>th</sup> Mediterranean Conference on Chemical Engineering. 15<sup>th</sup>-18<sup>th</sup> November 2011. Barcelona (Spain)  
Type of presentation: Poster
- [23] F. Llovell, M. Belo, O. Vilaseca, J.A.P. Coutinho, L. F. Vega *Thermodynamic Modeling of the Solubility of Supercritical CO<sub>2</sub> and Other Gases on Ionic Liquids with the soft-SAFT Equation of State*. ISSF 2012. 10<sup>th</sup> International Symposium on Supercritical Fluids. 13<sup>th</sup>-16<sup>st</sup> May 2012. San Francisco (USA)  
Type of presentation: Oral



*List of contributions*

- [24] F. Llovell, O.Vilaseca, L. F. Vega *Accurate Thermophysical Characterization of Aqueous Systems with the soft-SAFT equation of state* 17th Symposium on Thermophysical Properties. 24th-29th June 2012. Boulder (USA)  
Type of presentation: Oral
- [25] O. Vilaseca, F.Llovell, R.M.Marcos, L. F. Vega *Transferable Molecular Models for the Calculation of Thermodynamic and Transport Properties of Common Hydrofluorocarbon Refrigerants and New Alternative Blends with the Soft-SAFT Equation.* 17th Symposium on Thermophysical Properties. 24th-29th June 2012. Boulder (USA)  
Type of presentation: Oral
- [26] R.M. Marcos, F. Llovell, O. Vilaseca, L. F. Vega *Predictive models for the estimation of thermodynamic and transport properties of hydrofluorocarbons using an extended version of the Soft-SAFT.* Equifase 2012. 8th-12th October 2012. Puerto Varas (Chile)  
Type of presentation: Oral
- [27] F. Llovell, M. Belo, O. Vilaseca, R.M.Marcos, J.A.P. Coutinho, L. F. Vega *Modelling of ionic liquids: a simple and accurate approach for the prediction of thermophysical properties.* Equifase 2012. 8th-12th October 2012. Puerto Varas (Chile)  
Type of presentation: Oral
- [28] O. Vilaseca, F. Llovell; L. F. Vega *Modeling the critical, interfacial and surface properties of ionic liquids.* 2012 AIChE Meeting. October 28<sup>th</sup>-November 2<sup>nd</sup> 2012. Pittsburgh (USA)  
Type of presentation: Oral
- [29] F. Llovell; O. Vilaseca, L. F. Vega *Phase, Interfacial, Derivative and Transport Properties of Aqueous Systems with the Soft-SAFT EoS.* 2012 AIChE Meeting. October 28<sup>th</sup>- November 2<sup>nd</sup> 2012. Pittsburgh (USA)  
Type of presentation: Oral

**Events organization**

[1] International Workshop on Electrostatic Effects in SoftMatter: Bringing Experiments, Theory and Simulation Together.

10<sup>th</sup>-11<sup>th</sup> April 2008. UAB. Bellaterra, Barcelona (Spain).

*Member of the organizing committee*

[2] 20 Years of the SAFT equation: Recent advances and challenges

19<sup>th</sup>-21<sup>st</sup> September 2010. UAB. Bellaterra, Barcelona (Spain).

*Member of the organizing committee*

## **Curriculum Vitæ**

Oriol Vilaseca i Vidal was born Capellades (Barcelona), Spain, on the 2nd of October of 1976. He started the five-year degree of Chemical Engineering in 1999 at the Universitat Rovira i Virgili (Tarragona). In his fourth year's degree he received an Erasmus grant and move for one year to Ecole Nationale Supérieure des Ingénieurs en Arts Chimiques Et Technologiques in Toulouse (France). Then after struggling with French language and learn some issues on molecular simulation he applied for a Seneca Grant and moved to the Universitat Autònoma de Barcelona to course his last year degree. Knowing about Dr. Lourdes Vega's group he carried on the Research Laboratory as a mandatory part of his degree, with the group Molsim directed by Dr. Lourdes Vega, starting his contact with equations of state and molecular simulations, especially with the soft-SAFT and molecular modeling. Finally he obtained his bachelor's degree in Chemical Engineering on July, 2004. In September 2004 he obtained the bachelor's degree in Industrial Technical Engineering. After that he has passed several scientific technical courses up to the present, he obtained a Master Degree in Health and Security, he is a Certified Environmental External Assessor and he has been certified as Project Manager for European Projects for the Project Management Institute (PMI).

In 2004, he enrolled in a national company as Junior Environmental Assessor for the reduction, reutilization and recycling of Construction and Demolition (C&D) waste in Spain. In 2006 after a couple of years he founded a Consulting and Engineering company, which is still running and expanding. Very recently (2011), he cofounded and was named CEO of an international company with local partners in the emerging market of Morocco, for the management and execution of international investments especially in the environmental, logistic and industrial sectors, as well as civil and engineering works. He is also the CEO of a recognized Spanish Group specialized in civil and engineering works.

## *Curriculum Vitae*

In September 2008, after obtaining the Master Degree on Materials' Science & Technology, he started his PhD program at the ICMAB-CSIC institution and at MATGAS Research Center under the supervision of professor Dr. Lourdes F. Vega. From this thesis work, Oriol Vilaseca i Vidal has published more than 10 publications in conference proceedings, a book chapter and some research articles in international journals, and he is preparing some more. He has contributed by means of oral or poster presentations to 29 conferences. He has been a member of the organizing committee of one international conference and one international symposium, the latter being organized on the occasion of having together the selected members of the evaluation committee that, on the 23th of July in 2012, based on the lights of the present study, will decide if he deserves the doctor's degree.

## **Curriculum Vitæ (Catalan)**

Encara recordo quan essent molt i molt petit, devia tenir uns tres o quatre anys, vaig passar amb el cotxe del meu pares per davant de la facultat de Física i Química de la Diagonal de Barcelona. Des d'aquell precís instant vaig saber que la meva vocació aniria encarrilada per allà, i no se'm va ocórrer altra cosa que, el dilluns següent preguntar-li a la meva professora de parvulari que: quan temps em faltava per anar a la Universitat i que si era gaire car allò d'estudiar en aquell lloc que a mi em semblava tant llunyà en el temps i en l'espai (jo vivia a 40 km i tenia 4 anys....)

Les coses de vegades no van prou ràpid segons els ulls d'un mateix, però tal i com va dir Albert Einstein “ No cal esperar el futur, arriba amb prou rapidesa!”. Quan un comença els estudis primaris sempre veu als de les classes del davant com en un estadi superior, i és per això que un vol fer-se gran, però quan arribem a vuitè de l'antiga primària , ens n' adonem que tot allò no ha fet més que començar i que, arribar a l' institut de secundària només significa que l'hora de decidir allò que hom vol ser és més a la vora que un no havia pensat i llavors ja tenim el futur per primer cop davant. En aquest punt de la vida acadèmica comença a perfilar-se el nostre caràcter científic, (de vegades fins i tot abans, encara recordo la cara que va posar el meu pare quan li vaig demanar amb uns 7 o 8 anys un microscopi i un joc del Quimicefa o el primer dia que vaig ser prou gran per entrar al laboratori de l'escola, quina meravella!!!!). És per això que sempre que miro enrere, em trobo entre els meus pensaments: al Pere Castells de l'IES Molí de Vila (per a mi el millor director d'institut que un pot tenir) amb ell vaig fer el primer “projecte de recerca” sobre la porositat del policlorur de vinil, a la Mar de ciències amb la seva metodologia pedagògica perfecte, a la Maria Antonia de filo que em va fer sortir de la “caverna”, al Salvador qui em fa reenganxar al meravellós món de les matemàtiques després d'un dels meus rampells de pubertat (vaig treure un 7.5 sobre 10 a mates per primera vegada a la vida i vaig pensar que era la professora, la Pepa, que havia sigut molt dura en la correcció del meu examen, total per un canvi de signe, i que per tant lo millor a partir d'aquell moment era que estudiés les mates pel meu compte.....encara

pago les conseqüències d'aquella sabia decisió), tampoc puc oblidar al Xicola que un dia després de la classe de filo on tractàvem el teorema de Pitàgores i les seves implicacions en el mètode científic, li vaig parlar sobre la unitat de l'u i la magnificència del zero, basant-me en la classe anterior on havíem vist el diferents sistemes logarítmics....després d'allò va decidir deixar l'ensenyament secundari i dedicar-se a donar classes de cuina tradicional catalana. Estic segur que li vaig fer trobar la línia que l'unia amb el seu punt vital següent....

Passen els quatre anys d'institut i entre intercanvis culturals, els primers "projectes de recerca", els viatges de final de curs, els treballs de cambrer de cap de setmana, els de les tardes en un taller de soldadura i els de l'estiu, recollint raïm a les nostres precioses vinyes del Penedès, o qualsevol cosa que pogués significar un dineret, els amors furtius i les activitats paral·leles que durant aquesta etapa realitzem, un ni se n'adona i ja torna a tenir el següent punt: quina carrera vull fer? Carrera, la vida si que és una veritable cursa, però de fons. Tot i que la geometria diu que la línia més curta entre dos punts és una recta, la vida em va ensenyar el contrari, de vegades cal fer un tom i un sobreesforç per arribar allà on volem arribar.

Així que arribat en aquest punt i donades les circumstàncies que de vegades envolten la vida de les persones, no tenia prou calers per anar a la universitat o sigui que començava el "Plan B" com diuen a les pelis d'acció. Vaig buscar un d'aquells reforçants treballs d'estiu per veure com podia muntar-me les coses per anar a la Uni el més aviat possible. Llavors van començar a unir-se els punts del passat i del present, l'única cosa que realment sabia fer quan vaig acabar l'institut era escriure mig-mig, sumar i restar, i fer de cambrer, per tant vaig comprar un Bar musical que estava al meu poble. Vaig pensar que era un bon medi per comprar barato i vendre car, com em va dir un anys més tard el meu padrí, aquell dia vaig comprendre que era el moment de vendre'l i tornar a buscar la recta que em conduiria al següent punt.

Després de passar-me un "estiu vital" o dos o tres, de viatge en viatge, Cap Verd, Marroc i el meu viatge espiritual a través de l'Atlas, allà vaig trobar un marroquí, en Bachir, que em parlava de la Geologia del seu país mentre jo intentava fer surf amb una planxa gegant, França, Holanda, Mèxic on vaig conèixer al Jose Javier Espinosa un maia superdotat que feia de guia per la

## *Curriculum Vitae*

península del Yucatán i em parlava de l'Astronomia i la perfecció dels calendaris Maies, la filosofia ancestral d'aquella avançada cultura i la poca importància que tenen els nostres actes personals en el global de l'univers, però que no obstant el més fàcil es buscar la nostra harmonia amb l'univers. Encara recordo el disgust que vaig tindre quan la meva germana em va dir al setembre....que havia estat adormit i que només quedaven places per Enginyeria Química a Tarragona, vaig pensar que era millor fer cas del Javier i seguir en harmonia, 4 anys i 9 mesos després sabia que havia triat el camí més curt. O sigui que per primera vegada, marxava del meu poble per anar a estudiar no sé què o no sé on....el primer any va ser força dur però vaig aprovar-les totes menys càlcul, si hagués anat a les classes de la Pepa!!!! segon tampoc va ser cap camí de roses. Els laboratoris innumerables amb les meves companyes la Vane, la Elena, la Bea i la perduda de la Cris (que encara té la orgànica penjada!), els treballs en equip (a mi l'independent!!) però finalment me'n vaig sortir prou bé tot i que vaig suspendre termodinàmica al setembre, sí, sí aquesta vegada vaig suspendre jo solet, afortunadament vaig entendre la lliçó de les mates de batxillerat...la professora amb qui vaig repetir l'assignatura no era altra que la Lourdes Vega, qui a partir d'aquell moment va ser fins avui la meva guia acadèmica a tots els efectes, encara utilitzo els apunts d'aquella assignatura que em va fer descobrir el meravellós món de la "termo", ara sí que lligaven el Quimicefa, el microscopi, la geologia, les poques mates que havia après, les molècules que somiava de petit i tot allò que pensava que em feien estudiar sense cap sentit....tot té un sentit en algun moment de la vida, només ens manca perspectiva! Com que finalment havia aprovat el càlcul....vaig entrar al despatx de la Lourdes per demanar-li informació d'allò de les beques Erasmus, em va donar la llista i em va dir tria.....però realment no vaig triar res, una cosa va portar a l'altra i l'any següent ja estava al Politècnic de Toulouse, sense tenir ni idea de francès, però ja m'ho deia la Marta de l'institut vine a classe...finalment va concloure; si un dia vas una temporada a França triomfaràs segur, ara tinc una empresa d'enginyeria al Marroc i el 90% de les converses són en Francès, Quelle bonne heure! Si els màsters, els cursets tots els projectes valorats en milions d'euros que he fet durant els últims set anys no tindrien cap valor si no hagués passat aquell any a França. Finalment l'any a la Ville Rose amb: el Xabier, el Raül, el Cortés, el Fèlix, la Karen, la Isabelica, el Diego, la Laia, la Ivonne *la cubana* i tants d'altres companys de viatge....es va acabar, i la Lourdes em va

## *Curriculum Vitae*

tornar a marcar la discontinua oferint-me una beca Erasmus per fer l'últim any de carrera a la UAB amb una beca Sèneca i poder realitzar el laboratori de recerca al seu grup, Molsim, allà va ser on vaig conèixer la soft-SAFT. La Lourdes ens havia parlat de les equacions d'estat a les classes de termo, però no comprenia la relació que aquelles fórmules podien tenir amb mi fins que vaig començar el doctorat ara fa quatre anys, i quina relació! La relació més important però és la que vaig començar ara fa sis anys amb l'Àngels, la mare dels meus dos fills l'Aina, la petita i el Miquel, l'hereu, com deia el meu avi que també portava el seu nom...sense ella no hauria pogut dedicar tots aquests esforços al treball del doctorat, els càlculs de matinada, els congressos, els pòsters, les presentacions que ha hagut d'aguantar.....això és amor.

I això és la ciència: passió i amor pel saber, filosofia, no té res a veure amb la física, les matemàtiques, la química és simplement intentar veure la línia que uneix els punts. Com no podia ser d'una altra manera, el següent punt que jo volia assolir ja ha arribat, estic acabant la meva tesis, tot i que uns anys més tard d'allò que jo havia previst quan tenia tres o quatre anys (les distàncies no sempre són rectes), i finalment la paciència, la constància, l'esforç personal i professional, l'ajuda de les persones clau, però també el valor per creure en mi mateix m'han portat fins aquí, el punt que uneix el següent punt....potser la vida també és un continu...

*Als meus avantpassats, amics i companys de viatge sense els quals no estaria aquí...*

*"I never think of the future. It comes soon enough"*

*Albert Einstein (1879-1955); German and US Physic*